Summer 8-15-2017

The Role of VIP SCN Neurons in Circadian Physiology and Behavior

Cristina Mazuski
Washington University in St. Louis

WASHINGTON UNIVERSITY IN ST. LOUIS

Division of Biology and Biomedical Sciences
Neurosciences

Dissertation Examination Committee:
Erik Herzog, Chair
Michael Bruchas
John Cirrito
Tim Holy
Paul Taghert

The Role of VIP SCN Neurons in Circadian Physiology and Behavior

by
Cristina Mazuski

A dissertation presented to
The Graduate School
of Washington University in
partial fulfillment of the
requirements for the degree
of Doctor of Philosophy

August 2017
St. Louis, Missouri

Table of Contents

List of Figures

Chapter 2.

Chapter 3.

Acknowledgments

When I started my PhD six years ago, I can honestly say I would not have imagined where I am today. My journey towards today has been truly life altering, and I cannot emphasize enough how much of where I am today is due to the people who have supported me along the way. Words will never be enough to express my gratitude.

To Erik, for his enthusiastic support. Six years ago, I first met Erik when he taught circadian rhythms in our Molecular Neuroscience Class. Immediately, the enthusiasm, excitement and passion Erik has for science and mentoring was clear and I knew he would be an amazing mentor. I am forever grateful for the experiences that Erik has given me; from teaching me how to section the SCN to encouraging me to pursue my interests in lab. Through good and bad, early morning lab meetings and last minute procrastination, Erik is the reason I am the scientist I am today.

To the previous and current members of the Herzog lab, especially Vania Carmona-Alcocer, Carmel Martin-Fairey, Sam Chen, Tracey Hermanstyne and Matt Tso, who have been with me through thick and thin. With their friendship and support they made the lab feel like a second home, always there to drink coffee, complain about the weather and of course have important scientific discussions. I would also like to thank Tatiana Simon, Daniel Granados-Fuentes, Paula

Nieto, Luciano Marpagan, Bill Schwartz, Jeff Jones and Cierra Smith for the good discussions and technical support that were an integral part of my PhD.

To Rayan, even from 4,198 miles away Rayan has been my number one supporter and absolutely indispensable throughout the last 5 years. His curiosity and constant questions about my research along with the support have helped me keep going to the end. Together we have built a foundation that has lasted through the ups and the downs and ultimately contributed to my life both scientifically and personally.

To my many other friends. I have had the good fortune of befriending many amazing people during my time in St. Louis, who are now spread out across the globe. The good times, deep philosophical discussions and friendship has impacted my life in some many little ways

And back to where it all began. I am and always will be truly grateful to my family - my mom, dad, Andrea, Paul and Richard and in Colombia, Virginia and el otro papa. Life is not always easy or smooth, but ultimately they have been and will always be there for me.

Cristina Mazuski

Washington University in St. Louis

August 2017

ABSTRACT OF THE DISSERTATION

The Role of VIP SCN Neurons in Circadian Physiology and Behavior

by

Cristina Mazuski

Doctor of Philosophy in Biology and Biomedical Sciences

Neurosciences

Washington University in St. Louis, 2017

Professor Erik Herzog, Chair

Located in the ventral hypothalamus, the suprachiasmatic nucleus (SCN) is necessary for entraining daily rhythms in physiology and behavior to environmental cues. Though the 20,000 neurons of the SCN uniformly express GABA, they differ greatly in neuropeptide content. One anatomically and functionally distinct class of neuropeptidergic SCN neurons is vasoactive intestinal polypeptide (VIP). Expressed by approximately 10% of SCN neurons, VIP is necessary for synchronizing single-cell SCN rhythms to produce coherent output and sufficient for entrainment. However, little is known about the firing activity of these neurons releases VIP and results in circadian entrainment. We utilized multielectrode array technology and optogenetics to optically tag VIP neurons expressing Channelrhodopsin-2 (ChR2) following three days of spontaneous activity recordings. We find that VIP neurons have circadian firing rates with two distinct patterns, irregular and tonic, that constitute two separate electrophysiological classes. Using optogenetic stimulation *in vitro* and *in vivo*, we show that high frequency firing intervals

are sufficient to phase shift and entrain circadian rhythms in gene expression and locomotor activity through VIP release. Interestingly, low frequency firing intervals do not phase shift the SCN *in vitro* and entrain behavioral rhythms more gradually. We also find that stimulation of VIP neurons can only phase delay and entrain rhythms during late subjective day and early subjective night. We conclude that VIP neurons entrain behavior in a time-of-day- and frequency- dependent manner.

Complementary to testing the sufficiency of VIP neuronal firing for entrainment, we tested the necessity of VIP neurons for circadian rhythms in the adult SCN circuit. Using Cre-lox technology *in vivo,* we triggered adult-onset apoptosis in VIP SCN neurons. We found that over 80% of these mice retained circadian rhythms. We contrast this to *Vip* null mice, where over 60% lose rhythms. A majority of our mice lacking VIP neurons had decreased locomotor activity periods and increased daily onset variability, which strongly correlated with the intensity of VIP staining. *In vitro*, deletion of VIP neurons leads to a dramatically reduced amplitude of circadian gene expression and decreases in synchrony on the single-cell level. We conclude that the difference between adult deletion of VIP neurons and *Vip* null mice suggests a role for VIP in SCN development and in the developed adult circuit VIP neurons are not necessary for rhythmicity.

Finally, we dissected the role of VIP SCN neurons in the daily rhythms in glucocorticoids, by characterizing the anatomy of VIP projections and testing the necessity of VIP neurons. We labeled VIP SCN neurons that project dorsally to the paraventricular nucleus of the hypothalamus (PVN) using a two-color tract tracing experiment. We concluded that a small bilateral subset of VIP SCN neurons projects to each side of the PVN. To test VIP neurons

function, we deleted VIP SCN neurons in the adult and measured corticosterone rhythms under constant conditions for 2 days. We find that rhythms in corticosterone are severely dampened with the loss of VIP neurons with peak corticosterone only reaching approximately 50% of wild-type levels. We conclude that VIP SCN neurons contribute stimulatory input to the circadian rhythm in corticosterone.

Taken together, these data suggest that VIP SCN neurons are a heterogeneous class of SCN neurons with multiple roles in adult SCN entrainment, development and the regulation of glucocorticoid rhythms.

Chapter 1.

Introduction

Properties of Circadian Rhythms

Circadian rhythms are endogenous near-24h oscillations that exist in both unicellular (Golden et al., 1997) and multicellular organisms (Panda et al., 2002). Evolving as a consequence of the predictable 24h rotation of the Earth, circadian rhythms allow organisms to anticipate and time daily physiological processes and behavior. These oscillations occur at molecular, cellular and system-wide levels in organisms as disparate as cyanobacteria, fungi, drosophila, mice and humans.

Generated by endogenous mechanisms, circadian rhythms are capable of self-sustained oscillations in the absence of environmental input. In constant conditions within a laboratory environment, this is termed 'free-running' and observed due to the difference between an organism's intrinsic period (e.g. mice = 23.7h) and the environmental period (24h). In real-world conditions, environmental input entrains an organism to the ambient environment. Light is the primary entraining cue (Czeisler, 1995), and temperature (Herzog and Huckfeldt, 2003), feeding (Mistlberger, 1994) and social activity (Fuchikawa et al., 2016) can function as secondary entraining cues. Entrainment occurs when daily perturbation phase delays or advances an organism's intrinsic circadian rhythm to sync with the environment.

Paradoxically, circadian rhythms must be **stable** – to properly 'keep track of time' - and **flexible** – to adjust to environmental changes. Stability is accomplished through robust endogenous oscillations. However, flexibility is necessary to adapt to long-term environmental changes such as seasonal changes in day-length and temperature. In recent history, modern lighting (de la

Iglesia et al., 2015) and air travel (Waterhouse et al., 2007) often push the circadian system past its limits, resulting in chronodisruption.

In humans, deficits in circadian rhythm entrainment increase the risk of a variety of maladies including diabetes (Hu and Jia, 2016), cancer (Wegrzyn et al., 2016), and neuropsychiatric disorders (McClung, 2007). For instance, humans that exhibit a late chronotype, colloquially known as 'late owls', are more prone to poor academic performance, weight gain, and depression (Fabbian et al., 2016). Therefore understanding how circadian rhythms phase shift and entrain to the environment is crucial for ameliorating these adverse effects.

The Mammalian Circadian Circuit

The Suprachiasmatic Nucleus

In mammals, the suprachiasmatic nucleus (SCN) is the master circadian pacemaker. Located in the ventral hypothalamus above the optic chiasm and alongside the third ventricle, the SCN is a small bilateral nucleus of approximately 20,000 neurons (Herzog, 2007). The SCN is both necessary and sufficient for generating circadian rhythms. Electrolytic ablation of the SCN results in complete behavioral arrhythmicity (Eastman et al., 1984), where rhythmic behaviors such as feeding, sleep and locomotor still occur but are no longer phase locked to a time of day. However, implantation of an embryonic graft SCN can restore circadian rhythms in behavior (Lehman et al., 1987). Importantly, the restored period of the animal matches the intrinsic period of the graft SCN and not the host.

SCN Input

The SCN receives light input primarily through the retino-hypothalamic tract (RHT) (Abrahamson and Moore, 2001). Specifically, in the retina intrinsically photosensitive retinal ganglion cells (ipRGCs) signal to the SCN. In addition to receiving input from rods and cones (Güler et al., 2008), ipRGCs express the photopigment melanopsin that responds to strong changes in light amplitude (Hankins et al., 2008). The terminals of the M1 subtype of ipRGCs synapse onto the SCN (Baver et al., 2008) and release PACAP and glutamate, which activate PAC1 (PACAP receptor) and NMDA receptors in the SCN (Hannibal et al., 2000, Hannibal et al., 2002, Ding et al., 1994). Functionally, ablation of the M1 ipRGCs result in the complete loss of light entrainment (Chen et al., 2011). Additionally, the SCN receives indirect light input from the intergeniculate leaflet (IGL) through the geniculohypothalamic tract (GHT), which releases NPY and serotonin (Pickard et al., 1999). Alterations in NPY signaling lead to minor deficits in light entrainment (Weber and Rea, 1997, Marchant et al., 1997). In addition to these two tracts there are numerous other projections to the SCN, including olfactory, cortical, amygdaloid, hippocampal, thalamic, and hypothalamic inputs (Krout et al., 2002, Moga and Moore, 1997). The role of these inputs is an ongoing area of research.

SCN Output

Rhythms in circadian physiology depend on direct neuronal connections from the SCN. Among others, neuroendocrine rhythms fail to be restored following SCN graft implantation, highlighting the importance of direct neuronal connections from the SCN (Meyer-Bernstein et al., 1998). Indeed, the SCN sends projections to many hypothalamic areas associated with

neuroendocrine and autonomic function including the subparaventricular zone (SPZ), the lateral hypothalamus (LH) and the paraventricular nucleus of the hypothalamus (PVN) (Abrahamson et al., 2001). Ultimately, very little is known about how SCN cell types mediate circadian output. Research into how SCN outputs control circadian rhythms in sleep, water intake (Gizowski et al., 2016) and glucocorticoid rhythms are active areas of interest.

Cellular SCN Rhythms

Individual SCN neurons have cell-autonomous rhythms in gene expression and spontaneous firing activity. These rhythms are self-sustained within cultured SCN explants and present within isolated SCN neurons. Ultimately, these single-cell rhythms couple together to drive system-wide circadian rhythms in physiology and behavior. At the cellular level, these rhythms are often imprecise, however the strong coupling within the SCN strengthens these rhythms to produce precise rhythmic output (Herzog et al., 2004).

The Molecular Clock

The molecular clock is a transcription-translation feedback loop (TTFL) composed of core clock genes such as *Clock*, *Bmal1*, *Period* (1 and 2) and *Cryptochrome* (1 and 2) that form the basis for circadian rhythms in gene expression (Takahashi, 2017). Specifically, the transcription factors BMAL1 and CLOCK form a heterodimer that activates the transcription of *Period* and *Cryptochrome* (Reppert and Weaver, 2002). Following translation, PERIOD and CRYPTOCHROME dimerize and suppress the activity of the CLOCK:BMAL1 heterodimer,

effectively inhibiting their own transcription (Shearman et al., 2000). This loop takes approximately 24 hours and results in roughly antiphase expression of BMAL1 and PERIOD.

Loss of function mutations that completely knock out any of the four main TTFL components result in system-wide arrhythmicity. *Bmal1* is the only single core clock gene whose null mutation is sufficient to knock out the clock. Double null mutations involving other core clock genes (*Clock* and *NPAS2* (DeBruyne et al., 2007), *Per1* and *Per2* (Bae et al., 2001), and *Cry1* and *Cry2* (Vitaterna et al., 1999)) are required to cause arrhythmicity due to their overlapping and compensatory roles.

Expression of the core clock genes is not limited to the SCN, but rather ubiquitous throughout the organism (Yoo et al., 2004). In many tissues including liver, lungs and adrenal glands, the TTFL drives cyclic expression of transcripts, resulting in rhythmic expression of over 40% of the genome (Zhang et al., 2014). However, the SCN is one of the few tissues that expresses self-sustained rhythms that can persist for weeks to months.

Firing Activity

The SCN exhibits circadian rhythms in firing activity at circuit and single-cell levels. These rhythms are primarily driven through the rhythmic expression of ion channels that cyclically alter the electrophysiological properties of SCN neurons (Herzog et al., 2017). Perturbations to the core molecular clock alter the circadian rhythm in firing activity indicating that these rhythms are dependent on a functional molecular clock (Herzog et al., 1998, Albus et al., 2002).

However, circadian firing activity can also feed back and alter the properties of the core molecular clock at a single-cell, circuit and behavioral levels. Pharmacological blockade of voltage-gated sodium channels using TTX reduces the amplitude and desynchronizes circadian rhythms in gene expression (Yamaguchi et al., 2003). Genetic manipulation of potassium channels including *Kv1.4* and *Kv4.2* alters the fundamental period of the molecular clock (Granados-Fuentes et al., 2012). Induction of SCN firing can phase shift and entrain circadian rhythms in gene expression and behavior (Jones et al., 2015).

Unlike the comparatively slow changes in gene expression oscillations that rely on transcription and translation, SCN neurons can quickly modulate firing activity in response to perturbation. *In vivo* multi-unit activity recordings reveal a subset of light-sensitive SCN neurons that rapidly alter their firing rates in response to retinal input (Tsuji et al., 2016, Meijer et al., 1996). In vitro studies reveal changes in SCN firing rate in response to a variety of non-photic signaling molecules including melatonin and NPY (Hablitz et al., 2015, Hablitz et al., 2014). These studies indicate that short-term SCN firing rate plays a crucial role in integrating inputs into the SCN.

Most electrophysiological SCN studies have focused on changes in SCN neuronal firing rate also known as the mean firing frequency:

$$\text{Mean firing frequency} = \text{number of spikes} / \text{time}$$

where time bins can range from 10 seconds to 10 minutes. Firing rate is a quick way to simplify complex SCN activity recordings, but can risk oversimplifying data that occurs on the millisecond timescale. This patterning is also known as the instantaneous firing frequency.

$$\text{Instantaneous firing frequency} = 1 / [(n+1)_{\text{spike time}} - n_{\text{spike time}}]$$

Early SCN studies identified 3 main patterns of firing activity present within SCN neurons – tonic, irregular and bursting (Pennartz et al., 1998). Pharmacological studies suggest that separate ionic conductances are responsible for the oscillations in mean firing rate versus millisecond firing pattern (Pennartz et al., 2002, Ikeda et al., 2003). Recent studies have linked SCN firing patterns with light-responsivity and sleep regulation (Sakai, 2014, Tsuji et al., 2016). However these correlations do not fully explain the observed variability of SCN firing patterns.

Additionally, no in-depth studies have considered the role of spontaneous SCN firing rate or pattern on activity-dependent neurotransmission within the SCN. Membrane depolarization triggers calcium dependent signaling cascades that facilitate the binding of synaptic and dense core vesicles and release of contents from the neuron. Application of TTX on the SCN that greatly reduces firing activity can block phase shifts in gene expression (Jones et al., 2015) and reduce synchrony (Yamaguchi et al., 2003) similar to antagonists that directly block SCN neurotransmission (VPAC2 antagonist (Aton et al., 2005), V1a/V1b antagonists(Yamaguchi et al., 2013)). This strongly suggests that SCN neurotransmission is mediated through firing activity. Ultimately, how firing activity contributes to neurotransmission in the SCN is not well understood.

SCN Neurotransmission

SCN neurons signal through fast GABAergic neurotransmission and slow neuropeptidergic signaling. Most if not all SCN neurons synthesize and release GABA that signals through the

$GABA_A$ receptor (Belenky et al., 2003). However, SCN neurons vary greatly in their neuropeptidergic content (Abrahamson and Moore, 2001). Though up to 40 different SCN neuropeptides have been identified (Hatcher et al., 2008), research has focused on three neuropeptides with region-specific SCN expression: Vasoactive polypeptide (VIP) expressed in the core of the SCN, Arginine vasopressin (AVP) expressed in the shell and Gastrin-releasing peptide (GRP) in the mid- SCN. Of these, VIP is the most potent neuropeptide in SCN function and the focus of this dissertation.

Vasoactive Intestinal Polypeptide (VIP)

Physiology and Release of VIP

VIP is a 28-amino acid polypeptide that was originally isolated in the gastrointestinal tract (Said and Mutt, 1970). In the mammalian brain, VIP is found in the cortex, hippocampus, brainstem and hypothalamus. Within the hypothalamus, VIP is particularly enriched in the SCN, where it is synthesized and expressed by approximately 10% of SCN neurons. VIP cell bodies are restricted to the ventral SCN, but VIPergic processes densely project throughout the whole SCN (Abrahamson and Moore, 2001). Rhythms in VIP mRNA have been reported with peak levels occurring during nighttime (Okamoto et al., 1991, Yang et al., 1993). Rhythms in VIP release are less well understood due to the inherent difficulties of quantifying VIP release. However, VIP is rhythmically released under entrained conditions (Francl et al., 2010), released following nighttime light pulses (Shinohara et al., 1998) and may show rhythmicity under constant conditions (Shinohara et al., 1994, Francl et al., 2010).

How VIP release occurs from neurons is not well understood. Within individual neurons, VIP is stored within dense core vesicles as opposed to clear synaptic vesicles that store small-molecular fast neurotransmitters like GABA (Castel et al., 1996). This has implications for the release of VIP. The long-standing view in neuroscience is that dense core vesicle contents are only released through high calcium levels achieved through high frequency firing (typical stimulation paradigms exceed 40Hz). This is in contrast to synaptic vesicles, which are more readily released through single action potentials. Despite the importance of neuropeptidergic neurotransmission, dense core vesicle fusion has largely been studied in invertebrates, large neuromuscular synapses and hippocampal neurons (Xia et al., 2009, Pecot-Dechavassine and Brouard, 1997). Given the relatively low firing rates found in SCN neurons (sustained firing rates rarely exceed 10-15Hz during daytime) and the importance of neuropeptidergic neurotransmission within the SCN, surprisingly little is known about how VIP or any other neuropeptide is released from SCN neurons.

VIP Signaling

VIP primarily signals through two receptors, VPAC1 and VPAC2. Only VPAC2 is present in high levels within the SCN. VPAC2 belongs to the secretin family of Gs-protein coupled receptor and is expressed by 70-95% of SCN neurons (An et al., 2012, Kalló et al., 2004). Upon binding of VIP, VPAC2 signals through parallel changes in adenylate cyclase and phospholipase C (An et al., 2011), which result in downstream modulations of voltage gated channels, pre-synaptic regulation of GABA release and alterations in transcription via CREB (Meyer-Spasche and Piggins, 2004, Pakhotin et al., 2006).

VIP Functionality

Functionally, VIP is necessary for circadian synchrony. Loss of VIP or its receptor VPAC2 results in behavioral arrhythmicity in 60-70% of animals with the remaining mice running with shorter periods and low-amplitude rhythms. The loss of VIP signaling causes single cell rhythms in gene expression and firing activity to become arrhythmic or desynchronized from each other. This effect can be rescued by daily applications of VPAC2R agonists verifying that VIP signaling is both necessary and sufficient for SCN synchrony (Aton et al., 2005, Harmar, 2003, Colwell et al., 2003, Hughes et al., 2004).

VIP signaling also plays a role in photic entrainment. Some VIP neurons receive direct retinal input (Fernandez et al., 2016). Following a retinal light pulse, some VIP neurons express cFOS and release VIP (Castel et al., 1997, Shinohara et al., 1998). In vivo injections of VIP have phase shifting effects on locomotor activity resulting in a phase delay in early nighttime that mimic the effects seen with bright retinal light pulses (Piggins et al., 1995, Albers et al., 1991). In vitro daily application of VIP is sufficient to phase shift and entrain the SCN in vitro (An et al., 2011). Mechanistically, addition of VIP increases IPSC frequency (Itri et al., 2004) and promotes the expression of PERIOD1 and PERIOD2 during nighttime (Nielsen et al., 2002). Paradoxically, higher dosages of VIP can lower SCN synchrony, which may allow the SCN to more rapidly phase shift and entrain to the local light schedule, a phenomenon known as phase tumbling (An et al., 2013).

Finally, VIP plays a role in SCN output. VIP SCN neurons project to the subparaventricular zone (SPZ), the paraventricular nucleus of the hypothalamus (PVN) and the paraventricular nucleus of the thalamus (PVT) (Abrahamson and Moore, 2001, Abrahamson et al., 2001). Mice deficient in VIP lose rhythms in corticosterone (Loh et al., 2007) and estrous signaling (Miller et al., 2004). Ultimately, little is known about how these neurons contribute to specific circadian behavioral rhythms.

Cell Specific Manipulations

In summary, the SCN is a complex nucleus with heterogeneous rhythms in gene expression and firing activity that signals through many neuropeptides. To understand how the circadian circuit integrates environmental input into coherent behavioral output, we must understand the contribution of specific cell types or regions. By targeting specific SCN cell types, we can **characterize** rhythms, **disrupt** cell-specific rhythms and understand the **function** of cell-specific neural circuitry necessary for circadian behavior. This dissertation uses this tripartite approach to understanding the role of VIP SCN neurons in circadian physiology and behavior.

Cre-Lox Recombination

With Cre-Lox recombination, we can now target specific cell types within the SCN. Briefly, Cre is a DNA recombinase that interacts with sites known as *loxP* sequences to initiate site-specific recombination. This can be used to express or delete DNA sequences. For example, to express channelrhodopsin-2 (ChR2) within VIP neurons, we cross the VIP-ires-Cre mouse line with a transgenic line that contains a loxP-flanked STOP cassette preventing the transcription of ChR2.

Cre is expressed only in VIP-expressing neurons, therefore site-specific recominbation necessary for deleting the STOP cassette that prevents ChR2 expression occurs only in VIP neurons. This results in VIP specific expression of ChR2. Depending on the experimental question, this technology can be adapted to target other cell types and delete or express different constructs.

Observing/Characterizing Rhythms in Specific SCN Cell Types

Previous studies have measured region-specific SCN rhythms (core versus shell) using single-cell slice electrophysiology, PERIOD2::LUC bioluminescent imaging or PERIOD1:VENUS fluorescent imaging. However, interrogating the role of specific SCN cell types within these regions has been limited. Using Cre driver lines that target cell types within the SCN, researchers can drive the expression of fluorophores, bioluminescent reporters and other constructs to observe and characterize cell-specific rhythms. Recent reports characterize circadian rhythms in calcium and membrane voltage within VIP and AVP neurons (Enoki et al., 2017) and gene expression within SCN glia (Tso et al., 2017). Short term VIP firing activity was characterized through targeted VIP expression of fluorescent reporters (Hermanstyne et al., 2016) suggesting that VIP neurons have slightly higher firing rates than non-VIP neurons. Additionally electrophysiological studies characterized monosynaptic SCN connections by activating SCN VIP neurons using cell-specific expression of ChR2, concluding that approximately 50% of SCN neurons respond to GABA signaling from VIP neurons(Fan et al., 2015). In **Chapter 2**, we expand upon this literature by identifying and characterizing the multi-day firing activity of single VIP neurons. We conclude that VIP neurons have circadian patterns of firing activity and predominantly fire in irregular or tonic patterns.

Disrupting Rhythms in Specific SCN Cell Types

Global loss-of-function mutations have been critical in identifying the core molecular clock genes (*Bmal1, Clock, Period, Cryptochorme*) and other genes that regulate circadian period (*Casein-kinase epsilon*) and synchrony (*Vip, Vipr2*). Restricting these genetic manipulations to specific cell types permits more in-depth interrogation of how the SCN circuit functions and which cell types are ultimately more important for generating circadian rhythms. Reversible genetic manipulation of Neuromedin-S (NMS) SCN neurons (~40% of SCN neurons including a majority of VIP and AVP neurons) suggested that rhythms within NMS SCN neurons are necessary for circadian rhythms in behavior (Lee et al., 2015). Loss of the molecular clock in AVP neurons lengthens the behavioral period and weakens intercellular coupling (Mieda et al., 2015). Interestingly, overexpression of Clock Δ19 in VIP neurons does not yield a circadian phenotype (Lee et al., 2015), suggesting that on their own VIP neurons are not sufficient to set the behavioral period. In **Chapter 3** we examine the effects of ablating VIP neurons in the adult SCN. Interestingly, we find that adult loss of VIP neurons produces a milder phenotype than global knockout of VIP signaling.

Testing the Function of SCN Cell-specific Circuitry

Cell-specific targeting allows unprecedented interrogation of neural circuits that control behavior at multiple levels. Fully dissecting a circuit involves multiple components: from understanding anatomical connectivity to testing necessity of signaling and the sufficiency of firing activity for behavior. These techniques are particularly useful for understanding SCN output circuits. Recent

reports in the drosophila model dissect how the Leucokinin neuropeptidergic circuit regulates locomotor activity downstream of clock neurons (Cavey et al., 2016) and how SCN AVP neurons time the circadian rhythm in water intake in the mouse (Gizowski et al., 2016). In this dissertation we test the role of VIP SCN circuitry in locomotor activity and glucocorticoid rhythms. In **Chapter 2**, we test how the different firing patterns of SCN VIP neurons phase shift and entrain circadian rhythms in gene expression and locomotor activity. Interestingly, SCN VIP activity also causes acute inhibition of locomotor activity. We conclude that SCN VIP neurons phase shift and entrain circadian rhythms in a time-of-day- and frequency- dependent manner. In **Chapter 4**, we present preliminary data on VIP SCN neurons that project to the paraventricular nucleus of the hypothalamus and dampen the daily rhythms in corticosterone.

References

ABRAHAMSON, E. E., LEAK, R. K. & MOORE, R. Y. 2001. The suprachiasmatic nucleus projects to posterior hypothalamic arousal systems. *Neuroreport,* 12**,** 435-440.

ABRAHAMSON, E. E. & MOORE, R. Y. 2001. Suprachiasmatic nucleus in the mouse: retinal innervation, intrinsic organization and efferent projections. *Brain Research,* 916**,** 172-191.

ALBERS, H. E., LIOU, S. Y., STOPA, E. G. & ZOELLER, R. T. 1991. Interaction of colocalized neuropeptides: functional significance in the circadian timing system. *Journal of Neuroscience,* 11**,** 846-851.

ALBUS, H., BONNEFONT, X., CHAVES, I., YASUI, A., DOCZY, J., VAN DER HORST, G. T. & MEIJER, J. H. 2002. Cryptochrome-deficient mice lack circadian electrical activity in the suprachiasmatic nuclei. *Current Biology,* 12**,** 1130-1133.

AN, S., HARANG, R., MEEKER, K., GRANADOS-FUENTES, D., TSAI, C. A., MAZUSKI, C., KIM, J., DOYLE, F. J., PETZOLD, L. R. & HERZOG, E. D. 2013. A neuropeptide speeds circadian entrainment by reducing intercellular synchrony. *Proceedings of the National Academy of Sciences of the United States of America,* 110**,** 61.

AN, S., IRWIN, R. P., ALLEN, C. N., TSAI, C. & HERZOG, E. D. 2011. Vasoactive intestinal polypeptide requires parallel changes in adenylate cyclase and phospholipase C to entrain circadian rhythms to a predictable phase. *Journal of neurophysiology,* 105**,** 2289-2296.

AN, S., TSAI, C., RONECKER, J., BAYLY, A. & HERZOG, E. D. 2012. Spatiotemporal distribution of vasoactive intestinal polypeptide receptor 2 in mouse suprachiasmatic nucleus. *The Journal of comparative neurology,* 520**,** 2730-2741.

ATON, S. J., COLWELL, C. S., HARMAR, A. J., WASCHEK, J. & HERZOG, E. D. 2005. Vasoactive intestinal polypeptide mediates circadian rhythmicity and synchrony in mammalian clock neurons. *Nat.Neurosci,* 8**,** 476-483.

BAE, K., JIN, X., MAYWOOD, E. S., HASTINGS, M. H., REPPERT, S. M. & WEAVER, D. R. 2001. Differential functions of mPer1, mPer2, and mPer3 in the SCN circadian clock. *Neuron,* 30**,** 525-536.

BAVER, S. B., PICKARD, G. E. & SOLLARS, P. J. 2008. Two types of melanopsin retinal ganglion cell differentially innervate the hypothalamic suprachiasmatic nucleus and the olivary pretectal nucleus. *Eur.J.Neurosci.*

BELENKY, M. A., SAGIV, N., FRITSCHY, J. M. & YAROM, Y. 2003. Presynaptic and postsynaptic GABA A receptors in rat suprachiasmatic nucleus. *Neuroscience,* 118**,** 909-923.

CASTEL, M., BELENKY, M., COHEN, S., WAGNER, S. & SCHWARTZ, W. J. 1997. Light-induced c-Fos expression in the mouse suprachiasmatic nucleus: immunoelectron microscopy reveals co-localization in multiple cell types. *Eur.J.Neurosci.,* 9**,** 1950-1960.

CASTEL, M., MORRIS, J. & BELENKY, M. 1996. Non-synaptic and dendritic exocytosis from dense-cored vesicles in the suprachiasmatic nucleus. *Neuroreport,* 7**,** 543-547.

CAVEY, M., COLLINS, B., BERTET, C. & BLAU, J. 2016. Circadian rhythms in neuronal activity propagate through output circuits. *Nature neuroscience,* 19**,** 587.

CHEN, S. K., BADEA, T. C. & HATTAR, S. 2011. Photoentrainment and pupillary light reflex are mediated by distinct populations of ipRGCs. *Nature,* 476**,** 92-95.

COLWELL, C. S., MICHEL, S., ITRI, J., RODRIGUEZ, W., TAM, J., LELIEVRE, V., HU, Z., LIU, X. & WASCHEK, J. A. 2003. Disrupted circadian rhythms in VIP- and PHI-deficient mice. *American journal of physiology. Regulatory, integrative and comparative physiology,* 285**,** 49.

CZEISLER, C. A. 1995. The effect of light on the human circadian pacemaker. [Review]. *Ciba Foundation Symposium,* 183**,** 253-254.

DE LA IGLESIA, H. O., FERNÁNDEZ-DUQUE, E., GOLOMBEK, D. A., LANZA, N., DUFFY, J. F., CZEISLER, C. A. & VALEGGIA, C. R. 2015. Access to electric light is associated with shorter sleep duration in a traditionally hunter-gatherer community. *Journal of biological rhythms,* 30**,** 342-350.

DEBRUYNE, J. P., WEAVER, D. R. & REPPERT, S. M. 2007. CLOCK and NPAS2 have overlapping roles in the suprachiasmatic circadian clock. *Nature neuroscience,* 10**,** 543.

DING, J. M., CHEN, D., WEBER, E. T., FAIMAN, L. E., REA, M. A. & GILLETTE, M. U. 1994. Resetting the biological clock: mediation of nocturnal circadian shifts by glutamate and NO. *Science,* 266**,** 1713-1717.

EASTMAN, C. I., MISTLBERGER, R. E. & RECHTSCHAFFEN, A. 1984. Suprachiasmatic nuclei lesions eliminate circadian temperature and sleep rhythms in the rat. *Physiol Behav.,* 32**,** 357-368.

ENOKI, R., ODA, Y., MIEDA, M., ONO, D., HONMA, S. & HONMA, K.-I. 2017. Synchronous circadian voltage rhythms with asynchronous calcium rhythms in the suprachiasmatic nucleus. *Proceedings of the National Academy of Sciences,* 114**,** E2476-E2485.

FABBIAN, F., ZUCCHI, B., DE GIORGI, A., TISEO, R., BOARI, B., SALMI, R., CAPPADONA, R., GIANESINI, G., BASSI, E. & SIGNANI, F. 2016. Chronotype, gender and general health. *Chronobiology international,* 33**,** 863-882.

FAN, J., ZENG, H., OLSON, D. P., HUBER, K. M., GIBSON, J. R. & TAKAHASHI, J. S. 2015. Vasoactive intestinal polypeptide (VIP)-expressing neurons in the suprachiasmatic nucleus provide sparse GABAergic outputs to local neurons with circadian regulation occurring distal to the opening of postsynaptic GABAA ionotropic receptors. *Journal of Neuroscience,* 35**,** 1905-1920.

FERNANDEZ, D. C., CHANG, Y.-T., HATTAR, S. & CHEN, S.-K. 2016. Architecture of retinal projections to the central circadian pacemaker. *Proceedings of the National Academy of Sciences***,** 201523629.

FRANCL, J. M., KAUR, G. & GLASS, J. D. 2010. Regulation of vasoactive intestinal polypeptide release in the suprachiasmatic nucleus circadian clock. *Neuroreport,* 21**,** 1055-1059.

FUCHIKAWA, T., EBAN-ROTHSCHILD, A., NAGARI, M., SHEMESH, Y. & BLOCH, G. 2016. Potent social synchronization can override photic entrainment of circadian rhythms. *Nature communications,* 7.

GIZOWSKI, C., ZAELZER, C. & BOURQUE, C. W. 2016. Clock-driven vasopressin neurotransmission mediates anticipatory thirst prior to sleep. *Nature,* 537**,** 685-688.

GOLDEN, S. S., ISHIURA, M., JOHNSON, C. H. & KONDO, T. 1997. Cyanobacterial circadian rhythms. *Annual review of plant biology,* 48**,** 327-354.

GRANADOS-FUENTES, D., NORRIS, A. J., CARRASQUILLO, Y., NERBONNE, J. M. & HERZOG, E. D. 2012. IA channels encoded by Kv1. 4 and Kv4. 2 regulate neuronal firing in the suprachiasmatic nucleus and circadian rhythms in locomotor activity. *Journal of Neuroscience,* 32**,** 10045-10052.

GÜLER, A. D., ECKER, J. L., LALL, G. S., HAQ, S., ALTIMUS, C. M., LIAO, H.-W., BARNARD, A. R., CAHILL, H., BADEA, T. C. & ZHAO, H. 2008. Melanopsin cells are the principal conduits for rod–cone input to non-image-forming vision. *Nature,* 453**,** 102-105.

HABLITZ, L. M., MOLZOF, H. E., ABRAHAMSSON, K. E., COOPER, J. M., PROSSER, R. A. & GAMBLE, K. L. 2015. GIRK channels mediate the nonphotic effects of exogenous melatonin. *Journal of Neuroscience,* 35**,** 14957-14965.

HABLITZ, L. M., MOLZOF, H. E., PAUL, J. R., JOHNSON, R. L. & GAMBLE, K. L. 2014. Suprachiasmatic nucleus function and circadian entrainment are modulated by G protein-coupled inwardly rectifying (GIRK) channels. *The Journal of physiology,* 592**,** 5079-5092.

HANKINS, M. W., PEIRSON, S. N. & FOSTER, R. G. 2008. Melanopsin: an exciting photopigment. *Trends in neurosciences,* 31**,** 27-36.

HANNIBAL, J., HINDERSSON, P., KNUDSEN, S. M., GEORG, B. & FAHRENKRUG, J. 2002. The photopigment melanopsin is exclusively present in pituitary adenylate cyclase-activating polypeptide-containing retinal ganglion cells of the retinohypothalamic tract. *J Neurosci,* 22**,** RC191.

HANNIBAL, J., MØLLER, M., OTTERSEN, O. P. & FAHRENKRUG, J. 2000. PACAP and glutamate are co-stored in the retinohypothalamic tract. *The Journal of comparative neurology,* 418**,** 147-155.

HARMAR, A. J. 2003. An essential role for peptidergic signalling in the control of circadian rhythms in the suprachiasmatic nuclei. *J Neuroendocrinol,* 15**,** 335-8.

HATCHER, N. G., ATKINS, N., ANNANGUDI, S. P., FORBES, A. J., KELLEHER, N. L., GILLETTE, M. U. & SWEEDLER, J. V. 2008. Mass spectrometry-based discovery of circadian peptides. *Proceedings of the National Academy of Sciences,* 105**,** 12527-12532.

HERMANSTYNE, T. O., SIMMS, C. L., CARRASQUILLO, Y., HERZOG, E. D. & NERBONNE, J. M. 2016. Distinct Firing Properties of Vasoactive Intestinal Peptide-Expressing Neurons in the Suprachiasmatic Nucleus. *Journal of biological rhythms,* 31**,** 57-67.

HERZOG, E. D. 2007. Neurons and networks in daily rhythms. *Nature reviews. Neuroscience,* 8**,** 790-802.

HERZOG, E. D., ATON, S. J., NUMANO, R., SAKAKI, Y. & TEI, H. 2004. Temporal precision in the mammalian circadian system: a reliable clock from less reliable neurons. *J Biol Rhythms,* 19**,** 35-46.

HERZOG, E. D., HERMANSTYNE, T., SMYLLIE, N. J. & HASTINGS, M. H. 2017. Regulating the suprachiasmatic nucleus (SCN) circadian clockwork: interplay between cell-autonomous and circuit-level mechanisms. *Cold Spring Harbor perspectives in biology,* 9**,** a027706.

HERZOG, E. D. & HUCKFELDT, R. M. 2003. Circadian entrainment to temperature, but not light, in the isolated suprachiasmatic nucleus. *Journal of neurophysiology,* 90**,** 763-770.

HERZOG, E. D., TAKAHASHI, J. S. & BLOCK, G. D. 1998. Clock controls circadian period in isolated suprachiasmatic nucleus neurons. *Nature neuroscience,* 1**,** 708-713.

HU, C. & JIA, W. 2016. Linking MTNR1B variants to diabetes: the role of circadian rhythms. *Diabetes,* 65**,** 1490-1492.

HUGHES, A. T., FAHEY, B., CUTLER, D. J., COOGAN, A. N. & PIGGINS, H. D. 2004. Aberrant gating of photic input to the suprachiasmatic circadian pacemaker of mice lacking the VPAC2 receptor. *J Neurosci,* 24**,** 3522-6.

IKEDA, M., SUGIYAMA, T., WALLACE, C. S., GOMPF, H. S., YOSHIOKA, T., MIYAWAKI, A. & ALLEN, C. N. 2003. Circadian dynamics of cytosolic and nuclear Ca 2+ in single suprachiasmatic nucleus neurons. *Neuron,* 38**,** 253-263.

ITRI, J., MICHEL, S., WASCHEK, J. A. & COLWELL, C. S. 2004. Circadian rhythm in inhibitory synaptic transmission in the mouse suprachiasmatic nucleus. *Journal of neurophysiology,* 92**,** 311-319.

JONES, J. R., TACKENBERG, M. C. & MCMAHON, D. G. 2015. Manipulating circadian clock neuron firing rate resets molecular circadian rhythms and behavior. *Nature neuroscience,* 18**,** 373-375.

KALLÓ, I., KALAMATIANOS, T., WILTSHIRE, N., SHEN, S., SHEWARD, W. J., HARMAR, A. J. & COEN, C. W. 2004. Transgenic approach reveals expression of the VPAC2 receptor in phenotypically defined neurons in the mouse suprachiasmatic nucleus and in its efferent target sites. *The European journal of neuroscience,* 19**,** 2201-2211.

KROUT, K. E., KAWANO, J., METTENLEITER, T. C. & LOEWY, A. D. 2002. CNS inputs to the suprachiasmatic nucleus of the rat. *Neuroscience,* 110**,** 73-92.

LEE, I. T., CHANG, A. S., MANANDHAR, M., SHAN, Y., FAN, J., IZUMO, M., IKEDA, Y., MOTOIKE, T., DIXON, S. & SEINFELD, J. E. 2015. Neuromedin s-producing neurons act as essential pacemakers in the suprachiasmatic nucleus to couple clock neurons and dictate circadian rhythms. *Neuron,* 85**,** 1086-1102.

LEHMAN, M. N., SILVER, R., GLADSTONE, W. R., KAHN, R. M., GIBSON, M. & BITTMAN, E. L. 1987. Circadian rhythmicity restored by neural transplant.

Immunocytochemical characterization of the graft and its integration with the host brain. *Journal of Neuroscience,* 7**,** 1626-1638.

LOH, D. H., ABAD, C., COLWELL, C. S. & WASCHEK, J. A. 2007. Vasoactive intestinal peptide is critical for circadian regulation of glucocorticoids. *Neuroendocrinology,* 88**,** 246-255.

MARCHANT, E. G., WATSON, N. V. & MISTLBERGER, R. E. 1997. Both neuropeptide Y and serotonin are necessary for entrainment of circadian rhythms in mice by daily treadmill running schedules. *Journal of Neuroscience,* 17**,** 7974-7987.

MCCLUNG, C. A. 2007. Circadian genes, rhythms and the biology of mood disorders. *Pharmacology & therapeutics,* 114**,** 222-232.

MEIJER, J. H., WATANABE, K., DÉTÀRI, L. & SCHAAP, J. 1996. Circadian rhythm in light response in suprachiasmatic nucleus neurons of freely moving rats. *Brain research,* 741**,** 352-355.

MEYER-BERNSTEIN, E. L., JETTON, A. E., MATSUMOTO, S. I., MARKUNS, J. F., LEHMAN, M. N. & BITTMAN, E. L. 1998. Effects of suprachiasmatic transplants on circadian rhythms of neuroendocrine function in golden hamsters. *Endocrinology,* 140**,** 207-218.

MEYER-SPASCHE, A. & PIGGINS, H. D. 2004. Vasoactive intestinal polypeptide phase-advances the rat suprachiasmatic nuclei circadian pacemaker in vitro via protein kinase A and mitogen-activated protein kinase. *Neuroscience letters,* 358**,** 91-94.

MIEDA, M., ONO, D., HASEGAWA, E., OKAMOTO, H., HONMA, K.-I., HONMA, S. & SAKURAI, T. 2015. Cellular clocks in AVP neurons of the SCN are critical for interneuronal coupling regulating circadian behavior rhythm. *Neuron,* 85**,** 1103-1116.

MILLER, B. H., OLSON, S. L., TUREK, F. W., LEVINE, J. E., HORTON, T. H. & TAKAHASHI, J. S. 2004. Circadian clock mutation disrupts estrous cyclicity and maintenance of pregnancy. *Current Biology,* 14**,** 1367-1373.

MISTLBERGER, R. E. 1994. Circadian food-anticipatory activity: formal models and physiological mechanisms. *Neuroscience & Biobehavioral Reviews,* 18**,** 171-195.

MOGA, M. M. & MOORE, R. Y. 1997. Organization of neural inputs to the suprachiasmatic nucleus in the rat. *Journal of Comparative Neurology,* 389**,** 508-534.

NIELSEN, H. S., HANNIBAL, J. & FAHRENKRUG, J. 2002. Vasoactive intestinal polypeptide induces per1 and per2 gene expression in the rat suprachiasmatic nucleus late at night. *The European journal of neuroscience,* 15**,** 570-574.

OKAMOTO, S., OKAMURA, H., MIYAKE, M., TAKAHASHI, Y., TAKAGI, S., AKAGI, Y., FUKUI, K., OKAMOTO, H. & IBATA, Y. 1991. A diurnal variation of vasoactive intestinal peptide (VIP) mRNA under a daily light-dark cycle in the rat suprachiasmatic nucleus. *Histochemistry and Cell Biology,* 95**,** 525-528.

PAKHOTIN, P., HARMAR, A. J., VERKHRATSKY, A. & PIGGINS, H. 2006. VIP receptors control excitability of suprachiasmatic nuclei neurones. *Pflügers Archiv : European journal of physiology,* 452**,** 7-15.

PANDA, S., HOGENESCH, J. B. & KAY, S. A. 2002. Circadian rhythms from flies to human. *Nature,* 417**,** 329-335.

PECOT-DECHAVASSINE, M. & BROUARD, M. O. 1997. Large dense-core vesicles at the frog neuromuscular junction: characteristics and exocytosis. *Journal of neurocytology,* 26**,** 455-465.

PENNARTZ, C. M., DE JEU, M. T., GEURTSEN, A. M., SLUITER, A. A. & HERMES, M. L. 1998. Electrophysiological and morphological heterogeneity of neurons in slices of rat suprachiasmatic nucleus. *J Physiol,* 506 (Pt 3)**,** 775-93.

PENNARTZ, C. M. A., DE JEU, M. T. G., BOS, N. P. A., SCHAAP, J. & GEURTSEN, A. M. S. 2002. Diurnal modulation of pacemaker potentials and calcium current in the mammalian circadian clock. *Nature,* 416**,** 286.

PICKARD, G. E., SMITH, B. N., BELENKY, M., REA, M. A., DUDEK, F. E. & SOLLARS, P. J. 1999. 5-HT1B receptor-mediated presynaptic inhibition of retinal input to the suprachiasmatic nucleus. *J Neurosci,* 19**,** 4034-45.

PIGGINS, H. D., ANTLE, M. C. & RUSAK, B. 1995. Neuropeptides phase shift the mammalian circadian pacemaker. *The Journal of neuroscience : the official journal of the Society for Neuroscience,* 15**,** 5612-5622.

REPPERT, S. M. & WEAVER, D. R. 2002. Coordination of circadian timing in mammals. *Nature,* 418**,** 935-41.

SAID, S. I. & MUTT, V. 1970. Polypeptide with broad biological activity: isolation from small intestine. *Science,* 169**,** 1217-1218.

SAKAI, K. 2014. Single unit activity of the suprachiasmatic nucleus and surrounding neurons during the wake–sleep cycle in mice. *Neuroscience,* 260**,** 249-264.

SHEARMAN, L. P., SRIRAM, S., WEAVER, D. R., MAYWOOD, E. S., CHAVES, I., ZHENG, B., KUME, K., LEE, C. C., HASTINGS, M. H. & REPPERT, S. M. 2000. Interacting molecular loops in the mammalian circadian clock. *Science,* 288**,** 1013-1019.

SHINOHARA, K., HONMA, S., KATSUNO, Y., ABE, H. & HONMA, K.-I. 1994. Circadian rhythms in the release of vasoactive intestinal polypeptide and arginine-vasopressin in organotypic slice culture of rat suprachiasmatic nucleus. *Neuroscience letters,* 170**,** 183-186.

SHINOHARA, K., TOMINAGA, K. & INOUYE, S. T. 1998. Luminance-dependent decrease in vasoactive intestinal polypeptide in the rat suprachiasmatic nucleus. *Neuroscience letters,* 251**,** 21-24.

TAKAHASHI, J. S. 2017. Transcriptional architecture of the mammalian circadian clock. *Nature Reviews Genetics,* 18**,** 164-179.

TSO, C. F., SIMON, T., GREENLAW, A. C., PURI, T., MIEDA, M. & HERZOG, E. D. 2017. Astrocytes regulate daily rhythms in the suprachiasmatic nucleus and behavior. *Current Biology,* 27**,** 1055-1061.

TSUJI, T., TSUJI, C., LUDWIG, M. & LENG, G. 2016. The rat suprachiasmatic nucleus: the master clock ticks at 30 Hz. *The Journal of physiology,* 594**,** 3629-3650.

VITATERNA, M. H., SELBY, C. P., TODO, T., NIWA, H., THOMPSON, C., FRUECHTE, E. M., HITOMI, K., THRESHER, R. J., ISHIKAWA, T. & MIYAZAKI, J. 1999. Differential regulation of mammalian period genes and circadian rhythmicity by cryptochromes 1 and 2. *Proceedings of the National Academy of Sciences,* 96**,** 12114-12119.

WATERHOUSE, J., REILLY, T., ATKINSON, G. & EDWARDS, B. 2007. Jet lag: trends and coping strategies. *The Lancet,* 369**,** 1117-1129.

WEBER, E. T. & REA, M. A. 1997. Neuropeptide Y blocks light-induced phase advances but not delays of the circadian activity rhythm in hamsters. *Neuroscience letters,* 231**,** 159-162.

WEGRZYN, L. R., TAMIMI, R. M., ROSNER, B. A., BROWN, S. B., STEVENS, R. G., ELIASSEN, A. H., LADEN, F., WILLETT, W. C., HANKINSON, S. E. & SCHERNHAMMER, E. S. 2016. ROTATING NIGHT SHIFT WORK AND RISK OF BREAST CANCER IN THE NURSES'HEALTH STUDIES. *American journal of epidemiology*.

XIA, X., LESSMANN, V. & MARTIN, T. F. J. 2009. Imaging of evoked dense-core-vesicle exocytosis in hippocampal neurons reveals long latencies and kiss-and-run fusion events. *Journal of cell science,* 122**,** 75-82.

YAMAGUCHI, S., ISEJIMA, H., MATSUO, T., OKURA, R., YAGITA, K., KOBAYASHI, M. & OKAMURA, H. 2003. Synchronization of cellular clocks in the suprachiasmatic nucleus. *Science,* 302**,** 1408-12.

YAMAGUCHI, Y., SUZUKI, T., MIZORO, Y., KORI, H., OKADA, K., CHEN, Y., FUSTIN, J.-M. M., YAMAZAKI, F., MIZUGUCHI, N., ZHANG, J., DONG, X., TSUJIMOTO, G., OKUNO, Y., DOI, M. & OKAMURA, H. 2013. Mice Genetically Deficient in Vasopressin V1a and V1b Receptors Are Resistant to Jet Lag. *Science (New York, N.Y.),* 342**,** 85-90.

YANG, J., CAGAMPANG, F. R. A., NAKAYAMA, Y. & INOUYE, S.-I. T. 1993. Vasoactive intestinal polypeptide precursor mRNA exhibits diurnal variation in the rat suprachiasmatic nuclei. *Molecular brain research,* 20**,** 259-262.

YOO, S. H., YAMAZAKI, S., LOWREY, P. L., SHIMOMURA, K., KO, C. H., BUHR, E. D., SIEPKA, S. M., HONG, H. K., OH, W. J., YOO, O. J., MENAKER, M. & TAKAHASHI, J. S. 2004. PERIOD2::LUCIFERASE real-time reporting of circadian dynamics reveals persistent circadian oscillations in mouse peripheral tissues. *Proc Natl Acad Sci U S A,* 101**,** 5339-46.

ZHANG, R., LAHENS, N. F., BALLANCE, H. I., HUGHES, M. E. & HOGENESCH, J. B. 2014. A circadian gene expression atlas in mammals: implications for biology and medicine. *Proceedings of the National Academy of Sciences,* 111**,** 16219-16224.

Chapter 2.

VIP neurons of the SCN entrain circadian rhythms with distinct firing patterns

This chapter is adapted from the manuscript currently under review:

Mazuski, C., Abel J.H., Chen, S., Hermanstyne, T.O., Doyle III, F.J., & Herzog, E.D. VIP neurons of the SCN entrain circadian rhythms with distinct firing patterns

Abstract

The mammalian suprachiasmatic nucleus (SCN) functions as a master circadian pacemaker, integrating environmental input to align physiological and behavioral rhythms to local time cues. Approximately 10% of SCN neurons express vasoactive intestinal polypeptide (VIP); however, it is unknown if VIP neurons affect entrainment of rhythms through the modulation of firing activity and subsequent modulation of VIP release. To identify physiologically relevant firing patterns, we optically tagged VIP neurons and characterized spontaneous firing over three days. VIP neurons had circadian rhythms in firing rate and exhibited two classes of instantaneous firing activity. We next tested whether physiologically relevant firing affected circadian rhythms through VIP release. We found that VIP neuron stimulation with high, but not low, frequencies shifted gene expression rhythms *in vitro* through VIP signaling. *In vivo*, high frequency VIP neuron activation rapidly entrained circadian locomotor rhythms. Thus, VIP neurons communicate daily cues through firing activity and VIP release to entrain molecular and behavioral circadian rhythms.

Introduction

Circadian rhythms are a ubiquitous adaptation to the 24-h daily cycle on Earth. Found in organisms as disparate as *Arabidopsis*, *Drosophila*, *Synechococcus*, and humans, these daily oscillations occur at molecular, cellular and systems levels, ultimately entraining an organism to environmental cycles (Dunlap, 1999). Dysregulation in the circadian system, also known as chronodisruption, is associated with a variety of physiological maladies in humans including diabetes, cancer, insomnia, and affective disorders (Van Someren, 2000, Musiek et al., 2013, McClung, 2011). Understanding how cellular circadian oscillators integrate environmental signals, communicate with each other, and entrain to their environment is key to preventing and treating chronodisruption.

The suprachiasmatic nucleus (SCN) is a master circadian pacemaker, which detects local light input through retinal release of glutamate and PACAP (Eastman et al., 1984, Ding et al., 1997, Harrington et al., 1999, Hannibal et al., 2000). Located in the ventral hypothalamus, the approximately 20,000 GABAergic neurons comprising the SCN are unique in that many express self-sustained and spontaneously synchronizing circadian rhythms in firing activity and gene expression (Cassone et al., 1993, Reppert and Weaver, 2002, Welsh et al., 1995). These rhythms are maintained through a near-24 h transcription-translation feedback loop of core clock genes including *Bmal1*, *Clock*, *Period1 and 2 (Per1 and 2)*, and *Cryptochrome1 and 2* (Ko and Takahashi, 2006, Okamura et al., 2002). Recently, researchers have shown that electrical stimulation of all SCN neurons was sufficient to phase shift and entrain circadian rhythms in gene expression and behavior (Jones et al., 2015). However, it is poorly understood how firing activity and neurotransmission from specific cell types within the SCN contribute to entrainment.

Although uniformly GABAergic (Moore and Speh, 1993), SCN neurons vary significantly in their neuropeptide content (Abrahamson and Moore, 2001). One anatomically and functionally distinct class of neurons expresses vasoactive intestinal polypeptide (VIP). Though neurons expressing VIP only make up approximately 10% of SCN neurons (Abrahamson and Moore, 2001), VIP neuron projections densely innervate the SCN and the majority of SCN neurons express its receptor VPAC2 (An et al., 2012). Functionally, genetic loss of VIP or VPAC2R weakens synchrony among SCN neurons and dramatically reduces circadian rhythms in the SCN and in behavior (Aton et al., 2005, Maywood et al., 2006, Brown et al., 2007). Additionally, exogenous application of VIP increases GABAergic neurotransmission(Reed et al., 2002), induces clock gene expression(Nielsen et al., 2002), and phase shifts daily rhythms in the SCN and locomotor activity (An et al., 2011, Piggins et al., 1995). With the development of Cre-lox technology allowing cell-type specific manipulation of SCN neurons, researchers found that VIP neurons have sparse monosynaptic connections to approximately 50% of SCN neurons (Fan et al., 2015). However, to-date there have been no studies testing the functional role of VIP neurons in behavior.

Herein, we take a cell-to-systems approach to understand how firing of VIP neurons contributes to circadian entrainment. We used optical tagging to identify VIP SCN neurons and characterize their firing patterns across multiple days. Using physiologically relevant firing frequencies, we then tested the role of VIP neuron firing in phase shifting and entrainment *in vitro* and *in vivo* via optogenetic stimulation. We conclude that VIP neurons can use firing frequency to phase shift circadian gene expression and behavior, ultimately resulting in entrainment to the local schedule.

Results

Optical tagging of VIP SCN neurons on multielectrode arrays reveals daily rhythms in firing activity

To understand how VIP neurons integrate and communicate within the SCN, we first needed to identify and characterize the firing activity of VIP neurons. To do so, we optically tagged VIP SCN neurons within a high-density SCN culture plated on multielectrode arrays (MEAs).

Specifically, following multiday spontaneous activity recordings from SCN MEA neurons, we activated channelrhodpsin-2 (ChR2) expressed solely within VIP neurons (VIPCre crossed with floxed-ChR2) using blue light pulses (**Figure 1a**). To identify VIP neurons, we calculated the interspike interval histogram (ISIH) of each neuron that fired during the 1 h stimulation and found neurons whose firing matched the stimulation pattern (10.6 ± 1.7%, mean ± SEM, **Figure 1b**). To verify that VIP neurons selectively fired synchronously during the stimulation, we cross-correlated firing between each pair of active neurons. As predicted, we found that only VIP neurons increased firing synchronously in response to stimulation, while some non-VIP neurons decreased firing approximately 10-20 ms following stimulation, consistent with inhibitory neurotransmission from VIP SCN neurons (**Figure 1c**).

Based on our identification during stimulation, we classified the prior spontaneous activity firing as VIP or non-VIP (**Figure 2**). Overall, we discriminated multiday electrical activity from 40 VIP neurons and 543 non-VIP neurons across 8 MEA preparations. Although previous reports differ on whether VIP SCN neurons exhibit circadian firing rhythms(Hermanstyne et al., 2016,

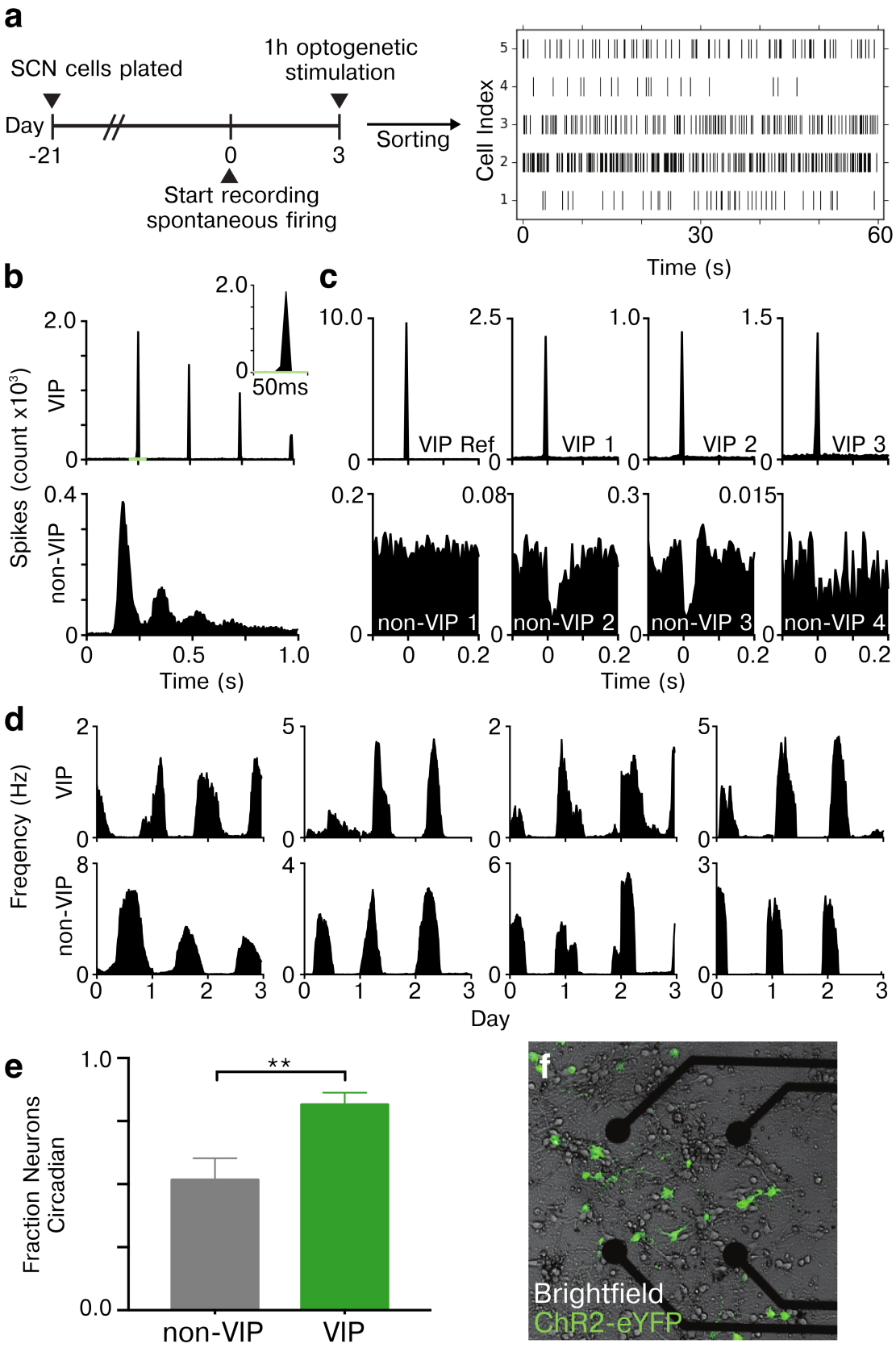
a
SCN cells plated
1h optogenetic stimulation
Day
-21
0
3
Start recording spontaneous firing
Sorting
Cell Index
Time (s)
b
c
Spikes (count x10³)
VIP
non-VIP
50ms
Time (s)
VIP Ref
VIP 1
VIP 2
VIP 3
non-VIP 1
non-VIP 2
non-VIP 3
non-VIP 4
d
Freqency (Hz)
Day
e
Fraction Neurons Circadian
**
non-VIP
VIP
f
Brightfield
ChR2-eYFP

Figure 1. Characterizing multiday spontaneous firing activity of identified VIP SCN neurons within a multielectrode array culture.

a) SCN neurons were categorized as VIP-positive (VIP) or –negative (non-VIP) by optically tagging VIP neurons using optogenetic stimulation after 3 days of spontaneous activity recording. Multiday firing was sorted from 563 SCN neurons identified on 8 multielectrode arrays plated and cultured for 3 weeks from VIPChR2 mice. Raster plots of five representative SCN neurons show how their spike times over one minute differed in mean rate and pattern. b) The inter-spike interval histograms during optogenetic stimulation illustrate how a representative VIP (top) neuron fired at the stimulation frequency (4 Hz) with a precision of <10ms (top right inset) and a non-VIP neuron (bottom) fired in a ChR2-independent pattern. c) To further characterize the evoked firing of VIP neurons, we cross-correlated spike times between concurrently recorded SCN neurons during optogenetic stimulation. A VIP reference neuron (top left panel) fired synchronously with 3 other representative VIP (top panels), but not 4 representative non-VIP neurons (bottom panels). Note that some non-VIP neurons (#2 and #3) decreased their firing following stimulation of VIP neurons, indicative of postsynaptic inhibition. d) Four representative VIP (top) and non-VIP (bottom panels) SCN neurons showing circadian firing patterns over the three days of recording. e) A greater fraction of VIP neurons were circadian (81.6 ±4.7%) compared to non-VIP neurons (51.7 ± 8.5%, Chi-squared test **$p < 0.00001$). f) eYFP fluorescence (green) reveals the subset of SCN neurons expressing ChR2 near four of the 60 electrodes.

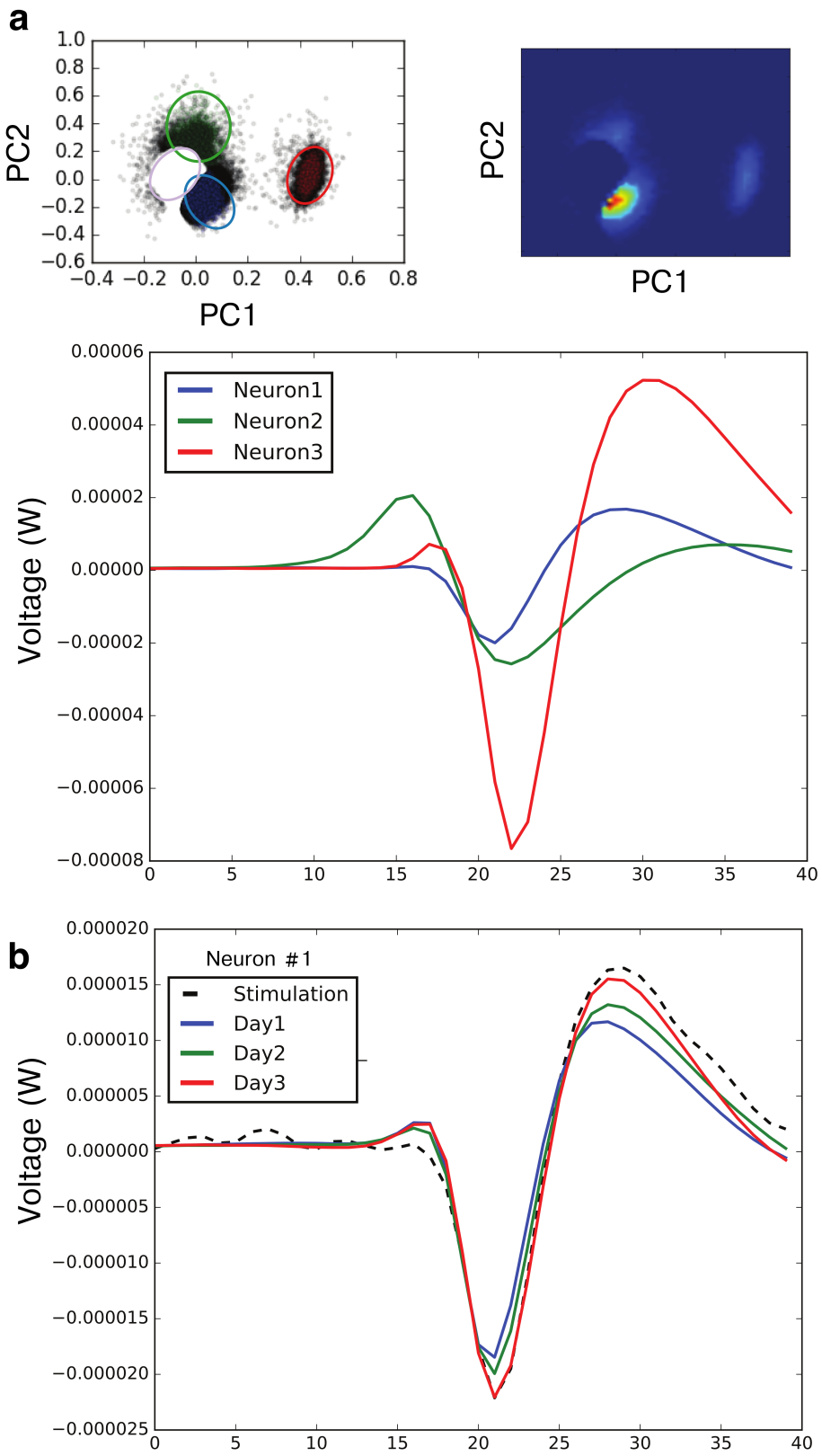
a
PC2
PC1
PC2
PC1
Neuron1
Neuron2
Neuron3
Voltage (W)
b
Neuron #1
Stimulation
Day1
Day2
Day3
Voltage (W)

Figure 2. Spontaneous electrical firing from individual neurons can be reliably tracked across multiple days (supplemental information)

We used a recursively applied PCA with Gaussian mixture model (GMM) clustering to discriminate firing from single SCN neurons across multiple days on multielectrode arrays before and during optogenetic stimulation. The automated analysis was performed blinded to the identity of the neuron (VIP or non-VIP). a) On this representative electrode, we identified 3 clusters (circled in top panel) and their corresponding average extracellular waveforms (bottom panel). b) Neuron1 from the above analysis was identified as VIP-positive. The spike waveform during optogenetic stimulation (dashed line) correlated with the mean spontaneous activity waveforms recorded over the prior three days from the same electrode.

Fan et al., 2015), we found that VIP neurons were more likely to exhibit circadian rhythms in firing than non-VIP neurons (81.5 ± 4.0% compared to 51.7 ± 8.5%, **Figure 1d-e**).

Since our experimental design relied on direct ChR2-induced increases in firing within VIP neurons, we tested these assumptions. As utilized and quantified by previous researchers (Hermanstyne et al., 2016, Fan et al., 2015, Brancaccio et al., 2013), Cre-lox recombination selectively drives transgene expression within VIP neurons. Additionally, we verified that only ChR2-positive SCN neurons fired precisely in response to light pulses using whole-cell patch clamp recordings (**Figure 3**). Finally, within our MEA preparation we validated that VIP neurons responded to light pulses within 5 ms (**Figure 4**). In conclusion, optical tagging reliably identified the multiday firing activity of VIP SCN neurons.

VIP neurons fire with either tonic or irregular patterns

Previous studies have described three classes of firing patterns in the SCN (tonic, irregular, and bursting) (Pennartz et al., 1998), however it is poorly understood whether these firing patterns vary with neuropeptide cell type, time of day, or across multiple days. To address this, we analyzed spike timing and frequency to characterize instantaneous firing patterns of circadian SCN neurons that could be tracked for multiple days (33 VIP and 268 non-VIP).

Based on the ISIH of spontaneous activity, we also observed three distinct classes of firing patterns within SCN neurons: tonic, irregular, and bursting (**Figure 5a-b**). Strikingly, individual SCN neurons did not change their firing pattern (tonic, irregular, or bursting) with time of day, or across multiple days, including during periods of rapidly increasing or decreasing firing activity

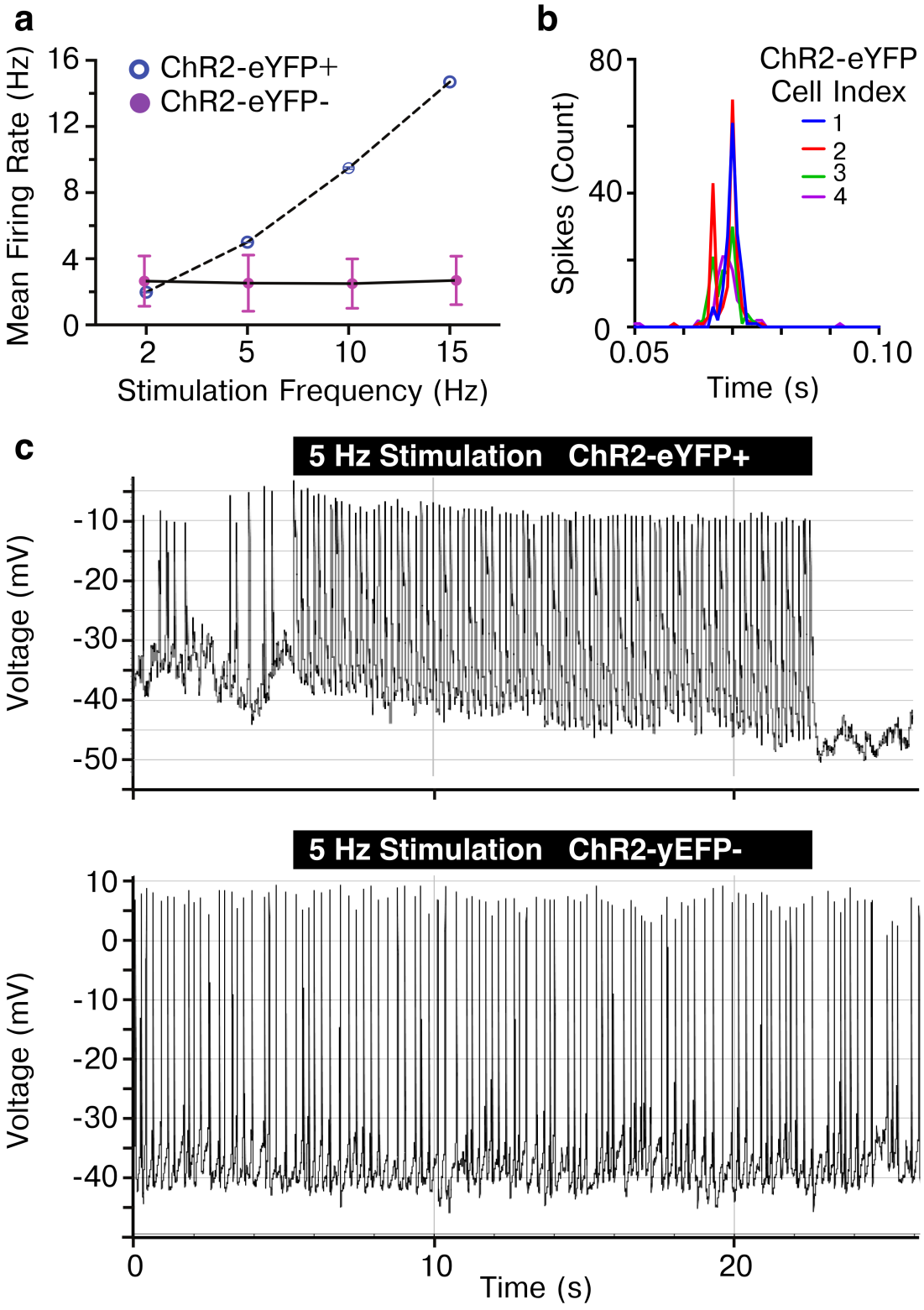
a
Mean Firing Rate (Hz)
16
12
8
4
0
ChR2-eYFP+
ChR2-eYFP-
2
5
10
15
Stimulation Frequency (Hz)
b
Spikes (Count)
80
40
0
ChR2-eYFP
Cell Index
1
2
3
4
0.05
0.10
Time (s)
c
5 Hz Stimulation ChR2-eYFP+
Voltage (mV)
-10
-20
-30
-40
-50
5 Hz Stimulation ChR2-yEFP-
Voltage (mV)
10
0
-10
-20
-30
-40
0
10
20
Time (s)

Figure 3. Only ChR2 positive SCN neurons increase firing in response to optogenetic stimulation (supplemental information)

a) Using whole-cell patch clamp, we recorded from neurons within VIPChR2 SCN slices while stimulating at 2, 5, 10, or 15 Hz. ChR2-eYFP positive neurons (n = 5) matched their firing to the stimulation frequency, while ChR2-eYFP negative neurons (n = 5) in the same SCN slice did not. b) ChR2-eYFP positive neurons followed the stimulation frequency within 10ms as revealed by the interspike interval histogram (15 Hz stimulation, n = 4 neurons). c) Representative traces show a ChR2-eYFP positive neuron that increased its firing rate in response to 5 Hz stimulation, while ChR2-eYFP negative firing did not change. These results indicate that the presence of ChR2 is necessary for light-evoked increases in firing.

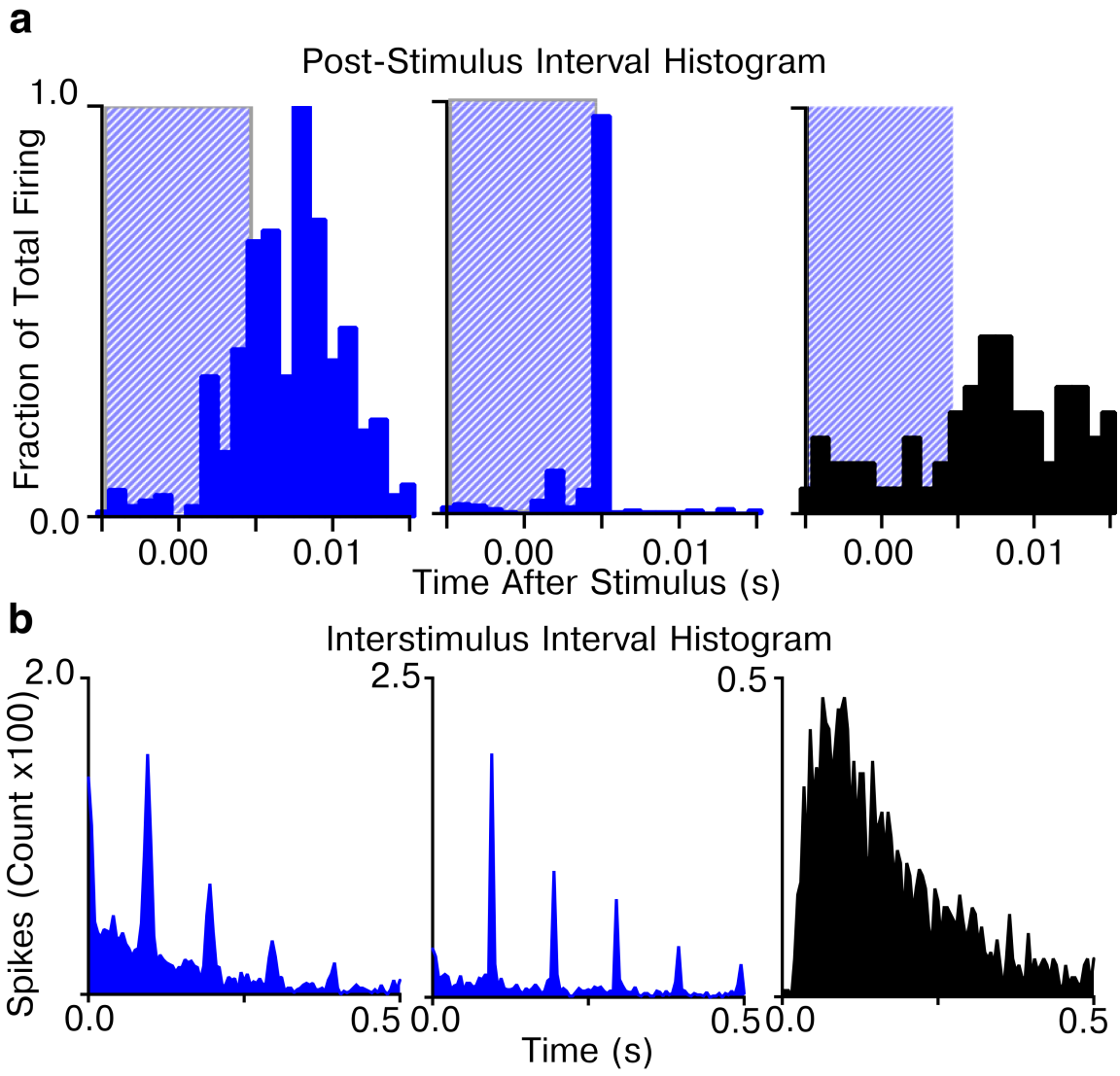
a
Post-Stimulus Interval Histogram
1.0
0.0
Fraction of Total Firing
0.00
0.01
0.00
0.01
0.00
0.01
Time After Stimulus (s)
b
Interstimulus Interval Histogram
2.0
2.5
0.5
Spikes (Count x100)
0.0
0.5
0.0
0.5
0.0
0.5
Time (s)

Figure 4. VIPChR2 neurons fire within 10ms of stimulation (Supplemental information)

a) The post-stimulus histogram (PSTH) of SCN neuronal firing following a 10ms laser flash (blue box) showed that 100% of neurons identified as VIPergic (blue) fired reliably within 10ms of the stimulation, while non-VIP neurons (black) did not respond to the flashes. b) Corresponding ISIH for two VIP (blue) and one non-VIP (black) neurons during 10Hz stimulation. The VIP neuron fired at 0.1s intervals whereas the non-VIP neuron (black) did not. Thus, the ISIH or the PSTH accurately identified VIP neurons on multielectrode arrays.

(**Figure 5c**). We used unbiased, hierarchical clustering based on the ISIH and the dominant instantaneous firing rate (DIFR, the peak of the ISIH) to cluster VIP and non-VIP neurons into classes of firing pattern (**Figure 5d**). This method revealed two clusters of VIP neurons (tonic and irregular) and three clusters of non-VIP neurons (tonic, irregular, and bursting). On average, the DIFR trended higher in tonic neurons than irregular neurons and did not differ between VIP and non-VIP neurons (**Figure 5e**). In contrast, non-VIP bursting neurons fired in doublets or triplets of spikes with a DIFR above 100Hz.

Separately, we used the same hierarchical clustering method to characterize VIP SCN neurons from intracellular daytime adult SCN slice recordings. The firing recorded from these VIP neurons also reliably clustered into tonic or irregular firing classes (**Figure 6**). Taken together, these data indicate that SCN neurons have distinct electrophysiological profiles that are stable across the circadian day, and consistent from day to day. We conclude that, despite representing only 10% of SCN neurons, VIP neurons are an electrophysiologically heterogeneous group, exhibiting either tonic or irregular firing, that predominantly fire around 5-10Hz (**Figure 5e-f**).

High frequency firing of VIP neurons phase shifts circadian gene expression rhythms *in vitro*

To test if VIP firing influences circadian entrainment, we stimulated VIP neurons with two firing frequencies. Based on our characterization of VIP neurons, we picked two stimulation paradigms that represent the high and low frequency ranges of VIP neurons: high instantaneous frequency (HIF, doublets of 20 Hz at 2 Hz) and low instantaneous frequency (LIF, 4 Hz pulses evenly spaced). These stimulation patterns had the same number of spikes per second (4 Hz), but

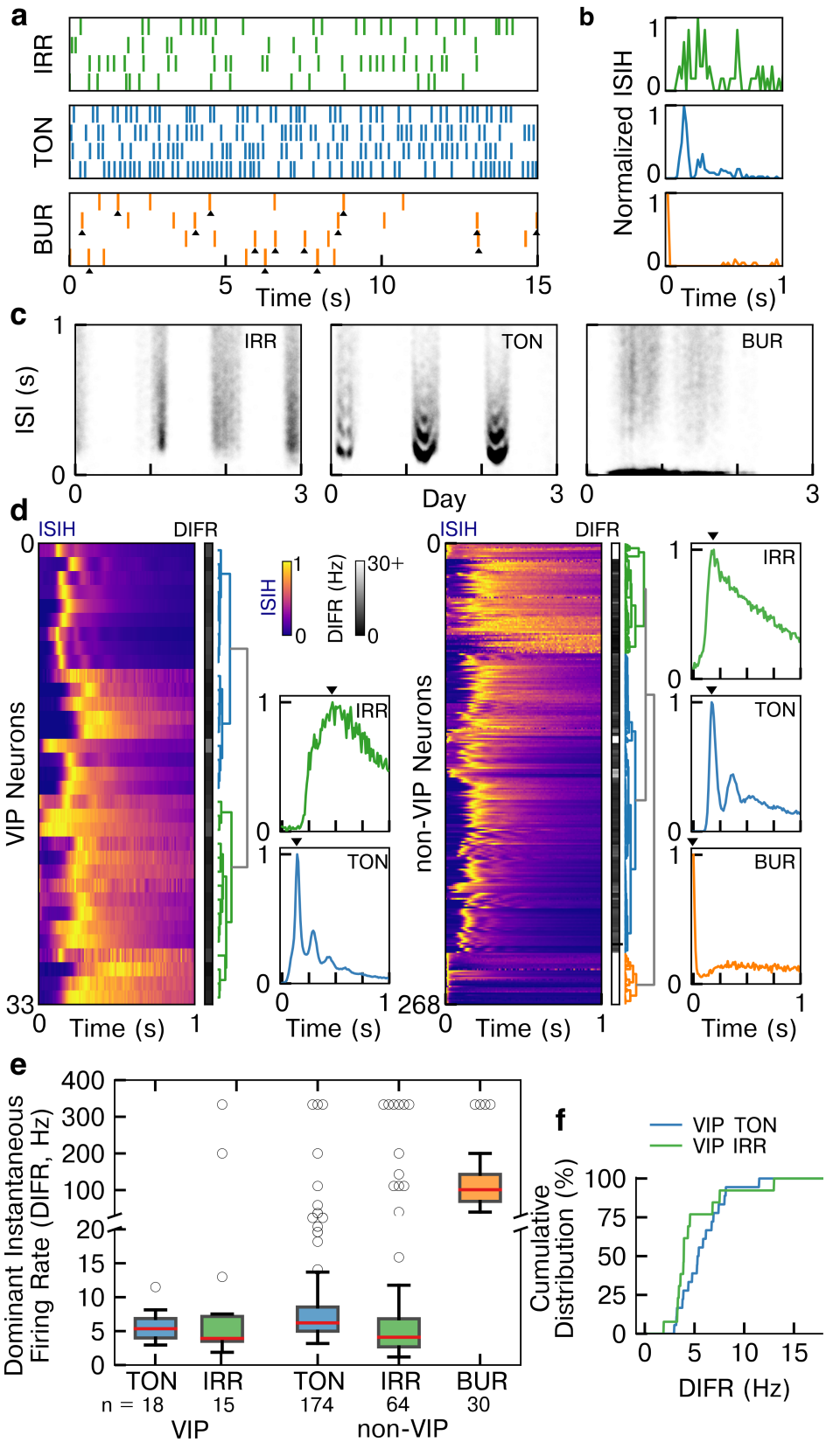
a
IRR
TON
BUR
0
5
10
15
Time (s)
b
Normalized ISIH
1
0
Time (s)
c
ISI (s)
IRR
TON
BUR
Day
d
ISIH
DIFR
VIP Neurons
non-VIP Neurons
DIFR (Hz)
30+
33
268
e
Dominant Instantaneous Firing Rate (DIFR, Hz)
400
300
200
100
20
15
10
5
TON
IRR
BUR
n = 18
15
174
64
30
VIP
non-VIP
f
VIP TON
VIP IRR
Cumulative Distribution (%)
100
75
50
25
DIFR (Hz)

Figure 5. Hierarchical clustering reveals two classes of VIP SCN neurons based on their daily firing patterns.

SCN neurons exhibited one of three different daytime firing patterns: Tonic (TON), irregular (IRR) or bursting (BUR). a) Raster plots show the spike times over a minute from a representative neuron in each class. Black arrows indicate when the bursting neuron fired multiple tightly spaced doublets or triplets. b) The interspike interval histograms (ISIH) corresponding to the neurons in a. Note that the TON neuron had precise spike timing with a sharp peak in the ISIH, while the IRR neuron exhibited imprecise timing between spikes and the BUR neuron had a precise short-interval component occurring at imprecise long intervals. c) Short-term firing patterns were stable across multiple days shown by three representative SCN neurons. Note that the daily appearance of multiple bands during tonic firing corresponds to harmonics resulting from skipped spikes. c) Unbiased hierarchical clustering of each neuron's ISIH and dominant instantaneous firing rate (DIFR) identified three classes of non-VIP, and two classes of VIP neurons (blue = tonic, green = irregular, orange = bursting). Insets show a representative normalized ISIH for each firing class. The DIFR (black arrows) measures the dominant frequency of firing, not the maximum or average firing frequency. d) Quantification of the DIFR from each class (n = the number of neurons recorded within each class; median interquartile range in Hz, TON VIP 5.3 ± 2.8, IRR VIP 3.9 ± 3.7, TON Non-VIP 6.2 ± 3.6, IRR Non-VIP 4.1 ± 4.1, BUR Non-VIP 101.0 ± 73.6). e) The cumulative frequency distribution shows that both TON and IRR VIP neurons had similar DIFR with nearly all firing between 5-10 Hz.

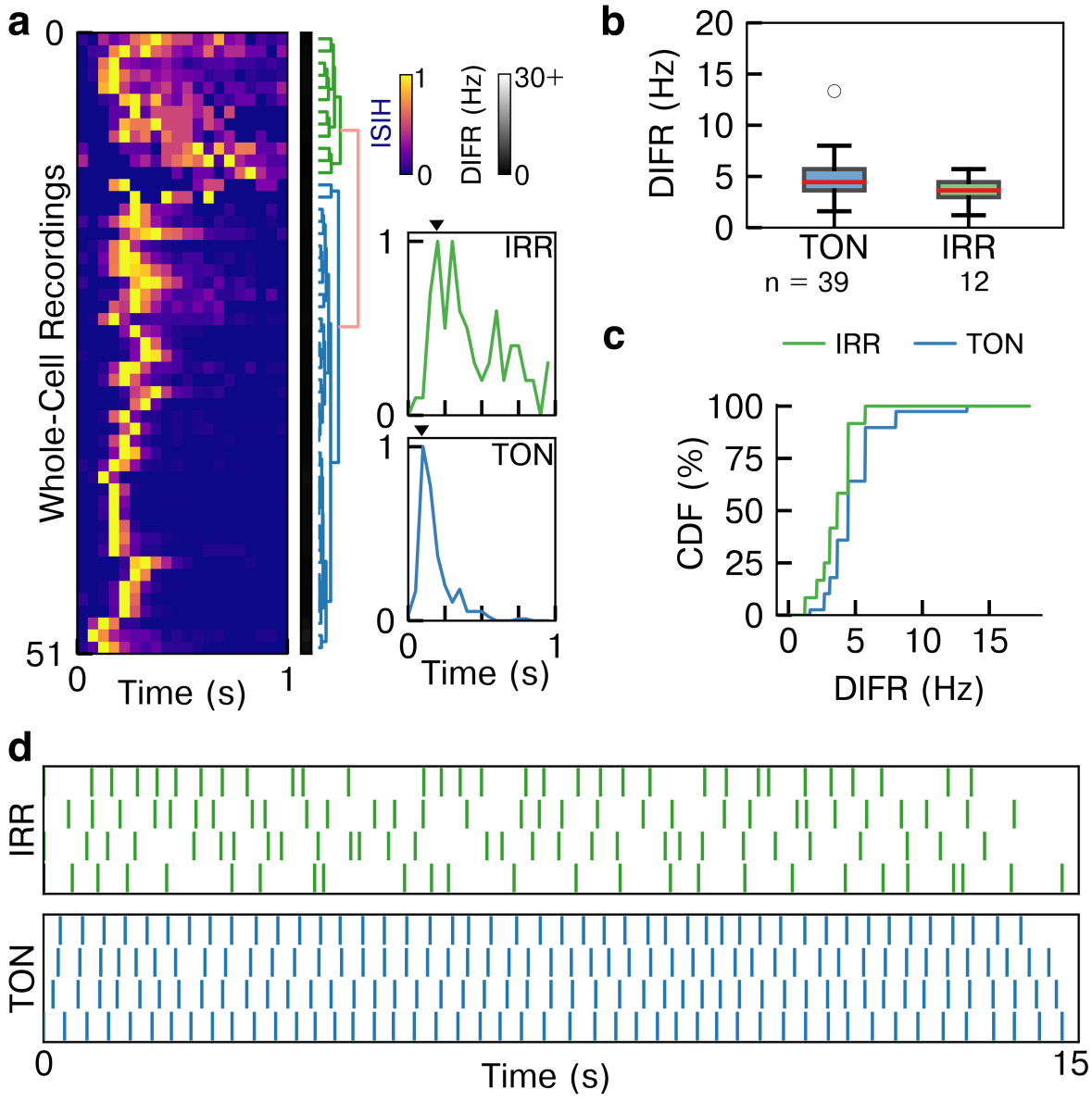
a
0
51
Whole-Cell Recordings
0
Time (s)
1
ISIH
1
0
DIFR (Hz)
30+
0
1
IRR
0
1
TON
0
0
1
Time (s)
b
DIFR (Hz)
20
15
10
5
0
TON
IRR
n = 39
12
c
IRR
TON
CDF (%)
100
75
50
25
0
0
5
10
15
DIFR (Hz)
d
IRR
TON
0
Time (s)
15

Figure 6. VIP neurons within an intact SCN slice fire in either tonic or irregular patterns (Supplemental Information)

a) Unbiased hierarchical clustering revealed tonic and irregular VIP in 60s whole-cell patch clamp recordings during daytime (right panel). b) Dominant instantaneous firing rate was calculated for each neuron from the ISIH peak, and a boxplot of dominant frequency is shown for each neuron class (tonic/irregular). Observed DIFR fell predominantly between 2 Hz and 10 Hz (tonic VIP 4.5 (1.4) Hz; irregular VIP 2.8 (1.4) Hz; all values median (interquartile range)). c) Cumulative frequency distribution plot shows the percentage of VIP neurons that fire at specific frequencies. d) 60s raster plots of 2 representative neurons show the differences in spike timing.

differed in spike timing. Both HIF and LIF evoked firing in VIP neurons on MEAs, which reliably followed the stimulation frequency (**Figure 7**). During the 1 h of stimulation we observed no evidence of depolarization block or habituation in stimulated VIP neurons.

We stimulated VIP neurons within intact SCN slices with HIF and LIF frequencies and found that only HIF frequencies shifted circadian gene expression. Briefly, we cultured SCN explants expressing ChR2 in VIP neurons and *Period2::Luciferase* (*PER2::LUC,* a knock-in fusion that reports PER2 protein abundance) or littermate controls lacking ChR2 expression. Following baseline bioluminescence recording of PER2 levels from the entire SCN, we stimulated all SCN for 1 h near the peak of PER2 expression (Circadian time, CT 9-12) with HIF or LIF patterns. We chose to stimulate at this time because it has been reported as the time when exogenous VIP application evoked large delays in PER2 rhythms (An et al., 2011). HIF stimulation significantly delayed the daily rhythms of SCN PER2 expression by over 1.5 h, whereas LIF stimulation did not (**Figure 8**). Additionally, three consecutive days of stimulation yielded similar results (**Figure 9**). Thus, firing of VIP neurons can phase delay circadian gene expression but only if stimulated at sufficiently high frequencies.

To test whether the resulting phase delay was mediated by increases in VIP signaling, we stimulated SCN PER2 explants expressing ChR2 in VIP neurons with HIF frequencies in the presence of 10 um VPAC2R antagonist or vehicle control. We found that the presence of the antagonist reduced the resulting phase shift (**Figure 8c**). Thus, our data suggests that HIF firing of VIP neurons releases VIP, which phase delays circadian gene expression.

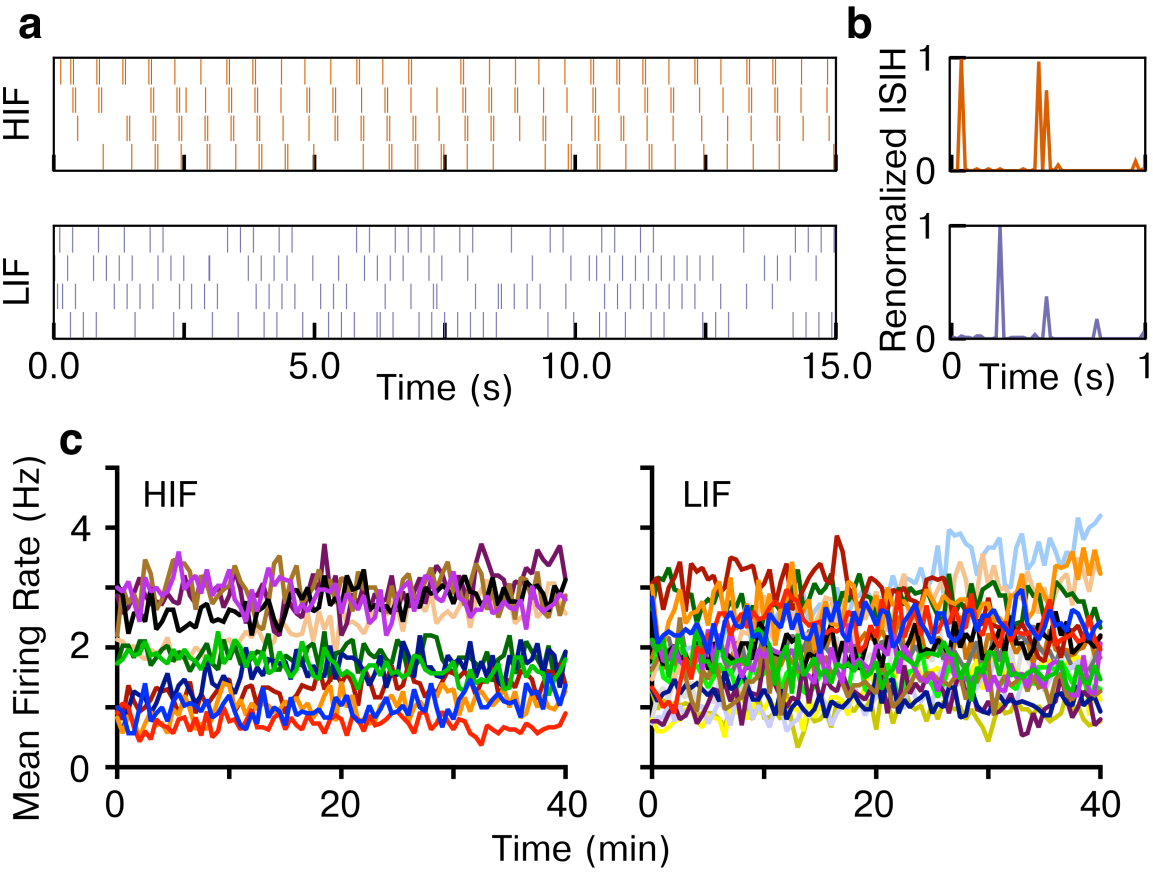
a
HIF
LIF
0.0
5.0
10.0
15.0
Time (s)
b
Renormalized ISIH
1
0
1
0
0
Time (s)
1
c
Mean Firing Rate (Hz)
HIF
LIF
4
2
0
0
20
40
0
20
40
Time (min)

Figure 7. VIPChR2 neurons fire reliably in response to 40 min of HIF or LIF stimulation

To test whether VIP neurons reliably fire at HIF and LIF frequencies, we stimulated VIPChR2 MEA cultures for 40 min with either frequency. a) 60s raster plots of two representative VIP neurons firing at HIF and LIF frequencies. The MEA recordings occasionally miss spikes (due largely to the proximity of a neuron to the electrode) but the pattern of spike timing is consistent with the stimulation b) as illustrated by the ISIH. c) VIP firing binned at 30s showed no change over a 40-min period with either HIF or LIF indicating that individual neurons show no evidence of habituation or depolarization block in response to HIF or LIF stimuli.

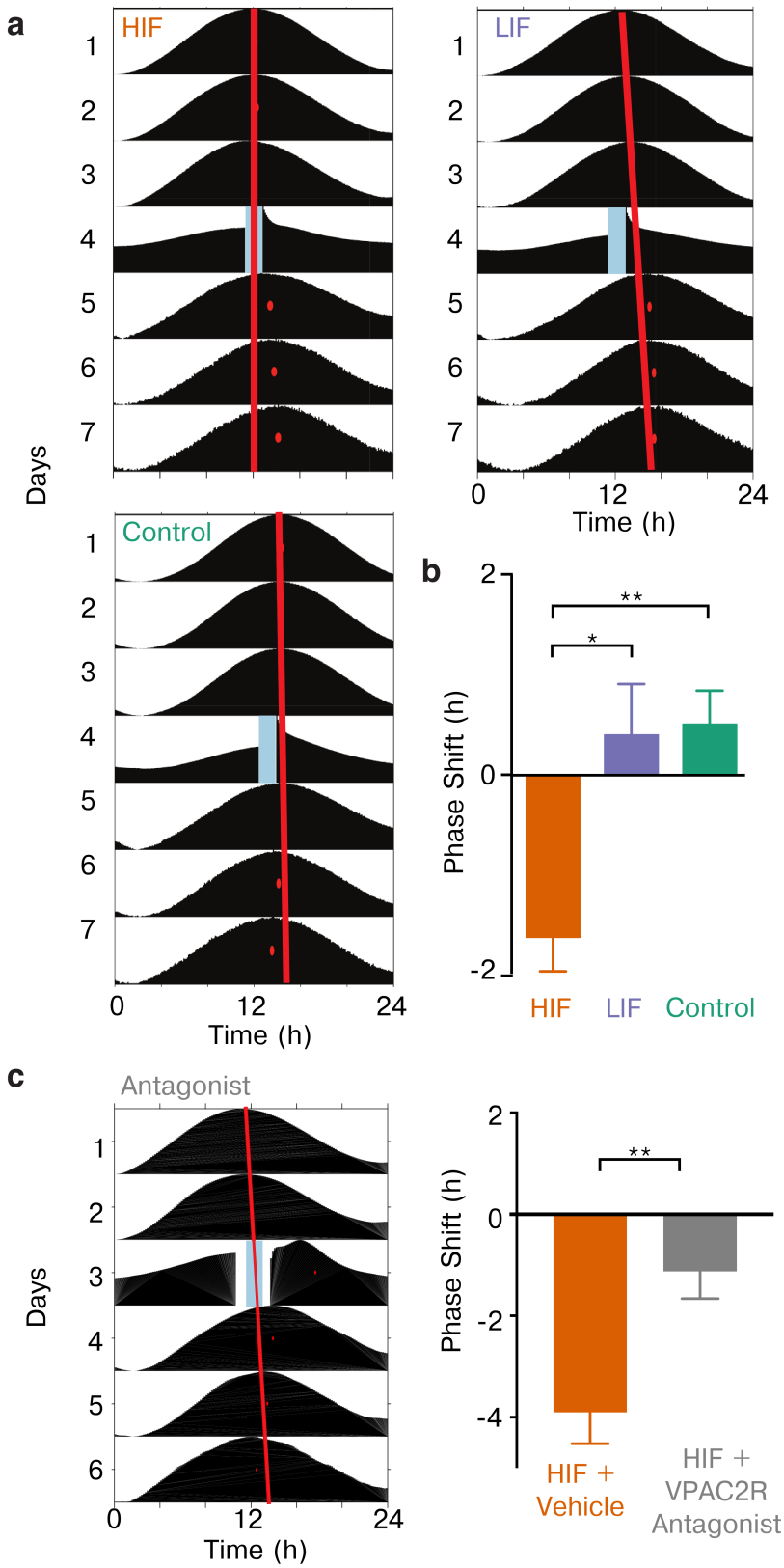
a
HIF
LIF
Control
Days
1
2
3
4
5
6
7
0
12
24
Time (h)
b
Phase Shift (h)
2
0
-2
*
**
HIF
LIF
Control
c
Antagonist
Phase Shift (h)
2
0
-2
-4
**
HIF + Vehicle
HIF + VPAC2R Antagonist

Figure 8. Optogenetic Stimulation of VIP SCN neurons phase delays circadian rhythms in PER2 expression.

a) Representative PER2::LUC actograms from three SCN slices. In the top two traces, ChR2 expressed in VIP neurons was activated for 1 h (blue bar) on the fourth day of recording with high (HIF) or low (LIF) frequencies. Control SCN received either HIF or LIF stimulation, but lacked ChR2. Note the large delay in the time of the daily PER2 (red dots) on the days after HIF stimulation relative to the extrapolated unperturbed phase (red line). b) HIF stably delayed PER2 rhythms compared to either LIF or control conditions (-1.6 ± 0.3 h, HIF, 0.4 ± 0.5, LIF, 0.5 ± 0.3, control; *$p < 0.05$ and **$p < 0.01$, one-way ANOVA with Tukey's posthoc test, n= 9, 10 and 32 SCN slices, respectively). c) VPAC2 antagonist treatment during HIF stimulation reliably reduces the resulting phase shift, shown by a representative actogram (left) and the group summary. (-3.902 0.6178, HIF + Vehicle, -1.124 0.5381, HIF + VPAC2R Antagonist; **$p < 0.01$, unpaired t-test, n = 7, 7 SCN slices, respectively).

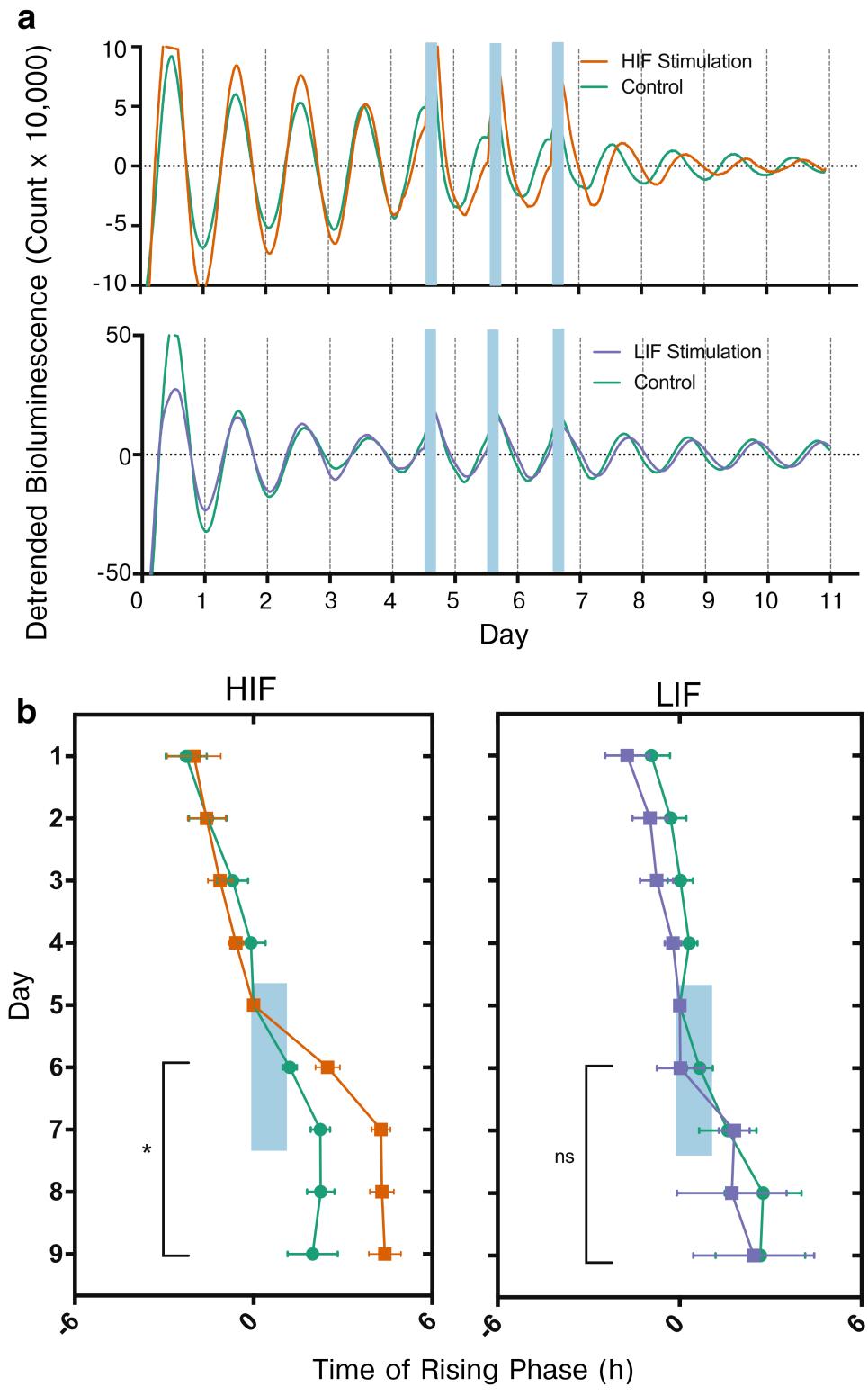
a
Detrended Bioluminescence (Count x 10,000)
HIF Stimulation
Control
LIF Stimulation
Control
Day
b
HIF
LIF
Day
*
ns
Time of Rising Phase (h)

Figure 9. HIF but not LIF stimulation of VIP neurons shifts clock gene rhythms in SCN slices. (Supplemental Information)

a) Representative bioluminescence traces show that daily HIF stimulation (blue bars) phase delayed PER2 circadian rhythms compared to control SCN explants, while LIF stimulation did not. B) Using the rising phase as a reliable phase marker, we found that HIF stimulation sufficed to change the phase of PER2 expression compared to controls (n = 8, VIPChR2 and 7, control, Watson-Williams test for days 6 – 9, *$p < 0.05$). LIF stimulation failed to phase shift PER2 gene expression (n = 5 VIPChR2 SCN and n = 10 control SCN, Watson-Williams test for days 6-9, $p = 0.5$)

Activation of VIP neurons induces cFOS expression throughout the SCN *in vivo*

Although VIP neuronal cell bodies localize to the ventral SCN, VPAC2 receptor is expressed in nearly all SCN neurons (An et al., 2012). Consistent with these anatomical data, we found that activation of VIP neurons *in vivo* increases cFOS protein throughout the SCN. Briefly, freely moving mice expressing ChR2 in VIP neurons (VIPChR2) and littermate controls received blue laser light via an implanted fiber optic cannula aimed at the SCN. After 1 h of 15Hz stimulation at CT 13, 88.9 ± 4.0% (mean ± SEM, n = 4 mice; **Figure 10a**) of VIP neurons expressed cFOS, a marker of neuronal activation. Furthermore, cFOS expression increased roughly 5-fold in the ventral SCN and almost 4-fold in the dorsal SCN (**Figure 10b**) compared to controls. We conclude that high frequency *in vivo* stimulation of VIP neurons increases activity both within VIP neurons and throughout the SCN.

Activation of VIP neurons entrains locomotor activity *in vivo*

Next, we found that firing of VIP neurons underlies their role in circadian entrainment. Briefly, we monitored wheel-running activity before, during and after stimulation of SCN VIP neurons *in vivo* from mice enucleated to remove ambient light input and implanted with a fiber optic cannula. Before stimulation, all mice showed free-running circadian rhythms in locomotion (in hours, 23.4 ± 0.1, VIPChR2, 23.4 ± 0.2, Control, mean ± SEM, n = 7, 4). Mice then received daily HIF stimulation for 1 h for up to 30 days and only VIPChR2 mice entrained to the stimulation (**Figure 11a**). We calculated a phase response curve (**Figure 11b**) and found that surprisingly, only stimulation of VIP neurons between CT 10 – 18 lead to phase shifts and entrainment. Additionally, we observed that stimulation of VIP neurons acutely suppressed wheel running (**Figure 11c**) similar to light-induced masking.

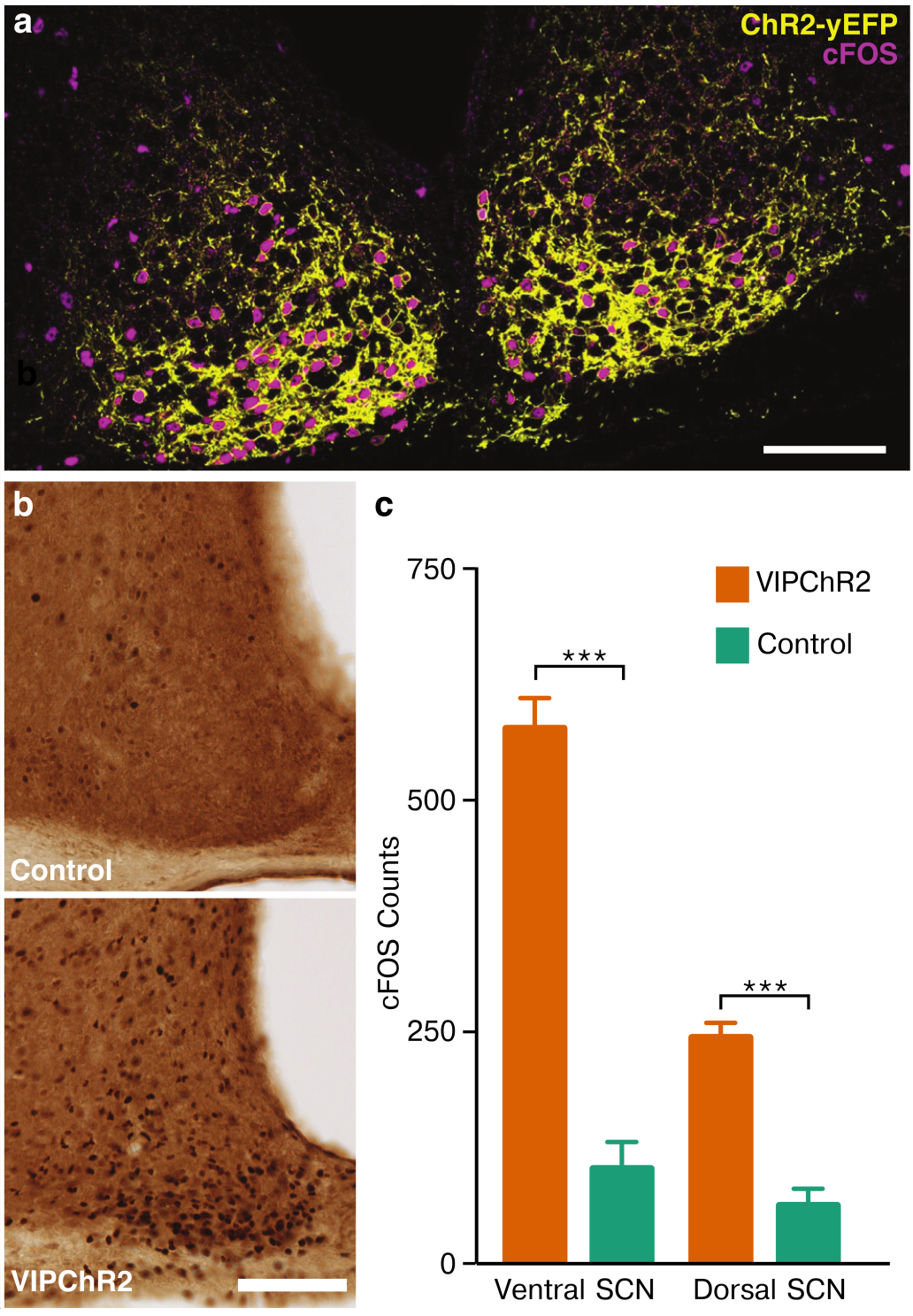
a
ChR2-yEFP
cFOS
b
b
Control
VIPChR2
c
750
500
250
0
cFOS Counts
VIPChR2
Control
***
***
Ventral SCN
Dorsal SCN

Figure 10. Activation of SCN VIP neurons *in vivo* induces cFOS expression throughout the SCN.

a) Representative image of the bilateral SCN showing cFOS induction (magenta) within VIPChR2 neurons (yellow) after 1 h of 15 Hz stimulation *in vivo* at CT13 (scale bar = 100um). b) The number of SCN cells expressing cFOS protein was higher in VIPChR2 (bottom) than control (top panel) mice after 1 h of 15 Hz stimulation at CT13. *In vivo* optogenetic stimulation of VIP neurons increased cFOS expression throughout the SCN (577.8 ± 33.0, Ventral SCN VIPChR2, 103.0 ± 56.9, Ventral SCN Control, 244.5 ± 15.6 Dorsal SCN VIPChR2, 63.0 ± 17.9 Dorsal SCN Control; unpaired Student's t-test ***$p<0.001$, n= 4 mice).

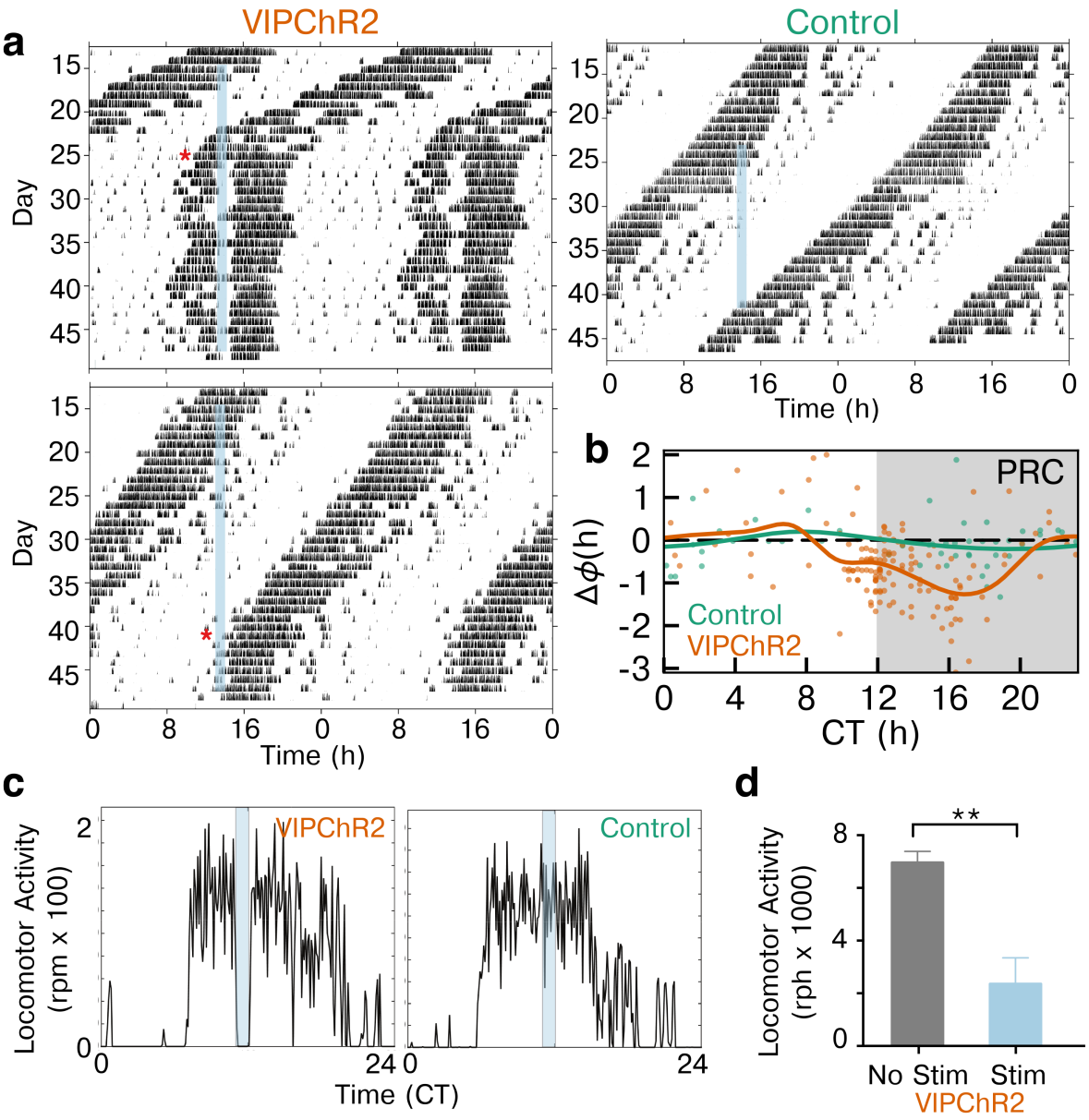
a
VIPChR2
Control
Day
Time (h)
b
PRC
Δφ(h)
Control
VIPChR2
CT (h)
c
VIPChR2
Control
Locomotor Activity
(rpm x 100)
Time (CT)
d
Locomotor Activity
(rph x 1000)
**
No Stim
Stim
VIPChR2

Figure 11. Stimulation of VIP neurons in vivo entrains locomotor activity.

a) Daily locomotor activity of two representative mice entrained to HIF stimulation of SCN VIP neurons (blue bar) compared to a control mouse lacking ChR2. Actograms show wheel revolutions per 6 min (black bars) recorded from enucleated mice for almost 50 days. Note that the two VIPChR2 mice, with slightly different periods, reached stable entrainment (*) only when the stimulation occurred around early subjective night. b) Average phase response curves following stimulation of VIPChR2 (orange, n = 7) and control mice (green, n = 4) show the change in phase (dots) on the day after stimulation at different circadian times. Note that activation of VIP neurons entrained daily locomotor rhythms through phase delays when delivered during the late subjective day and early subjective night. c) Representative activity profiles of 2 mice show that HIF stimulation of VIP neurons acutely reduced running wheel activity in VIPChR2 (left), but not control (right), mice. d) Wheel revolutions during optogenetic stimulation (CT 12-18, 1 h of HIF) decreased nearly four-fold compared to baseline in VIPChR2 mice (2355.0 ± 981.1 during stimulation vs. 6958.0 ± 418.9 with no stimulation, n = 6 mice, paired Student's t-test **$p < 0.01$).

Finally, we found that firing frequency plays a role in VIP-mediated entrainment *in vivo*. Mice were randomly assigned to receive either 1h of daily HIF or LIF stimulation for 4-10 days between CT 10-15. Then, following at least 4 days of free-running activity, the mice received the other (LIF or HIF, respectively) stimulation for 4-10 days at the same time of day (**Figure 12a**). Overall, we found that either stimulation frequency entrained locomotor activity (**Figure 12c**), however HIF stimulation entrained more rapidly (**Figure 12b**). We conclude that firing of VIP neurons results in circadian entrainment and the frequency of firing determines the speed of entrainment.

Discussion

We consistently identified VIP SCN neurons that fired with either tonic or irregular patterns in extracellular and intracellular, slice and long-term multielectrode recordings, suggesting that spike timing characterizes functional classes of SCN neurons. These may correlate with the two populations of SCN VIP neurons that appear during development (Ban et al., 1997). We hypothesize that these firing patterns relate to different functional roles of SCN VIP neurons as previously suggested (Kawamoto et al., 2003). For example, these spontaneous firing patterns may identify VIP neurons that transduce direct vs. indirect retinal input (Fernandez et al., 2016) or that project primarily within the SCN to maintain synchrony among SCN neurons (Abrahamson and Moore, 2001) vs. outside the SCN to targets including the paraventricular nucleus of the hypothalamus and paraventricular nucleus of the thalamus (Abrahamson et al., 2001) to regulate daily rhythms in hormone release. Similar anatomical subgroups of brainstem serotonergic neurons have been associated, for example, with regulating distinct behaviors including respiration and aggression through distinct brain target

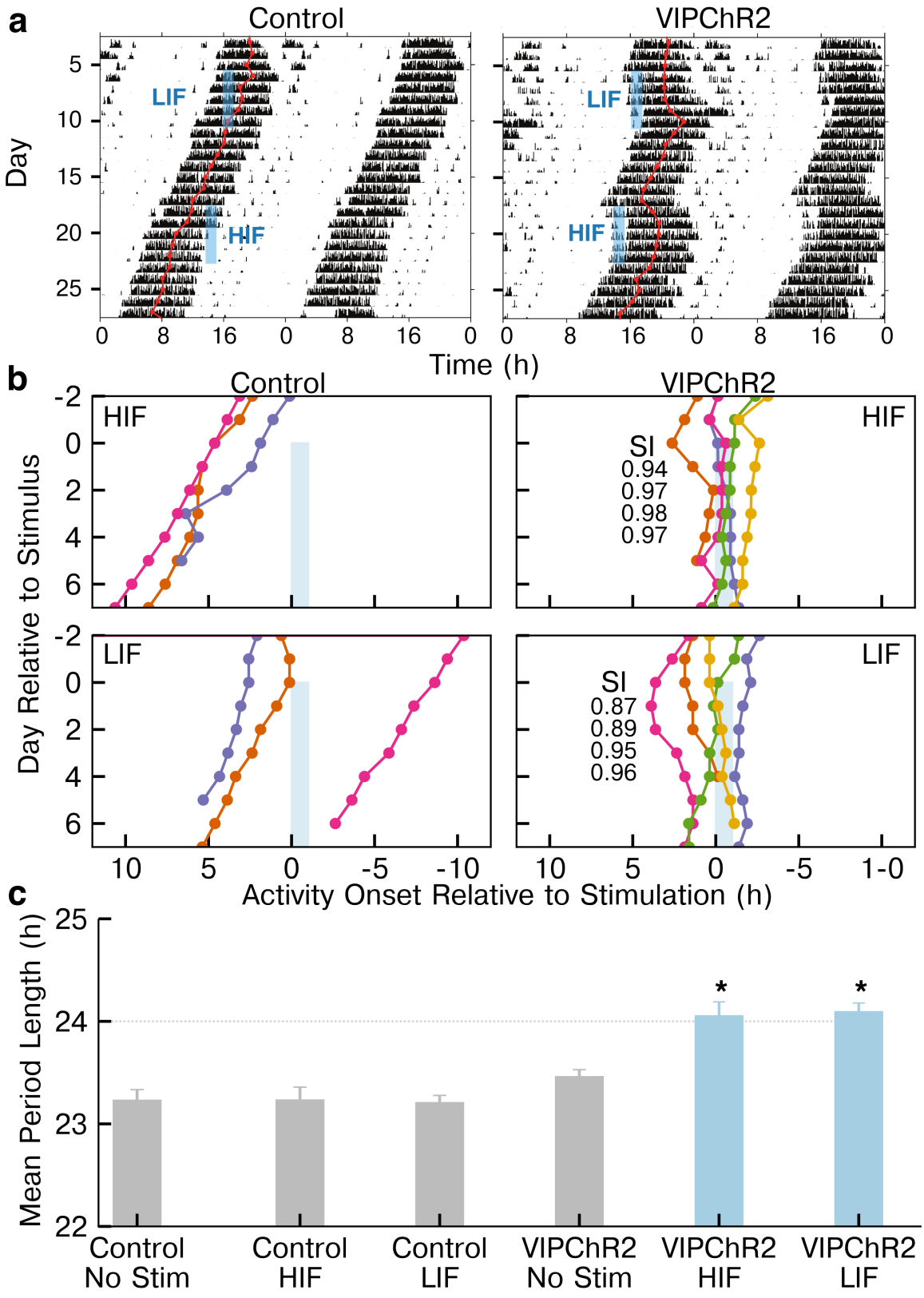
a
Control
VIPChR2
LIF
HIF
Day
Time (h)
b
Control
VIPChR2
HIF
LIF
SI
0.94
0.97
0.98
0.97
SI
0.87
0.89
0.95
0.96
Day Relative to Stimulus
Activity Onset Relative to Stimulation (h)
c
Mean Period Length (h)
Control No Stim
Control HIF
Control LIF
VIPChR2 No Stim
VIPChR2 HIF
VIPChR2 LIF

Figure 12: Instantaneous firing pattern affects locomotor rhythm entrainment.

a) Representative actograms show how daily optogenetic stimulation with HIF or LIF (blue bar) differentially entrained VIPChR2, but not control, mice. The daily acrophase (red circles and lines) of control mice in constant darkness free-ran through the days of stimulation. In contrast, daily HIF stimulation produced a large delay and rapidly entrained locomotor rhythms. Daily LIF stimulation, while having smaller effects on phase, also entrained. b) Daily stimulation entrained daily activity onsets to within 2 h of the stimulation in both HIF and LIF but not in control mice. Each color represents an individual mouse. HIF stimulation immediately resulted in tight clustering, as shown by the higher synchrony index (SI), while LIF stimulation gradually entrained to the stimulation, as seen by the gradually increasing SI. c) Daily HIF or LIF stimulation synchronized locomotor rhythms to 24 h in VIPChR2, but not control, mice (one-way ANOVA with posthoc Tukey HSD *$p < 0.05$). Note that VIPChR2 mice displayed a period identical to controls while stimulation was off.

areas (Niederkofler et al., 2016). Future studies should elucidate whether the physiological classes of VIP neurons map to specific anatomical groups within the SCN and targets outside the SCN.

VIP SCN neurons change firing frequency with time of day, and high and low frequency firing of VIP SCN neurons differentially affects circadian entrainment, suggesting that VIP neurons can modulate entrainment by increasing their firing frequency. In the unperturbed circadian system, this would occur during mid to peak firing activity of VIP neurons. We hypothesize that the firing frequency of VIP neurons may contribute to phase shifting and entrainment to new light schedules (e.g. in seasonal entrainment (Lucassen et al., 2012), and jet lag (An et al., 2013)).

Our data suggest that high frequency stimulation increases signaling from VIP neurons more than low frequency stimulation. Given the well-established links between high frequency firing, dense core vesicle fusion and neuropeptide release (Verhage et al., 1991, Iverfeldt et al., 1989), we hypothesize that high frequency firing results in more VIP release than low frequency firing. In the SCN, specifically, high frequency stimulation produces phase shifts consistent with the magnitude and timing of VIP-induced shifts *in vitro* (An et al., 2011) and *in vivo* (Pantazopoulos et al., 2010, Piggins et al., 1995). In addition, our stimulation may alter the release of GABA. However, since fast neurotransmission is more tightly coupled to spike count, which was similar between HIF and LIF stimulation, we believe this to be less likely.

Entrainment through stimulation of VIP neurons only partially mimics entrainment seen previously through stimulating all SCN neurons (Jones et al., 2015). Specifically, increases in VIP activity fail to advance phase or alter period of locomotor activity during late subjective night. This suggests that VIP activity likely plays a role in light-induced phase delays, but not in light-induced phase advances. Since our VIP stimulation bypasses any retinal input, we hypothesize that there is gating within the SCN mediating light responses. In addition to VIP firing frequency, daily rhythms in VIP abundance or release probability (Francl et al., 2010, Shinohara et al., 1999, Okamoto et al., 1991), VPAC2 receptor abundance (An et al., 2012), and responses in downstream SCN neurons (Enoki et al., 2017, Fan et al., 2015) likely contribute to shaping the phase response curve to firing of VIP neurons and, ultimately, circadian entrainment.

Intriguingly, locomotor activity decreases during stimulation of SCN VIP neurons. This is consistent with a report correlating SCN firing with locomotor inactivity (van Oosterhout et al., 2012) and provides the first causal demonstration that firing increases within VIP SCN neurons inhibit locomotor activity. This, combined with the broad projections of patterns of SCN VIP neurons within the hypothalamus, suggests a role for VIP neurons in regulating circadian behaviors including sleep timing (Aston-Jones et al., 2001) and daily hormonal levels (Fahrenkrug et al., 2012, Loh et al., 2007). How VIP SCN neurons couple anatomically and functionally to behavioral circuits is an open question.

In conclusion, we addressed outstanding questions about how firing activity of VIP neurons alters circadian activity and behavior. By altering the instantaneous firing frequency of SCN VIP neurons, we found that firing of VIP neurons had a larger effect on circadian entrainment when

stimulated with short interspike intervals, regardless of the total number of action potentials. Strikingly, firing of VIP neurons shifted circadian phase only during the late subjective day and early subjective night. We conclude that VIP neurons can phase shift and ultimately entrain circadian behavior by firing during the day-to-night transition.

Materials and Methods

Animals. VIPCre knock-in mice (VIP$^{tm1(cre)Zjh}$, Jackson Laboratories), floxed ChR2 (Ai32, Gt(ROSA)26Sor$^{tm32(CAG-COP4*H134R/EYFP)Hze}$, Jackson Laboratories) and *Per2::Luc(Yoo et al., 2004)* knock-in mice (founders generously provided by Dr. Joseph Takahashi, UTSW) were housed in a 12h:12h light:dark cycle in the temperature and humidity controlled Danforth Animal Facility at Washington University in St. Louis. All animals were congenic on a C57BL/6JN background. Combinations of these genotypes were used for all experiments, with VIPChR2 animals being heterozygous for both VIPCre and floxed-ChR2 and controls being littermate animals heterozygous for only VIPCre or floxed-ChR2. Mice were genotyped by PCR before and by presence (ChR2-positive) or absence of eYFP fluorescence microscopy following each experiment. All procedures were approved by the Animal Care and Use Committee of Washington University and followed National Institutes of Health guidelines.

Multielectrode array cell electrophysiology. Homozygous VIPCre-J mice were crossed with homozygous floxed-ChR2 mice to generate heterozygous litters expressing ChR2 solely in VIP+ neurons (VIPChR2). Extracellular recordings were made from multielectrode arrays (Multichannel Systems, Reutlingen, Germany) plated with SCN cells as previously described (Aton et al., 2005, Webb et al., 2012, Freeman et al., 2013). Briefly, following decapitation, the

brains were rapidly removed from postnatal day 4-5 (P4-P5) VIPChR2 pups. We dissected the bilateral SCN from 250-um thick coronal brain slices, papain-dissociated and dispersed the cells at high density onto sixty, 30μm-diameter electrodes (200μm spacing) pre-treated with poly-D-lysine/laminin. Cultures were maintained in Air-DMEM (Dulbecco's Modified Eagles Medium, DMEM, supplemented with 10% fetal bovine serum for the first week of recording) for 3 weeks prior to recording.

Multielectrode arrays were covered with a fluorinated ethylene-polypropylene membrane before transfer to a recording incubator maintained at 36^{o}C. We waited 24h before the start of digitization to ensure culture health and stability. For extracellular recordings, spikes that exceeded a manually set threshold (~3-4 standard deviations from noise level) were digitized (1 ms before and after crossing the threshold; MC-Rack software, Multichannel Systems) at 20,000 Hz sampling. Subsequently, the culture was stimulated with 15ms pulses of light from a high-power 470nm LED (Cree XLamp XP-E2 Blue High Power LED, LEDsupply) at frequencies between 2-20Hz for 1h. Culture light intesntiy was verified to fall between 5 – 10 mW.

Whole-cell patch clamp electrophysiology. Whole cell patch clamp recordings from SCN neurons were obtained using the procedures described in Hermanstyne et al. (Hermanstyne et al., 2016). Specifically, SCN slices were prepared from 3 month old adult VIPChR2 heterozygous mice. After anesthesia with 1.25% Avertin, brains were removed into a cold cutting solution (in mM 240 sucrose, 2.5 KCL, 1.25 NaH_2Po_4, 25 $NaHCo_3$, 0.5 $CaCl_2$ and 7 $MgCl_2$, saturated with 95% O_2/5%Co_2). 300um coronal slices were cut on a Leica VT1000 S vibrating blade microtome and incubated in oxygenated artificial cerebrospinal fluid (in mM 125 NaCl, 2.5 KCL, 1.25

NaH_2PO_4, 25 $NaHCO_3$, 2 $CaCl_2$, 1 $MgCl_2$, 25 dextrose, saturated with 95% O_2/5% CO_2) for at least 1 h. Using glass pipettes (4-7 MΩ) containing an intracellular solution (in mM 120 $KMeSO_4$, 20 KCl, 10 HEPES, 0.2 EGTA, 8 NaCl 4 Mg-ATP 0.3 Tris-GTP, and 14 phosphocreatine), a "loose patch" cell-attached recording was obtained. A gigaOhm seal (>2 GΩ) was formed and spontaneous firing was recorded for approximately 1 min. We then evoked firing in ChR2-positive neurons with 15ms pulses from a 465 nm laser (DPPS MDL-III-447 100mW, 5% stability, Information Unlimited) positioned over the slice controlled by a TTL input from a Grass stimulator (S88, Grass Instrument Company, Quincy, MA) at the desired frequency (2 to 15Hz). Electrophysiological data were compiled and analyzed using ClampFit, Mini Analysis, and Prism 7.0 (Graphpad Software, La Jolla California).

Isolation of individual neuronal firing patterns. Software was created for semi-automated spike sorting to allow discrimination of neuronal activity from MEA recordings across multiple days. Briefly, time-stamped spikes from a given electrode were separated into 24-h epochs, subsampled by taking a random 10% of the total spikes from each epoch, and then sorted based on principal component analysis (PCA) and fitting a Gaussian mixture model (GMM) to the principal components that contained >10% of the explained variance using a Bayesian information criterion (BIC) cutoff. The noise was identified as the cluster with the average spike shape with the lowest magnitude. The data was split into each remaining cluster. PCA and GMM clustering and splitting was then applied recursively until each cluster could not be split based on the BIC cutoff. We used the Mahalanobis distance to keep only spikes sufficiently close to the center of the distribution. The PCA components and GMM parameters used to sort the subsampled day of spikes were saved and used to sort all spikes on that electrode from that day.

The spike trains identified on each electrode were then combined across days by correlating spike shapes (Pearson r >0.95) to recover the activity of a single neuron throughout the multiday recording. If neuronal firing could not be connected across multiple days, it was excluded from subsequent analysis. Firing activity during optogenetic stimulation was similarly sorted and matched to the third day of spontaneous firing to identify VIP+ neurons. This algorithm was constructed in the Python language using packages scipy (Walt et al., 2011), and scikit-learn (Pedregosa et al., 2011) for sorting, and neuroshare for reading raw MEA data files. All scripts used in spike sorting are publicly available at: http://github.com/JohnAbel/spikesort. This method produced similar numbers of circadian neurons and spike times to manual sorting (Freeman et al., 2013) in approximately 90% less time. To calculate circadian rhythmicity, we binned the average firing rate of each neuron over 10min. Using the MetaCycle package (Wu et al., 2016) (https://cran.r-project.org/web/packages/MetaCycle/index.html in R), we calculated circadian rhythmicity using JTK cycle and Lomb-Scargle (range 20 to 28h). If a neuron was deemed rhythmic with $p < 0.05$ after controlling for multiple comparisons on both methods, we considered that neuron circadian.

Classification of individual neuronal firing patterns. Neuronal firing patterns from the three days of spontaneous activity were identified in Python using scipy hierarchical clustering (Johnson, 1967) of interspike interval histogram (ISIH) with a bin size of 0.01 s and the dominant instantaneous firing rate (DIFR, the peak of the ISIH), using dynamic time warping (Salvador and Chan, 2007) as the correlation metric, and complete linkage. Varying ISIH bin size (0.005 s to 0.05 s) did not alter results significantly. The threshold for dendrogram cluster identification was set to 70% of the maximum distance between data points (default scikit-learn setting).

Following clustering, DFIR was identified with a bin size of 0.0001 s to construct summary statistics with high temporal resolution. In-slice recording and whole-cell patch clamp recording data were analyzed in an identical fashion, except ISIH bin size was changed to 0.05 s for patch clamp recording due to the short 60 s recording interval.

Recording and analysis of real-time clock gene expression. To record circadian PER2 protein expression, we crossed heterozygous VIPChR2 and *PER2::Luc* mice. Control mice were littermate animals lacking either VIPCre or floxed-ChR2. Adult (> P15) mice of both sexes were sacrificed with CO_2 and 300µm coronal brain slices were sectioned. The bilateral SCN was dissected out and cultured on Millicell-CM inserts (Millipore, Billerica, MA) in pre-warmed culture medium (AirDMEM supplemented with 10mM HEPES and 100uM beetle luciferin, Promega, Madison, WI). The sealed 35-mm Petri dishes (BD Biosciences, San Jose, CA) were transferred to a light-tight incubator kept at 36^{o}C. As described previously (Freeman et al., 2013, Aton et al., 2005), bioluminescence from the *Per2*-luciferase reporter was counted with a photomultiplier tube (PMT; HC135-11 MOD, Hamamatsu Corp., Shizuoka, Japan) in 6 min bins for at least three days prior to optogenetic stimulation. PMT recordings were paused during 1 h of optogenetic stimulation between CT9-12 for either one day or three consecutive days. Using a custom-made LED array (Cree XLamp XP-E2 Blue Color High powered LEDs, LEDsupply, Randolph, VT) that delivered light flashes (15 ms, 5 mW, 470 nm) per dish, SCN were stimulated for 1 h at either high (20 Hz pulses at 2 Hz) or low instantaneous frequencies (4 Hz). The LED array was powered by a supply (LEDD1B high-powered LED driver, Thorlabs, Newton, NJ) under TTL control from a stimulator (S88, Grass Instrument Company, Quincy, MA). Care was taken to minimize any mechanical disturbance to the SCN, and during

stimulation, the temperature underneath the LED array remained at 36^{o}C. After stimulation, the dishes were repositioned underneath their PMT and recording continued for at least four days.

For pharmacology experiments we stimulated VIPChR2 PER2 slices in the presence or absence of 10um VPAC2R antagonist in AirDMEM([D-p-Cl-Phe6,Leu17]-VIP, Tocris Bioscience, Bristol, UK). Following 1h of stimulation with HIF frequency, all slices were transferred briefly into a fresh, prewarmed dish of AirDMEM and then transferred back into their original dishes and placed back underneath their PMT channels.

All data were analyzed blinded to genotype. SCN traces that did not retain rhythmicity due to media evaporation or fungal infection were excluded (N=4), and all other data were analyzed in a stereotyped, reproducible manner. In addition, due to inherent variability in period and amplitude within our PMT systems, all comparable experiments were performed in the same incubator. Each experiment (HIF stimulation, LIF stimulation and antagonist treatment) represents at least 3 separate runs with control and experimental conditions run in parallel. Raw counts from the PMT were detrended using a running 24-hour smooth, discarding the first and last 12 h of the recording as previously described (Herzog et al., 2015). For single-pulse experiments, the data from the day of stimulation also was excluded from analyses. Circadian period was calculated from a linear fit to times of the daily acrophase of PER2 expression (baseline= second through fourth days of recording; after-stimulation= fifth through seventh days; Clocklab, Actimetrics). The difference between the baseline-extrapolated and observed acrophases in the three days following stimulation was reported as the phase shift. For PMT traces stimulated for three consecutive days, we used the rising phase as a stable phase marker. Given the natural spread of PER2, we normalized the data based on the rising phase on the day before stimulation.

In vivo stimulation of VIP+ neurons. To stimulate VIP+ neurons *in vivo*, mice underwent stereotactic surgery to implant a fiberoptic cannula capable of delivery light to the bilateral SCN. Specifically, anesthetized mice (2% Isofluorane) were placed into a stereotaxic device and implanted with a sterilized fiber-optic cannula (5.8 mm in length, 200uM diameter core, 0.39 NA; Thorlabs, Newton, NJ). The cannula was implanted at +0.4mm anterior, +0.0 mm lateral and -5.5 mm ventral to Bregma. Mice received analgesic treatment during recovery. Following recovery, mice were enucleated as previously described (Aton et al., 2004, Hermanstyne et al., 2016) so that mice did not respond to ambient light. Additionally, mice were tethered to a flexible fiberoptic cable (Thorlabs, Newton, NJ) attached to a laser (465 nm, 100 mW, 5% stability, DPPS MDL-III-447, Information Unlimited) and allowed to freely roam with *ad lib* access to food, water and an open-faced wheel in a custom-built cage. Wheel revolutions were counted with a reed switch (Clocklab, Actimetrics). After free-running locomotor behavior returned to pre-enucleation levels, mice were stimulated for up to 40 days with different frequency patterns (HIF or LIF). Mice that received both stimulation patterns had the order randomized and separated by at least four days without stimulation.

Immunohistochemistry. To test for neuronal activation, we measured cFOS protein induction in mice implanted with a fiberoptic aimed at the SCN after 1 h of stimulation (15Hz, 15ms pulses) during early subjective night (CT 13). Immediately following stimulation, mice were anesthetized with 1.25% Avertin (2,2,2-tribromoethanol and tert-amyl alcohol in 0.9% NaCl; 0.025 ml/g body weight) and transcardially perfused with phosphate-buffered saline (PBS) and 4% paraformaldehyde (PFA). The brain was rapidly dissected and transferred to 30% sucrose

following 24 h in 4% PFA. Frozen coronal sections cut at 40 um were collected in 3 separate wells. cFOS immunofluorescence or avidin-biotin immunohistochemistry was performed using two using a rabbit anti-cFOS antibody (Santa Cruz Biotechnology, Santa Cruz, CA). For immunofluorescence, free-floating sections were washed for 1 h in PBS, incubated overnight at 4^{o}C in anti-rabbit cFOS antibody (1:1000 in PBSGT). Slices were washed again and incubated for 2 h at room temperature in donkey anti-rabbit Cy3 secondary antibody (1:500 in PBSGT). Sections were washed again in PBS for 30min, mounted, and cover-slipped with DABCO (1,4-Diazobicyclo[2,2,2]-octane) mounting medium. Sections were imaged in 4-um z-stacks on a Nikon A1 Confocal microscope. Two independent investigators quantified the fraction of ChR2-eYFP positive neurons that also expressed nuclear cFOS and results differed by less than 10% per brain. For DAB immunohistochemistry, free-floating sections were incubated for 72 h in rabbit c-Fos antibody (1:2500). Subsequently, sections were processed with the avidin-biotin method for immunohistochemistry. Tissues were reacted in diaminobenzidine with 0.01% H_2O_2, mounted, dehydrated and cover-slipped. Sections were imaged using the Alafi Nanozoomer at Washington University in St. Louis Medical School. Tissues were always processed together and mid-SCN sections were selected from all animals for quantification. An investigator blinded to the genotype of the mouse quantified the number of cFOS positive cells within the SCN using ImageJ software. The SCN was located and boundaries were drawn to demarcate the ventral and dorsal SCN in each animal (250 um x150 um, ventral SCN per side, 150 um x 150 um, dorsal SCN per side).

Locomotor analysis. We identified the daily onset of locomotor activity from wheel running data in 15-min bins as the zero-crossing of the continuous wavelet transform using the Mexican Hat

wavelet as described for temperature rhythms (Leise et al., 2013). We calculated the phase response curve by identifying the change in activity onsets evoked by optogenetic stimulation compared to the same mouse under free running conditions. Calculating phase change in comparison to the same mouse under free-running conditions (rather than comparison with a separate control group) allowed inclusion of mice with visibly different periods. To measure the time to entrainment, we constructed Rayleigh plots of activity onset for days 2-10 of optogenetic stimulation and calculated the Kuramoto parameter (i.e. synchronization index)(Kuramoto, 2012). Finally, we measured optogenetically induced activity suppression by comparing wheel revolutions during the stimulated hours between CT 12 – 16 and equivalent time bins from free-running days with no stimulation.

References

ABRAHAMSON, E. E., LEAK, R. K. & MOORE, R. Y. 2001. The suprachiasmatic nucleus projects to posterior hypothalamic arousal systems. *Neuroreport,* 12, 435-440.

ABRAHAMSON, E. E. & MOORE, R. Y. 2001. Suprachiasmatic nucleus in the mouse: retinal innervation, intrinsic organization and efferent projections. *Brain Research,* 916, 172-191.

AN, S., HARANG, R., MEEKER, K., GRANADOS-FUENTES, D., TSAI, C. A., MAZUSKI, C., KIM, J., DOYLE, F. J., PETZOLD, L. R. & HERZOG, E. D. 2013. A neuropeptide speeds circadian entrainment by reducing intercellular synchrony. *Proceedings of the National Academy of Sciences of the United States of America,* 110, 61.

AN, S., IRWIN, R. P., ALLEN, C. N., TSAI, C. & HERZOG, E. D. 2011. Vasoactive intestinal polypeptide requires parallel changes in adenylate cyclase and phospholipase C to entrain circadian rhythms to a predictable phase. *Journal of neurophysiology,* 105, 2289-96.

AN, S., TSAI, C., RONECKER, J., BAYLY, A. & HERZOG, E. D. 2012. Spatiotemporal distribution of vasoactive intestinal polypeptide receptor 2 in mouse suprachiasmatic nucleus. *The Journal of comparative neurology,* 520, 2730-2741.

ASTON-JONES, G., CHEN, S., ZHU, Y. & OSHINSKY, M. L. 2001. A neural circuit for circadian regulation of arousal. *Nat Neurosci,* 4, 732-8.

ATON, S. J., BLOCK, G. D., TEI, H., YAMAZAKI, S. & HERZOG, E. D. 2004. Plasticity of circadian behavior and the suprachiasmatic nucleus following exposure to non-24-hour light cycles. *J Biol Rhythms,* 19, 198-207.

ATON, S. J., COLWELL, C. S., HARMAR, A. J., WASCHEK, J. & HERZOG, E. D. 2005. Vasoactive intestinal polypeptide mediates circadian rhythmicity and synchrony in mammalian clock neurons. *Nat.Neurosci,* 8, 476-483.

BAN, Y., SHIGEYOSHI, Y. & OKAMURA, H. 1997. Development of vasoactive intestinal peptide mRNA rhythm in the rat suprachiasmatic nucleus. *Journal of Neuroscience,* 17, 3920-3931.

BRANCACCIO, M., MAYWOOD, E. S., CHESHAM, J. E., LOUDON, A. S. I. & HASTINGS, M. H. 2013. A Gq-Ca 2+ axis controls circuit-level encoding of circadian time in the suprachiasmatic nucleus. *Neuron,* 78, 714-728.

BROWN, T. M., COLWELL, C. S., WASCHEK, J. A. & PIGGINS, H. D. 2007. Disrupted neuronal activity rhythms in the suprachiasmatic nuclei of vasoactive intestinal polypeptide-deficient mice. *Journal of neurophysiology,* 97, 2553-2558.

CASSONE, V. M., WARREN, W. S., BROOKS, D. S. & LU, J. 1993. Melatonin, the pineal gland, and circadian rhythms. *J Biol Rhythms,* 8 Suppl, S73-S81.

DING, J. M., FAIMAN, L. E., HURST, W. J., KURIASHKINA, L. R. & GILLETTE, M. U. 1997. Resetting the biological clock: mediation of nocturnal CREB phosphorylation via light, glutamate, and nitric oxide. *Journal of Neuroscience,* 17, 667-675.

DUNLAP, J. C. 1999. Molecular bases for circadian clocks. *Cell,* 96, 271-90.

EASTMAN, C. I., MISTLBERGER, R. E. & RECHTSCHAFFEN, A. 1984. Suprachiasmatic nuclei lesions eliminate circadian temperature and sleep rhythms in the rat. *Physiol Behav.,* 32, 357-368.

ENOKI, R., ONO, D., KURODA, S., HONMA, S. & HONMA, K.-I. 2017. Dual origins of the intracellular circadian calcium rhythm in the suprachiasmatic nucleus. *Scientific Reports,* 7.

FAHRENKRUG, J., GEORG, B., HANNIBAL, J. & JØRGENSEN, H. L. 2012. Altered rhythm of adrenal clock genes, StAR and serum corticosterone in VIP receptor 2-deficient mice. *Journal of molecular neuroscience : MN,* 48, 584-596.

FAN, J., ZENG, H., OLSON, D. P., HUBER, K. M., GIBSON, J. R. & TAKAHASHI, J. S. 2015. Vasoactive intestinal polypeptide (VIP)-expressing neurons in the suprachiasmatic nucleus provide sparse GABAergic outputs to local neurons with circadian regulation occurring distal to the opening of postsynaptic GABAA ionotropic receptors. *Journal of Neuroscience,* 35, 1905-1920.

FERNANDEZ, D. C., CHANG, Y.-T., HATTAR, S. & CHEN, S.-K. 2016. Architecture of retinal projections to the central circadian pacemaker. *Proceedings of the National Academy of Sciences*, 201523629.

FRANCL, J. M., KAUR, G. & GLASS, J. D. 2010. Regulation of vasoactive intestinal polypeptide release in the suprachiasmatic nucleus circadian clock. *Neuroreport,* 21, 1055-9.

FREEMAN, G. M., KROCK, R. M., ATON, S. J., THABEN, P. & HERZOG, E. D. 2013. GABA Networks Destabilize Genetic Oscillations in the Circadian Pacemaker. *Neuron,* 78, 799-806.

HANNIBAL, J., MØLLER, M., OTTERSEN, O. P. & FAHRENKRUG, J. 2000. PACAP and glutamate are co-stored in the retinohypothalamic tract. *The Journal of comparative neurology,* 418, 147-155.

HARRINGTON, M. E., HOQUE, S., HALL, A., GOLOMBEK, D. & BIELLO, S. 1999. Pituitary adenylate cyclase activating peptide phase shifts circadian rhythms in a manner similar to light. *J Neurosci,* 19, 6637-42.

HERMANSTYNE, T. O., SIMMS, C. L., CARRASQUILLO, Y., HERZOG, E. D. & NERBONNE, J. M. 2016. Distinct Firing Properties of Vasoactive Intestinal Peptide-Expressing Neurons in the Suprachiasmatic Nucleus. *Journal of biological rhythms,* 31, 57-67.

HERZOG, E. D., KISS, I. Z. & MAZUSKI, C. 2015. Chapter One-Measuring Synchrony in the Mammalian Central Circadian Circuit. *Methods in enzymology,* 552, 3-22.

IVERFELDT, K., SERFÖZÖ, P., ARNESTO, L. & BARTFAI, T. 1989. Differential release of coexisting neurotransmitters: frequency dependence of the efflux of substance P, thyrotropin releasing hormone and [3H] serotonin from tissue slices of rat ventral spinal cord. *Acta Physiologica,* 137, 63-71.

JOHNSON, S. C. 1967. Hierarchical clustering schemes. *Psychometrika,* 32, 241-254.

JONES, J. R., TACKENBERG, M. C. & MCMAHON, D. G. 2015. Manipulating circadian clock neuron firing rate resets molecular circadian rhythms and behavior. *Nature neuroscience,* 18, 373-375.

KAWAMOTO, K., NAGANO, M., KANDA, F., CHIHARA, K., SHIGEYOSHI, Y. & OKAMURA, H. 2003. Two types of VIP neuronal components in rat suprachiasmatic nucleus. *Journal of neuroscience research,* 74, 852-857.

KO, C. H. & TAKAHASHI, J. S. 2006. Molecular components of the mammalian circadian clock. *Hum Mol Genet,* 15 Spec No 2, R271-7.

KURAMOTO, Y. 2012. *Chemical oscillations, waves, and turbulence*, Springer Science & Business Media.

LEISE, T. L., INDIC, P., PAUL, M. J. & SCHWARTZ, W. J. 2013. Wavelet meets actogram. *Journal of biological rhythms,* 28, 62-68.

LOH, D. H., ABAD, C., COLWELL, C. S. & WASCHEK, J. A. 2007. Vasoactive intestinal peptide is critical for circadian regulation of glucocorticoids. *Neuroendocrinology,* 88, 246-255.

LUCASSEN, E. A., VAN DIEPEN, H. C., HOUBEN, T., MICHEL, S., COLWELL, C. S. & MEIJER, J. H. 2012. Role of vasoactive intestinal peptide in seasonal encoding by the suprachiasmatic nucleus clock. *The European journal of neuroscience,* 35, 1466-1474.

MAYWOOD, E. S., REDDY, A. B., WONG, G. K., O'NEILL, J. S., O'BRIEN, J. A., MCMAHON, D. G., HARMAR, A. J., OKAMURA, H. & HASTINGS, M. H. 2006. Synchronization and maintenance of timekeeping in suprachiasmatic circadian clock cells by neuropeptidergic signaling. *Current biology : CB,* 16, 599-605.

MCCLUNG, C. A. 2011. Circadian rhythms and mood regulation: insights from pre-clinical models. *European neuropsychopharmacology : the journal of the European College of Neuropsychopharmacology,* 21 Suppl 4, 93.

MOORE, R. Y. & SPEH, J. C. 1993. GABA is the principal neurotransmitter of the circadian system. *Neuroscience letters,* 150, 112-116.

MUSIEK, E. S., LIM, M. M., YANG, G., BAUER, A. Q., QI, L., LEE, Y., ROH, J. H., ORTIZ-GONZALEZ, X., DEARBORN, J. T., CULVER, J. P., HERZOG, E. D., HOGENESCH, J. B., WOZNIAK, D. F., DIKRANIAN, K., GIASSON, B. I., WEAVER, D. R., HOLTZMAN, D. M. & FITZGERALD, G. A. 2013. Circadian clock proteins regulate neuronal redox homeostasis and neurodegeneration. *The Journal of clinical investigation*.

NIEDERKOFLER, V., ASHER, T. E., OKATY, B. W., ROOD, B. D., NARAYAN, A., HWA, L. S., BECK, S. G., MICZEK, K. A. & DYMECKI, S. M. 2016. Identification of serotonergic neuronal modules that affect aggressive behavior. *Cell Reports,* 17, 1934-1949.

NIELSEN, H. S., HANNIBAL, J. & FAHRENKRUG, J. 2002. Vasoactive intestinal polypeptide induces per1 and per2 gene expression in the rat suprachiasmatic nucleus late at night. *The European journal of neuroscience,* 15, 570-574.

OKAMOTO, S., OKAMURA, H., MIYAKE, M., TAKAHASHI, Y., TAKAGI, S., AKAGI, Y., FUKUI, K., OKAMOTO, H. & IBATA, Y. 1991. A diurnal variation of vasoactive intestinal peptide (VIP) mRNA under a daily light-dark cycle in the rat suprachiasmatic nucleus. *Histochemistry and Cell Biology,* 95, 525-528.

OKAMURA, H., YAMAGUCHI, S. & YAGITA, K. 2002. Molecular machinery of the circadian clock in mammals. *Cell Tissue Res,* 309, 47-56.

PANTAZOPOULOS, H., DOLATSHAD, H. & DAVIS, F. C. 2010. Chronic stimulation of the hypothalamic vasoactive intestinal peptide receptor lengthens circadian period in mice and hamsters. *American journal of physiology. Regulatory, integrative and comparative physiology,* 299, 85.

PEDREGOSA, F., VAROQUAUX, G., GRAMFORT, A., MICHEL, V., THIRION, B., GRISEL, O., BLONDEL, M., PRETTENHOFER, P., WEISS, R. & DUBOURG, V. 2011. Scikit-learn: Machine learning in Python. *Journal of Machine Learning Research,* 12, 2825-2830.

PENNARTZ, C. M., DE JEU, M. T., GEURTSEN, A. M., SLUITER, A. A. & HERMES, M. L. 1998. Electrophysiological and morphological heterogeneity of neurons in slices of rat suprachiasmatic nucleus. *J Physiol,* 506 (Pt 3), 775-93.

PIGGINS, H. D., ANTLE, M. C. & RUSAK, B. 1995. Neuropeptides phase shift the mammalian circadian pacemaker. *The Journal of neuroscience : the official journal of the Society for Neuroscience,* 15, 5612-5622.

REED, H. E., CUTLER, D. J., BROWN, T. M., BROWN, J., COEN, C. W. & PIGGINS, H. D. 2002. Effects of vasoactive intestinal polypeptide on neurones of the rat suprachiasmatic nuclei in vitro. *Journal of neuroendocrinology,* 14, 639-646.

REPPERT, S. M. & WEAVER, D. R. 2002. Coordination of circadian timing in mammals. *Nature,* 418, 935-41.

SALVADOR, S. & CHAN, P. 2007. Toward accurate dynamic time warping in linear time and space. *Intelligent Data Analysis,* 11, 561-580.

SHINOHARA, K., FUNABASHI, T. & KIMURA, F. 1999. Temporal profiles of vasoactive intestinal polypeptide precursor mRNA and its receptor mRNA in the rat suprachiasmatic nucleus. *Molecular brain research*.

VAN OOSTERHOUT, F., LUCASSEN, E. A., HOUBEN, T., TJEBBE VANDERLEEST, H., ANTLE, M. C. & MEIJER, J. H. 2012. Amplitude of the SCN clock enhanced by the behavioral activity rhythm. *PLoS One,* 7, e39693.

VAN SOMEREN, E. J. 2000. Circadian and sleep disturbances in the elderly. *Exp Gerontol,* 35, 1229-37.

VERHAGE, M., MCMAHON, H. T., GHIJSEN, W. E. J. M., BOOMSMA, F., SCHOLTEN, G., WIEGANT, V. M. & NICHOLLS, D. G. 1991. Differential release of amino acids, neuropeptides, and catecholamines from isolated nerve terminals. *Neuron,* 6, 517-524.

WALT, S. V. D., COLBERT, S. C. & VAROQUAUX, G. 2011. The NumPy array: a structure for efficient numerical computation. *Computing in Science & Engineering,* 13, 22-30.

WEBB, A. B., TAYLOR, S. R., THOROUGHMAN, K. A., DOYLE III, F. J. & HERZOG, E. D. 2012. Weakly circadian cells improve resynchrony. *PLoS computational biology,* 8, e1002787.

WELSH, D. K., LOGOTHETIS, D. E., MEISTER, M. & REPPERT, S. M. 1995. Individual neurons dissociated from rat suprachiasmatic nucleus express independently phased circadian firing rhythms. *Neuron,* 14, 697-706.

WU, G., ANAFI, R. C., HUGHES, M. E., KORNACKER, K. & HOGENESCH, J. B. 2016. MetaCycle: an integrated R package to evaluate periodicity in large scale data. *Bioinformatics,* 32, 3351-3353.

YOO, S. H., YAMAZAKI, S., LOWREY, P. L., SHIMOMURA, K., KO, C. H., BUHR, E. D., SIEPKA, S. M., HONG, H. K., OH, W. J., YOO, O. J., MENAKER, M. & TAKAHASHI, J. S. 2004. PERIOD2::LUCIFERASE real-time reporting of circadian dynamics reveals persistent circadian oscillations in mouse peripheral tissues. *Proc Natl Acad Sci U S A,* 101, 5339-46.

Chapter 3.

Adult Deletion of VIP SCN Neurons results in a milder phenotype than *Vip* null mice

This chapter will be adapted for the manuscript:

Mazuski, C., Chen, S., & Herzog, E.D. Adult Deletion of VIP SCN Neurons results in a milder phenotype than *Vip* null mice. (in preparation)

Abstract

The suprachiasmatic nucleus (SCN) drives circadian rhythms in locomotion through coupled, single-cell oscillations. Genetic loss of *Vip* or its receptor *Vipr2* result in profound deficits in single-cell synchronization and coupling that lead to arrhythmic locomotor behavior in over 60% of the mice. To test whether this phenotype depends on loss of VIP signaling early in development or could be attributed to the role of VIP neurons in the developed SCN, we deleted SCN VIP neurons *in vivo* in adult mice through induction of the apoptotic pathway in cre-expressing VIP neurons. We found that over 80% of mice with loss of VIP SCN neurons retained daily rhythms, but with a short circadian period, more variable onsets and decreased duration of daily activity. In contrast, *in vitro* deletion of VIP neurons dramatically reduced the amplitude of circadian gene expression with minimal changes in period. In summary, loss of VIP neurons *in vivo* within the developed circadian circuit changes circadian period whereas early loss of VIP SCN neurons *in vitro* reduces circadian amplitude and synchrony. We conclude that in the adult VIP SCN neurons play an important role in regulating circadian period and suggest that neonatal VIP has an important role in development.

Introduction

Located in the ventral hypothalamus, the suprachiasmatic nucleus (SCN) is the dominant pacemaker that aligns physiological and behavioral rhythms to the local schedule (Herzog, 2007). Individual SCN neurons express cell autonomous oscillations driven through a negative transcription-translation feedback loop involving the 'core clock genes', which include *Bmal1*, *Clock*, *Period 1* and *2*, and *Cryptochrome 1* and *2* (Takahashi, 2017). Coupling of these single-cell oscillators through intercellular synchrony generates high amplitude, precise, circuit-wide rhythms capable of driving behavioral circadian rhythms (Herzog et al., 2004).

Network synchrony and rhythm generation primarily relies on intercellular neurotransmission. Disruption of intercellular communication reveals region and single-cell heterogeneity within the SCN (Yamaguchi et al., 2003, Webb et al., 2009), suggesting that perhaps a group of SCN neurons function as 'dominant' pacemakers. If these dominant pacemaking neurons exist, they would ultimately be necessary and sufficient for driving SCN rhythms. Studies have suggested that these dominant pacemaking neurons might be localized to the ventral SCN or 'core' rather than the dorsal SCN or 'shell' (Yan et al., 2007). *In vitro*, intercellular communication from the ventral SCN is necessary for dorsal SCN rhythms in gene expression (Yamaguchi et al., 2003), and the ventral SCN drives resynchronization of the dorsal SCN following perturbation (Taylor et al., 2017). *In vivo,* only microlesions localized to the medial-ventral SCN in hamsters are sufficient to cause behavioral arrhythmicity (Kriegsfeld et al., 2004).

One important class of ventral SCN neurons is the vasoactive intestinal polypeptide (VIP) neurons. VIP-expressing neurons comprise approximately 10% of SCN neurons (Abrahamson

and Moore, 2001). Global deletion of *Vip* or its receptor *Vipr2* yields results in 60% of the animals losing rhythms or exhibiting multiple periodicities (Colwell et al., 2003, Aton et al., 2005, Harmar et al., 2002). Mechanistically, the loss of rhythms is caused by decreases in the number of rhythmic SCN neurons and the loss of intercellular synchrony (Aton et al., 2005, Brown et al., 2007, Maywood et al., 2006). The strong phenotype seen in *Vip* null mice suggests that VIP neurons are prime candidates for driving population-wide circadian rhythms. Therefore, in order to test whether VIP neurons are necessary for circadian rhythms in behavior, we deleted VIP SCN neurons in the intact adult brain.

Critically, ablation of VIP neurons in the adult has never been tested. Using cre-mediated activation of the apoptotic pathway in VIP neurons, we tested the effects of localized VIP deletion in the adult intact network and the effects on locomotor behavior. Surprisingly, we found that the over 80% of the mice retained rhythmic locomotor behavior, a much milder phenotype than *Vip* null mice. Our results suggest that VIP neurons have an overlooked role in SCN development and conclude that in the developed SCN, VIP neurons regulate period but are ultimately not necessary for synchronized circadian rhythms.

Results

Adult-onset deletion of VIP neurons disrupts locomotor activity

To test the role of VIP SCN neurons in the developed adult circadian circuit, we ablated VIP SCN neurons *in vivo* and monitored circadian locomotor activity. To delete VIP, we stereotactically injected VIP-ires-Cre heterozygous mice with an AAV virus expressing Cre-dependent Caspase3 (see methods adapted from (Yang et al., 2013)). Expression of the Caspase3

construct within VIP neurons cell-autonomously triggered the apoptotic pathway resulting in specific cell death of VIP SCN neurons (experimental group is hereafter referred to as VIP-deleted). We sham injected VIP-ires-Cre mice (N = 2) with ACSF or injected the Caspase3 construct into mice that lacked Cre expression (N = 6) as controls (total N=8).

Following surgery and recovery, we monitored and recorded circadian wheel running behavior in entrained conditions (12:12 light-dark cycle) for at least 1-2 weeks. Mice were then placed in constant darkness for 2-3 weeks. At the conclusion of the experiment, mice were sacrificed to confirm the deletion of VIP SCN neurons. In total, 4 experimental mice injected with the Caspase3 construct retained wild-type levels of VIP expression in the SCN, most likely due to off target injections. We included these mice in our analysis as a separate group (termed unsuccessful VIP deletion).

Greater than 80% of VIP-deleted mice retained circadian rhythms in constant darkness. However, they ran with a significantly shorter period of locomotor activity and greater onset variability (22.66 ± 0.12 h, 0.90 ± 0.09 h, N = 16), compared to control mice (23.32 ± 0.08h and 0.44 ± 0.07h, N = 8) and unsuccessful VIP deletion groups (23.35 ± 0.09h, 0.33 ± 0.09h, N = 4, all values mean ± SEM, **Figure 1**). We contrast this to *Vip* null mice previously reported (Aton et al., 2005, Colwell et al., 2003) where more than 60% lost rhythms. VIP-deleted mice also ran with a significantly shortened duration of activity (7.09 ± 0.57 h) compared to control mice (9.77± 0.67 h); however

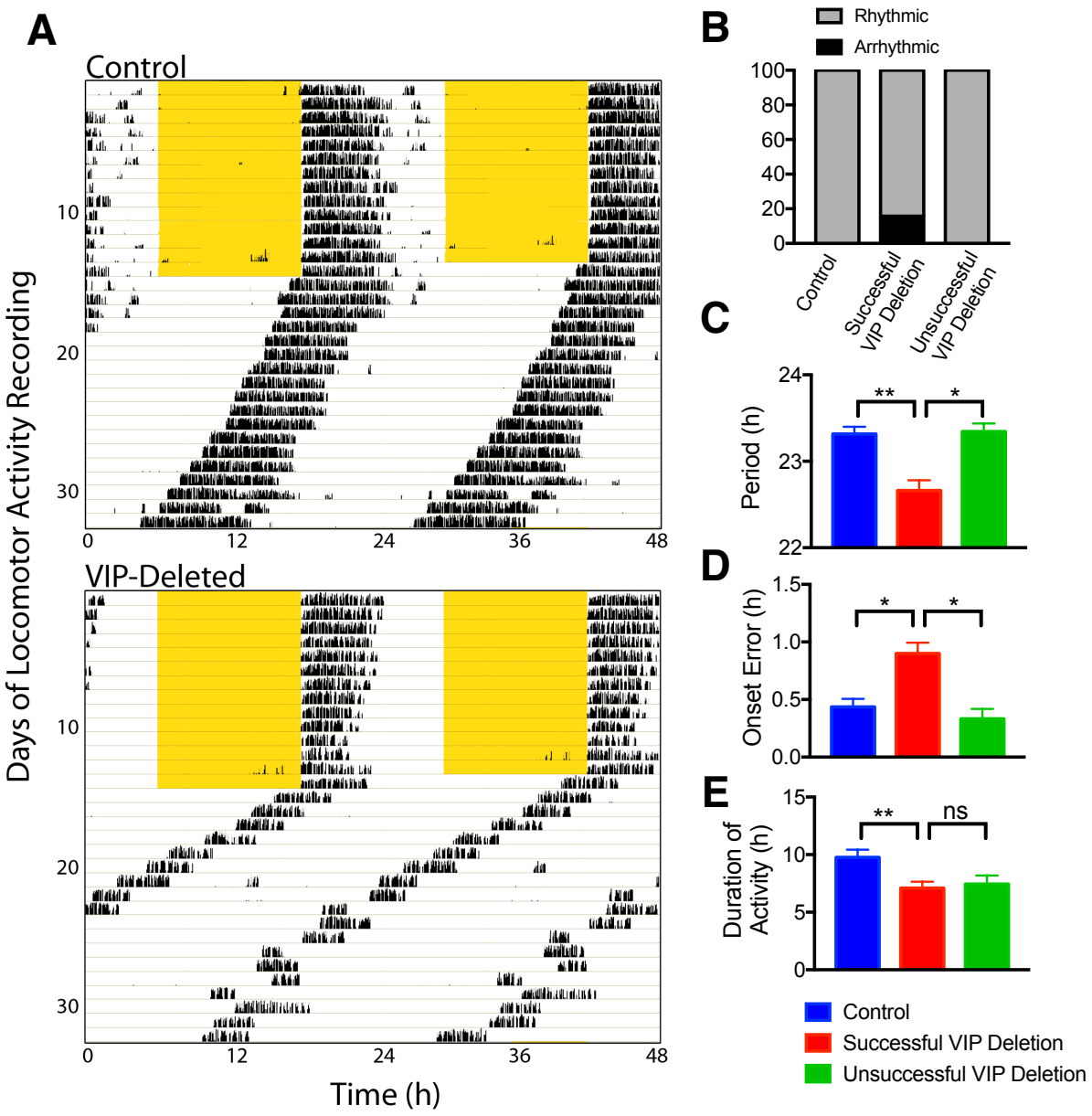
A
Control
VIP-Deleted
Days of Locomotor Activity Recording
10
20
30
0
12
24
36
48
Time (h)
B
Rhythmic
Arrhythmic
100
80
60
40
20
0
Control
Successful VIP Deletion
Unsuccessful VIP Deletion
C
Period (h)
24
23
22
**
*
D
Onset Error (h)
1.5
1.0
0.5
0.0
*
*
E
Duration of Activity (h)
15
10
5
0
**
ns
Control
Successful VIP Deletion
Unsuccessful VIP Deletion

Figure 1. Deletion of VIP neurons shortens locomotor behavior but rarely causes arrhythmicity. Representative actograms of circadian locomotor activity shown in **A** illustrate the dominant phenotype in VIP-deleted mice. **B)** Over 80% of mice with successful VIP deletion (16/19), all mice with unsuccessful VIP deletion (4/4) and all control mice (8/8) had circadian rhythms in locomotor activity. **C)** Successful deletion of VIP neurons in the adult mice shortened period (**p<0.01 *p<0.05 one-way ANOVA), **D)** increased onset variability (*p<0.05 Kruskal-Wallis test) and **E)** decreased the duration of activity (*p<0.05 one-way ANOVA).

this was not significantly different to mice with unsuccessful VIP deletion (7.45 ± 0.74h). In total, we quantified period, onset variability, total activity and duration of activity during entrained conditions and constant darkness (**Figure 2**).

Locomotor Phenotype in VIP-deleted mice correlates with VIP Staining Intensity

To test whether rhythmic locomotor activity resulted from any residual VIP staining, we quantified the deletion of VIP neurons. All mice were sacrificed during late subjective day (CT 7-10) when AVP staining intensity is high. Coronal brain sections were simultaneously processed for VIP and AVP staining and all images were taken with the same exposure to allow for accurate comparisons of fluorescent intensity.

As anticipated, in VIPCre Caspase3 injected animals we found significant reductions in VIP staining intensity but no changes in AVP intensity (**Figure 3A-3B**). Mice with unsuccessful VIP deletion had VIP staining intensity at levels comparable to control mice (**Figure 3B**). The majority of successful VIP deleted mice had VIP staining levels at or below background staining. Increasing expression levels of VIP in the SCN strongly correlated with increasing circadian locomotor period and decreasing day-to-day locomotor precision (**Figure 3C-D**). Daily locomotor duration did not correlate with VIP levels in the SCN (**Figure 3E**). **Figure 4** shows how VIP staining intensity in the SCN correlated with circadian behavioral deficits. Interestingly, three mice were arrhythmic although they had no detectable VIP staining similar to other VIP-deleted mice with short period locomotor patterns (**Figure 3C-E orange stars**). AVP staining intensity was not correlated with period, onset error or duration of activity.

Figure 2. Locomotor Activity Analyses of VIP-Deleted and Control Mice. (supplemental information)

Light-Dark Analyses (LD)

Group	Genotype	N	Injection	Period	Onset Error	Duration of Activity	Activity Per Day
Control#	C57J and P2L/+	6	AAV8-DIO-Caspase3	24.03 ± 0.03	0.26 ± 0.1	8.56 ± 0.88	19047 ± 3491
Control#	VIP-Cre	2	ACSF	24.01 ± 0.01	0.08 ± 0.04	7.97 ± 0.35	23970 ± 1534
Successful VIP Deletion	VIP-Cre	19	AAV8-DIO-Caspase3	24.01 ± 0.02	0.29 ± 0.06[A]	6.92 ± 0.35	16608 ± 1633
Unsuccessful VIP Deletion	VIP-Cre	4	AAV8-DIO-Caspase3	24.01 ± 0.02	0.06 ± 0.02[A]	7.78 ± 1.07	17723 ± 4913

Constant Darkness Analyses (DD)

Group	Genotype	N	Injection	Period	Onset Error	Duration of Activity	Activity Per Day
Control#	C57J and P2L/+	6	AAV8-DIO-Caspase3	23.36 ± 0.11[B]	0.36 ± 0.06[D]	9.74 ± 0.9[F]	18824 ± 3276
Control#	VIP-Cre	2	ACSF	23.19 ± 0.07[B]	0.68 ± 0.06[D]	9.84 ± 0.43[F]	24784 ± 2653
Successful VIP Deletion	VIP-Cre	*19	AAV8-DIO-Caspase3	22.66 ± 0.12[BC]	0.90 ± 0.09[DE]	7.08 ± 0.57[F]	13730 ± 1871
Unsuccessful VIP Deletion	VIP-Cre	4	AAV8-DIO-Caspase3	23.35 ± 0.09[C]	0.33 ± 0.09[E]	7.45 ± 0.74	18394 ± 3867

Control groups were combined for statistical tests
* N = 16 for period, onset error and duration of activity analyses due to arrhythmicity in 3 mice
ABCDEF all significant $p < 0.05$
A LD onset error – one-way ANOVA comparing successful and unsuccessful VIP deletion
B DD period – one-way ANOVA comparing control and successful VIP deletion
C DD period – one-way ANOVA comparing successful and unsuccessful VIP deletion
D DD onset error – Kruskal-Willis comparing control and successful VIP deletion
E DD onset error – Kruskal-Willis comparing successful and unsuccessful VIP deletion
F DD duration of activity – one-way ANOVA comparing control and successful VIP deletion

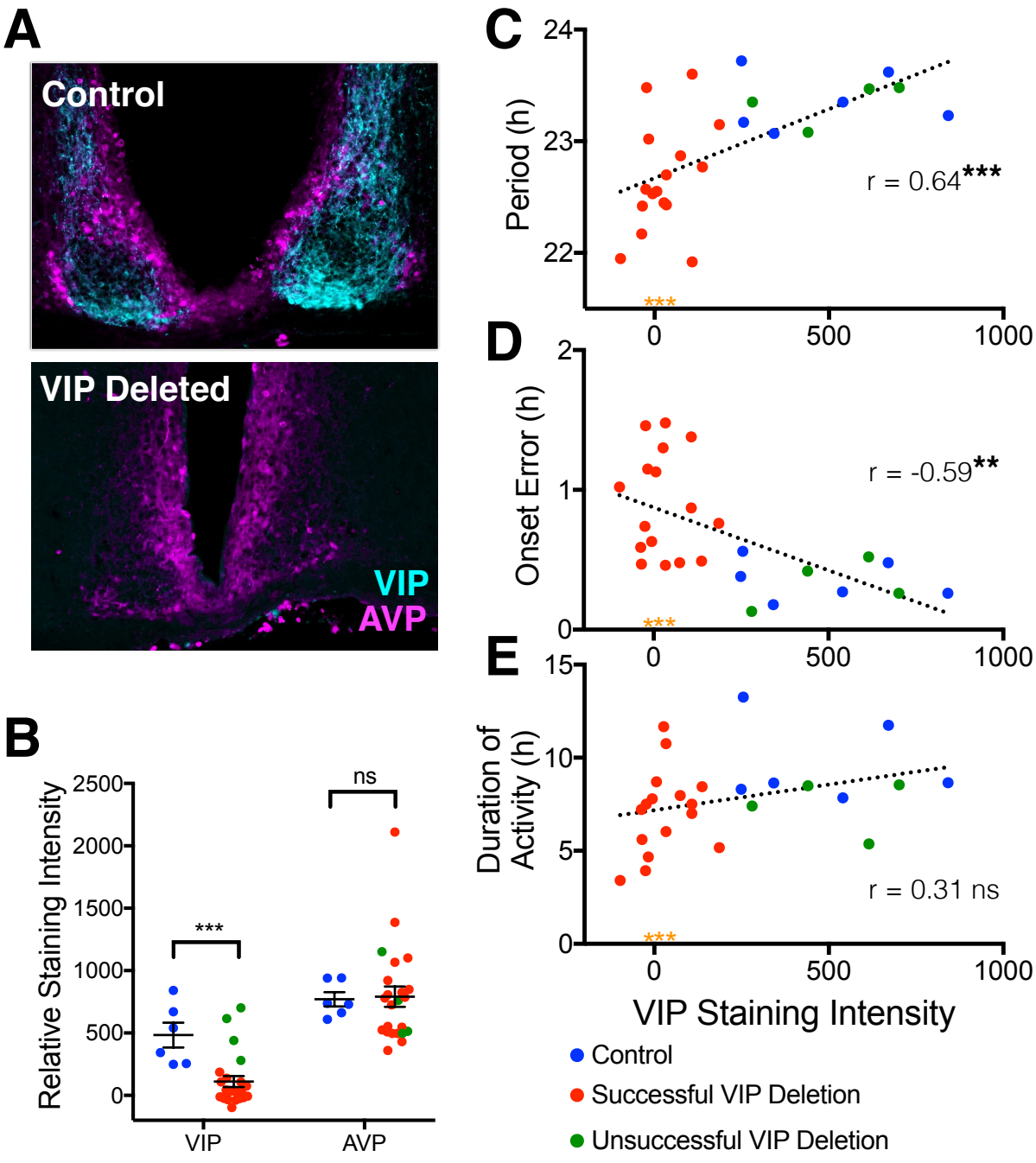
A
Control
VIP Deleted
VIP
AVP
B
Relative Staining Intensity
2500
2000
1500
1000
500
0
***
ns
VIP
AVP
C
Period (h)
24
23
22
r = 0.64***
***
0
500
1000
D
Onset Error (h)
2
1
0
r = -0.59**
***
0
500
1000
E
Duration of Activity (h)
15
10
5
0
r = 0.31 ns
***
0
500
1000
VIP Staining Intensity
Control
Successful VIP Deletion
Unsuccessful VIP Deletion

Figure 3. Phenotype correlates with VIP but not AVP staining intensity. A Representative VIP and AVP immunofluorescent staining of SCN coronal sections from Control and VIP deleted mice. **B** VIP but not AVP staining was significantly reduced in VIP-deleted mice compared to controls (483.4 ± 98.93 versus 110.9 ± 43.59 relative VIP fluorescence units, ***$p<0.0008$ unpaired t-test). Note that mice with unsuccessful VIP deletion (green) had VIP intensity levels comparable to control mice. **C)** Period and **D)** onset error correlated with VIP staining intensity (Pearson $r = 0.64$, $r = -0.59$ respectively ***$p<0.001$ **$p<0.01$). **E)** Interestingly while duration of activity was lower in VIP deleted animals compared to control it did not correlate with SCN VIP staining intensity. Note that the orange stars on the x-axis represent the relative VIP fluorescent staining of the 3 arrhythmic mice.

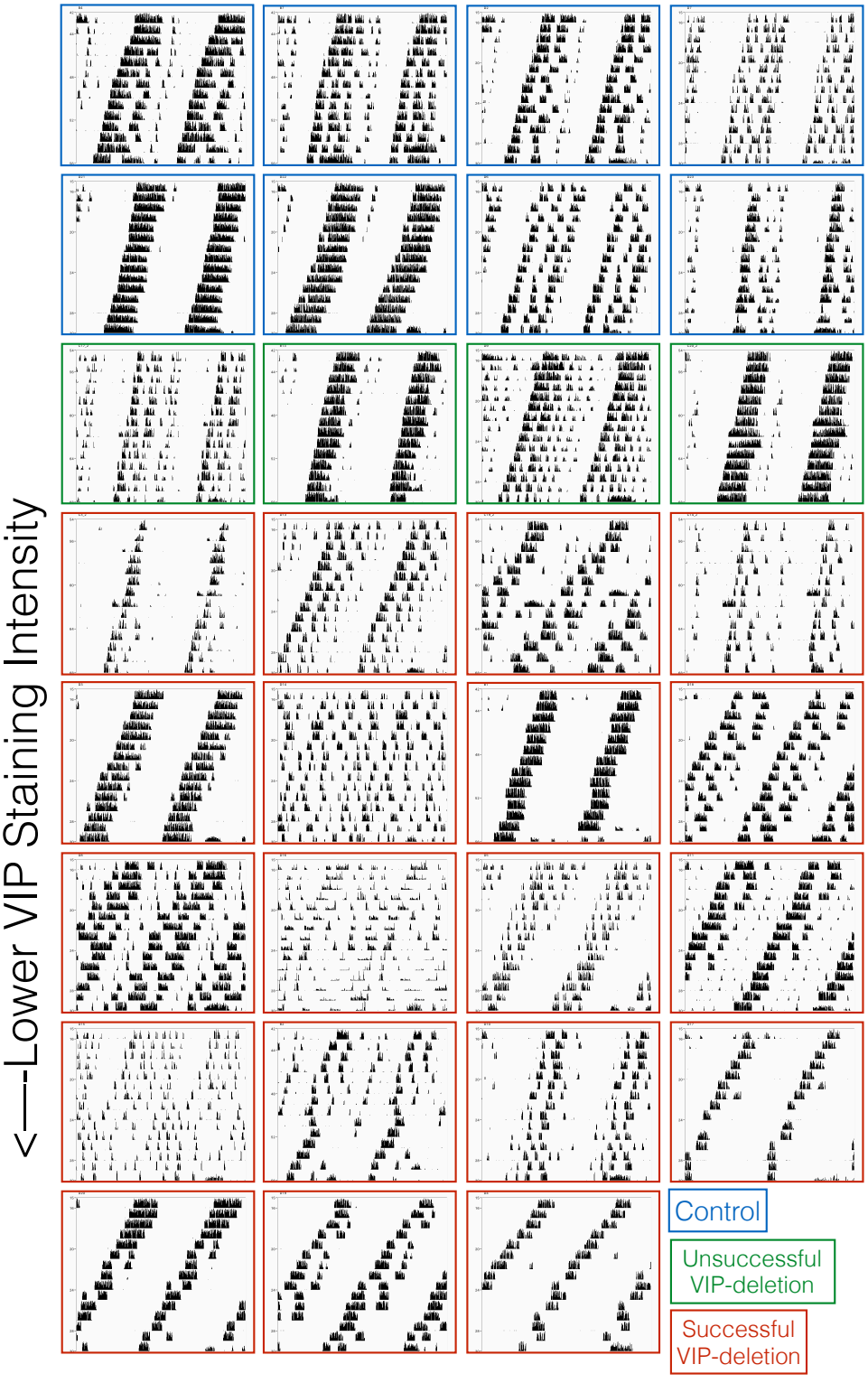
<—-Lower VIP Staining Intensity
Control
Unsuccessful VIP-deletion
Successful VIP-deletion

Figure 4. Visualizing the effects of VIP SCN loss on circadian locomotor behavior. (supplemental information)

2 week actograms of wheel running behavior in constant darkness are ordered based on VIP staining intensity.

VIP Deletion Correlates with Period2 Amplitude Decreases *in vitro*

To visualize VIP neuronal cell death in real-time in the isolated SCN, we transgenically expressed tdTOMATO in VIP neurons (VIP-ires-Cre crossed with floxed-Rosa-tdTOMATO) and then crossed onto a PERIOD2::Luciferase (PER2::LUC)(Yoo et al., 2004) background to visualize circadian gene expression. The resulting mice expressed tdTOMATO only in VIP neurons and PER2::LUC in all SCN neurons. Around postnatal day6, we sectioned the SCN and infected equivalent slices with either AAV-DIO-Casp3 to ablate VIP neurons or a control AAV virus expressing Cre-dependent eYFP. PER2 levels were recorded for a month and the slices were fluorescently imaged once a week to confirm deletion of VIP neurons and expression of the control virus.

Our results show that deletion of VIP neurons has minimal effects on the circadian period of the SCN, but reduces gene expression amplitude (**Figure 5A-B**). Interestingly, we find a strong correlation between the number of VIP neurons that remain and the amplitude of PER2 levels (**Figure 5C**). Ultimately, loss of VIP neurons appears to affect gene expression amplitude only when more than 80% have been deleted.

Discussion

Adult-onset of VIP neurons in vivo produced a milder phenotype than that seen in *Vip* null mice. Our results indicate that the phenotype resulted specifically from VIP SCN deletion. VIP staining intensity was strongly correlated to shortened activity period and onset variability and mice with unsuccessful VIP deletion showed period length and onset variability similar to wild-type mice.

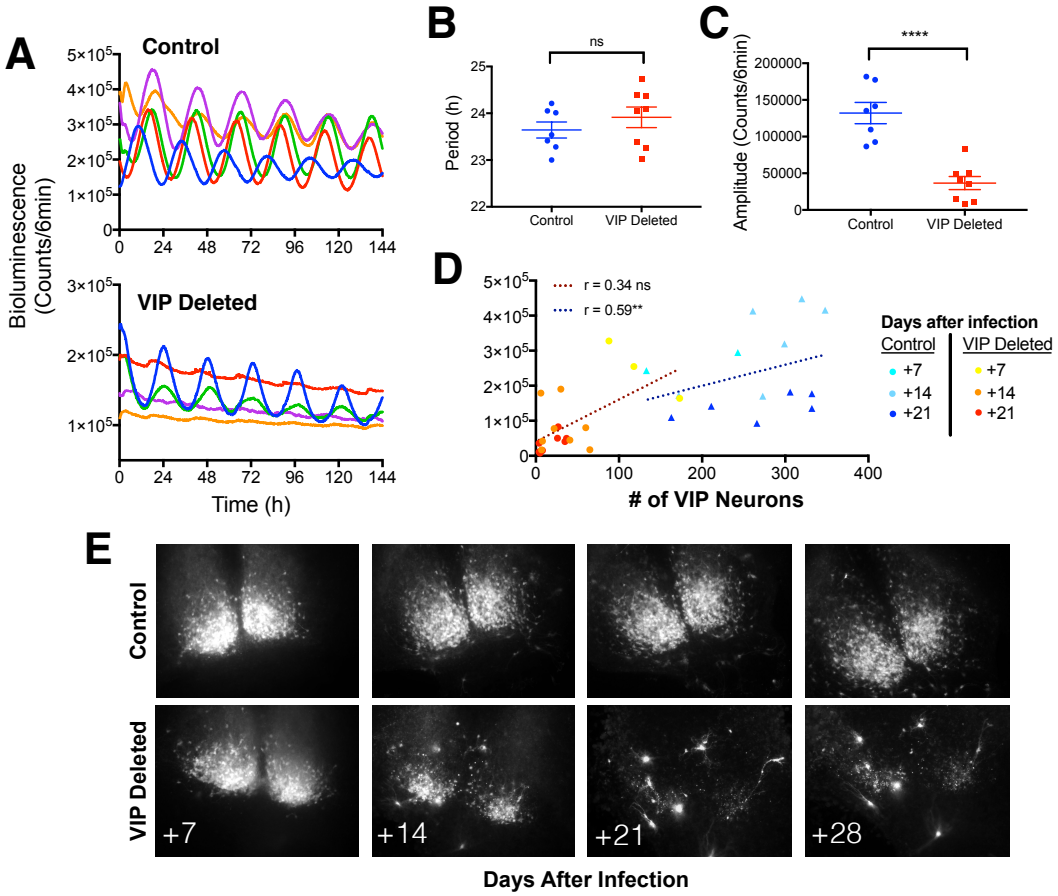
A
Control
VIP Deleted
Bioluminescence (Counts/6min)
Time (h)
B
ns
Period (h)
Control
VIP Deleted
C
****
Amplitude (Counts/6min)
Control
VIP Deleted
D
r = 0.34 ns
r = 0.59**
# of VIP Neurons
Days after infection
Control
+7
+14
+21
VIP Deleted
+7
+14
+21
E
Control
VIP Deleted
+7
+14
+21
+28
Days After Infection

Figure 5. Deletion of VIP neurons in vitro reduces the amplitude of PER2 gene expression. **A)** Representative traces of PERIOD2::Luciferase gene expression rhythms in VIP deleted and control SCN slices two weeks after viral infection. **C)** Amplitude but not **B)** period changes with deletion of VIP neurons (36,641 ± 14425 versus 132,085 ± 14425, peak to trough amplitude, VIP-deleted compared to control ****p<0.0001, unpaired t test) **D)** PER2 amplitude correlates to the number of remaining VIP neurons in VIP deleted (r = 0.59 **p<.001) but not in control across three weeks of recording. Control slices decrease in amplitude due to the age of slice but not number of VIP neurons. **E)** Representative time-lapse images of TDTOMATO expression driven by the *Vip* promoter illustrate the profound loss of VIP neurons after infection.

Interestingly, *in vitro* deletion of VIP neurons primarily led to a decrease in Period2 gene expression.

This is the first reported deletion of VIP signaling in the intact adult SCN. Previous studies concluded that VIP signaling was necessary for circadian behavior because a majority of *Vip* and *Vipr* null mice showed arrhythmic circadian activity. Critically, *Vip* and *Vipr* null mice develop in the absence of all VIP signaling, which is expressed not only in the SCN but also in the cortex, brainstem, retina, adrenals and gastro-intestinal tract (Gozes et al., 1987). Our current results suggest i) that the predominant arrhythmic locomotor phenotype in *Vip* null mice may be largely due to the overlooked role of VIP in development and ii) in the intact adult SCN other SCN neurons or mature SCN inputs maintain rhythmicity in the absence of VIP neurons.

SCN development begins in the embryo and continues up to two weeks after birth (Brooks and Canal, 2013). In the weeks following birth, the fetal SCN is susceptible to environmental perturbations that can have long-lasting effects into adulthood including enucleation and lighting schedules (Landgraf et al., 2014, Chew et al., 2017). VIP mRNA is first expressed in the SCN around birth (Hill et al., 1994), suggesting that VIP signaling may play an important role as the SCN is wired to respond and integrate environmental inputs. Additionally, clock gene expression differs between young SCN and adult SCN. One prominent example involves Cryptochrome 1 and 2 knockout mice, where adult mice are behaviorally arrhythmic, but young SCN retain rhythms (Ono et al., 2016). Due to these differences, studies that perturb signaling in the adult, developed SCN network are crucial to truly understanding the role of specific signaling pathways and neurons.

Our results support the idea that VIP neurons in the adult ultimately play a lesser role in generating rhythms as 'dominant' pacemakers, but rather work in concert with other neurons to set the period of the clock. Specifically, the presence and activity of VIP neurons lengthens locomotor activity. As previously demonstrated, activation of VIP neurons phase delays and lengthens locomotor activity (Chapter 2), which is consistent with the period shortening seen here in VIP-deleted mice. Ultimately, VIP neurons belong to a larger group of SCN neurons that drive circadian rhythms. Recent reports conclude that NMS+ SCN neurons, which comprise ~40% of SCN neurons including 95% of VIP neurons are ultimately necessary for generating rhythms (Lee et al., 2015).

Finally, while locomotor period and onset variability were strongly correlated with VIP SCN deletion, duration of activity was not. Rather, as a whole, mice that expressed Cre in VIP neurons and were injected with the AAV-DIO-Caspase3 construct had shorter activity durations than control mice. We suggest that this locomotor phenotype may be primarily driven by loss of VIP SCN projection neurons rather than loss of VIP SCN neurons that synapse within the SCN. Previous reports indicate that VIP SCN neurons are a heterogeneous group and that activation of VIP SCN neurons leads to decreases in locomotor activity during the early nighttime (Chapter 2). This intriguing result opens up the possibility of using adult-onset deletion of specific SCN neurons to dissect the networks that mediate SCN output including locomotor activity and hormonal fluctuations (see chapter 4).

Future Directions

Single-cell rhythms in gene expression

Ultimately the differences between our *in vitro* and *in vivo* results (period changes vs. amplitude changes) can be explained in several ways including: i) differences due to the age of ablation, where VIP signaling has different roles depending on the stage of SCN development, or ii) differences in SCN input, where SCN slices lack the circuit inputs still present *in vivo* in VIP-deleted mice that ultimately sustain synchrony. By measuring SCN synchrony at the single-cell level, we can answer this question.

Preliminary results using single-cell imaging of gene expression suggest that deletion of VIP neurons decreased the number of neurons that express circadian rhythms in gene expression and increased the proportion of arrhythmic cells (**Figure 6**). Interestingly, though *in vivo* deletion of VIP neurons resulted in more arrhythmic cells, it also resulted in a higher synchrony index among rhythmic cells, supporting the hypothesis that age of VIP ablation affects single-cell synchrony.

To further address how deletion of VIP neurons in vivo in the intact adult circuit alters single-cell rhythms in gene expression, we propose testing the correlation between locomotor phenotype, deletion of VIP neurons and disruption in single-cell gene expression within individual mice.

We stereotactically injected triple transgenic adult mice expressing tdTOMATO only in VIP neurons and Period2::Luciferase in all neurons (VIPCre/+; floxed-tdTOM/+; Per2::LUC/+) with

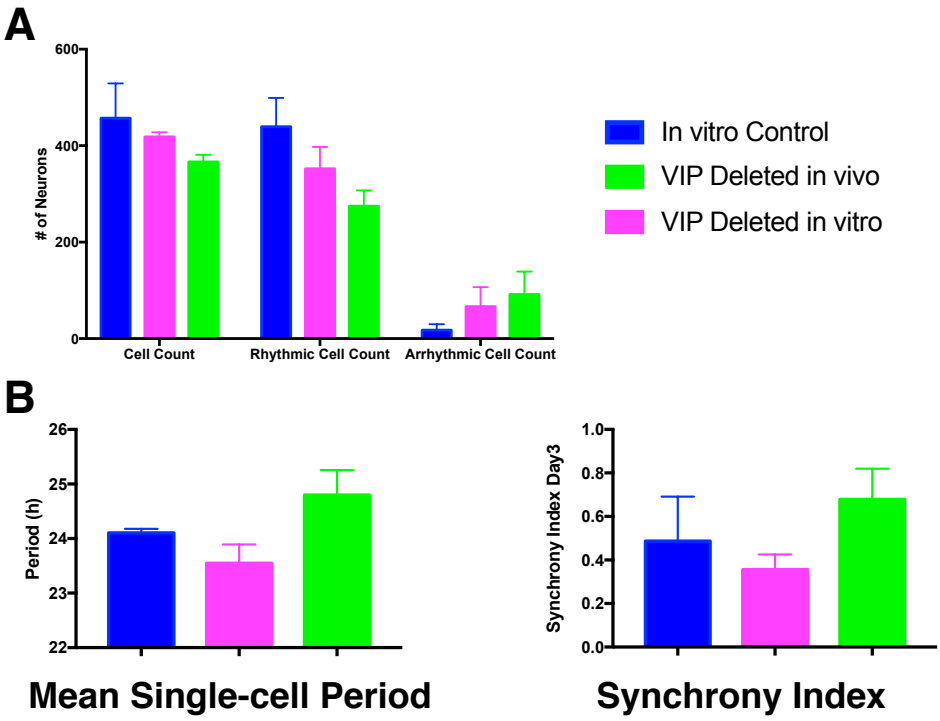
A
600
400
200
0
# of Neurons
Cell Count
Rhythmic Cell Count
Arrhythmic Cell Count
In vitro Control
VIP Deleted in vivo
VIP Deleted in vitro
B
26
25
24
23
22
Period (h)
Mean Single-cell Period
1.0
0.8
0.6
0.4
0.2
0.0
Synchrony Index Day3
Synchrony Index

Figure 6. Impairment of Single-cell gene expression rhythms in VIP-deleted mice. (Preliminary Data)

A The loss of VIP neurons leads to decreases in the number of detectable cells with circadian gene expression at the single-cell level and increases in the number of arrhythmic cells. **B** However, VIP-deletion that occurred in vitro leads to mild deficits in period and more severe deficits in synchrony than VIP-deletion in vivo. Additional experiments are necessary to confirm this finding and understand how VIP-deletion in vivo affects single-cell rhythms and we caution interpretation at this stage due to the different ages at which VIP deletion occurred, the different times in culture, and the different route of infection.

the AAV-DIO-Caspase3 construct or a control fluorescent virus. After collection of locomotor activity, we will section these brains and image single-cell gene expression using a CCD camera. This will allow us to correlate behavioral rhythms to single-cell gene expression rhythms and ultimately the number of remaining VIP neurons.

Impairment of Light-Responsiveness in VIP-deleted mice

Following deletion of VIP neurons *in vivo* and collection of locomotor activity under constant conditions, we tested the light-responsiveness of the circadian circuit. After re-entrainment, we delivered a light pulse at CT 15 and immediately switched the mice into constant conditions. We are currently analyzing this data to see if VIP-deleted mice show any indication of deficits in light mediated phase shifting. Follow-up experiments might include quantifying cFOS expression following an early night light pulse.

Methods

Animals All mice were housed in a 12h:12h light dark cycle in the temperature and humidity controlled Danforth Animal Facility at Washington University in St. Louis with ad lib access to food and water. Combinations of the following genotypes were used in all experiments: VIP-IRESCre knock-in mice (VIP$^{tm1(creZjh}$, Jackson Laboratories), *Per2:Luc* knock-in mice (founders generously provided by Dr. Joseph Takahashi, UTSW), tdTomato reporter mice (B6.Cg-Gt(ROSA)26Sor$^{tm9(CAG-tdTomato)Hze}$/J, Jackson Laboratories) and C57J mice. All procedures were approved by the Animal Care and Use Committee of Washington University and adhered to National Institutes of Health guidelines.

In Vivo Deletion of VIP Neurons To delete VIP neurons in vivo, VIP-ires-Cre mice were stereotactically injected with AAV8-Caspase3-TEVP virus at the level of the SCN. Briefly, anesthetized mice (2% Isofluorane) were placed into a stereotactic device and the virus (0.5 uL/side) was bilaterally injected into the SCN at +0.4mm anterior, +/- 0.15 mm lateral and -5.6mm ventral to Bregma. Control mice were either VIP-ires-Cre mice receiving sham surgery with ACSF injections or mice lacking Cre expression (C57J or Per2:Luc/+) receiving AAV8-Caspase3-TEVP injections. Mice received analgesic treatment during recovery.

Locomotor Activity Following recovery, mice were placed in custom-built wheel cages connected to Clocklab Actimetrics System, which allowed circadian monitoring of locomotor activity. Mice were maintained in 12h:12h light dark cycle for at least 7 days prior to being released into constant darkness. Following at least 3 weeks in constant darkness, mice were re-entrained to a 12h:12h light dark cycle prior to 1 h light pulse during CT 15. Following the light pulse mice were once again released into constant darkness. Locomotor data was collected from 3 separate rounds of mice and injections.

Locomotor activity was analyzed using Clocklab Actimetrics and custom built Python scripts. Period was calculated from at least one week of activity using Chi-squared periodogram. Onset variability was calculated through Clocklab by using a box filter to fit activity onsets and quantifying the error of the fit. Duration of activity was calculated as the time between onsets and offsets calculated using clocklab's box filter. Python scripts were used to quantify daily activity counts. All data were analyzed blinded to the genotype of the animal.

Immunohistochemistry Upon re-entrainment, all mice were perfused during a 3-h window during late subjective day (CT 7-10). Briefly, mice were anesthetized with 1.25% Avertin (2,2,2-tribromoethanol and tert-amyl alcohol in 0.9% NaCl; 0.025 ml/g body weight) and transcardially perfused with phosphate-buffered saline (PBS) and 4% paraformaldehyde (PFA). The brain was rapidly dissected and transferred to 30% sucrose the following day. Frozen coronal sections were cut at 40um in 3 separate wells. For VIP and AVP immunofluorescence, free-floating sections were washed for 1 h in PBS, then blocked in PBSGT (5% normal goat serum, 0.3% Triton and PBS) for 1h. Sections were transferred overnight to primary antibodies in PBSGT (rabbit anti-VIP 1:2000, Immunostar and mouse anti-AVP PS41 1:100). Slices were washed again and incubated for 2 h at room temperature with secondary antibodies (anti-rabbit 488 and anti-mouse 564). Sections were briefly stained with DAPI, washed again in PBS, mounted and cover-slipped with DABCO (1,4-Diazobicycol[2,2,2]-octane) mounting medium. All sections from a specific round were processed at the same time.

Sections were imaged on an epifluorescent microscope. The SCN was identified using the DAPI staining for each animal resulting in 2-5 SCN sections per animal. VIP and AVP staining images from the SCN were acquired using the same exposure and gain for every mouse in the round, allowing us to effectively compare intensities. An investigator blinded to the genotype of the mouse, drew boundaries around the SCN using ImageJ software and measured the mean intensity of VIP and AVP staining within those boundaries for each SCN section. Additionally, the background staining was calculated for each image from an area slightly lateral to the SCN that wasn't positively labeled for AVP or VIP. To calculate staining intensity across the SCN, individual images were ordered from anterior to posterior, and background was subtracted from

the corresponding images. Values reported are the maximum staining intensities for individual SCN.

Based on the staining, VIP-deleted mice were divided into two groups – successful VIP deletion and unsuccessful VIP deletion. Unsuccessful VIP deleted mice had VIP staining intensities that were on par with control mice. In addition the presence of VIP cell bodies and dense VIP-positive arborizations within the SCNs of these mice was confirmed visually.

In Vitro Deletion of VIP Neurons The SCN from triple transgenic mice heterozygous for VIP-ires-Cre, Rosa-tdtomato, and Per2:Luc was used during these experiments. Briefly, between postnatal day 6-7 (P6-P7), these mice were decapitated and brains were rapidly removed. The bilateral SCN was dissected from 300-um thick coronal brain slices, imaged to verify tdtomato fluorescence, and cultured on Millicell-CM inserts (Millipore, Billerica, MA) in pre-warmed culture medium (DMEM supplemented with 10mM HEPES and 10uM beetle luciferin, Promega, Madison, WI). The following day SCN were infected with 1-2ul of either AAV8-Caspase-TEVP or AAV9-DIO-eYFP viruses. The virus was applied directly on top of the slice. The sealed 35-m Petri dishes (BD Biosciences, San Jose, CA) were transferred to a light-tight incubator kept at 36C. Each slice was imaged on an epifluorescent microscope once per week to visualize the changes in number of VIP neurons and media was replaced every two weeks.

All data were analyzed blinded to genotype. Period data were analyzed with Chronostar using cosine fit on detrended data. Amplitude was calculated using a custom-written python script,

which measured the peak to trough difference from the raw data. Epifluorescent images for tdtomato neurons were quantified using ImageJ's built in cell counter.

References

ABRAHAMSON, E. E. & MOORE, R. Y. 2001. Suprachiasmatic nucleus in the mouse: retinal innervation, intrinsic organization and efferent projections. *Brain Research,* 916**,** 172-191.

ATON, S. J., COLWELL, C. S., HARMAR, A. J., WASCHEK, J. & HERZOG, E. D. 2005. Vasoactive intestinal polypeptide mediates circadian rhythmicity and synchrony in mammalian clock neurons. *Nat.Neurosci,* 8**,** 476-483.

BROOKS, E. & CANAL, M. M. 2013. Development of circadian rhythms: role of postnatal light environment. *Neuroscience & Biobehavioral Reviews,* 37**,** 551-560.

BROWN, T. M., COLWELL, C. S., WASCHEK, J. A. & PIGGINS, H. D. 2007. Disrupted neuronal activity rhythms in the suprachiasmatic nuclei of vasoactive intestinal polypeptide-deficient mice. *Journal of neurophysiology,* 97**,** 2553-2558.

CHEW, K. S., RENNA, J. M., MCNEILL, D. S., FERNANDEZ, D. C., KEENAN, W. T., THOMSEN, M. B., ECKER, J. L., LOEVINSOHN, G. S., VANDUNK, C. & VICAREL, D. C. 2017. A subset of ipRGCs regulates both maturation of the circadian clock and segregation of retinogeniculate projections in mice. *eLife,* 6**,** e22861.

COLWELL, C. S., MICHEL, S., ITRI, J., RODRIGUEZ, W., TAM, J., LELIEVRE, V., HU, Z., LIU, X. & WASCHEK, J. A. 2003. Disrupted circadian rhythms in VIP- and PHI-deficient mice. *American journal of physiology. Regulatory, integrative and comparative physiology,* 285**,** R939-49.

GOZES, I., SHANI, Y. & ROSTÈNE, W. H. 1987. Developmental expression of the VIP-gene in brain and intestine. *Molecular Brain Research,* 2**,** 137-148.

HARMAR, A. J., MARSTON, H. M., SHEN, S., SPRATT, C., WEST, K. M., SHEWARD, W. J., MORRISON, C. F., DORIN, J. R., PIGGINS, H. D., REUBI, J. C., KELLY, J. S., MAYWOOD, E. S. & HASTINGS, M. H. 2002. The VPAC(2) receptor is essential for circadian function in the mouse suprachiasmatic nuclei. *Cell,* 109**,** 497-508.

HERZOG, E. D. 2007. Neurons and networks in daily rhythms. *Nature reviews. Neuroscience,* 8**,** 790-802.

HERZOG, E. D., ATON, S. J., NUMANO, R., SAKAKI, Y. & TEI, H. 2004. Temporal precision in the mammalian circadian system: a reliable clock from less reliable neurons. *J Biol Rhythms,* 19**,** 35-46.

HILL, J. M., AGOSTON, D. V., GRESSENS, P. & MCCUNE, S. K. 1994. Distribution of VIP mRNA and two distinct VIP binding sites in the developing rat brain: relation to ontogenic events. *Journal of Comparative Neurology,* 342**,** 186-205.

KRIEGSFELD, L. J., LESAUTER, J. & SILVER, R. 2004. Targeted microlesions reveal novel organization of the hamster suprachiasmatic nucleus. *Journal of Neuroscience,* 24**,** 2449-2457.

LANDGRAF, D., KOCH, C. E. & OSTER, H. 2014. Embryonic development of circadian clocks in the mammalian suprachiasmatic nuclei. *Frontiers in neuroanatomy,* 8.

LEE, I. T., CHANG, A. S., MANANDHAR, M., SHAN, Y., FAN, J., IZUMO, M., IKEDA, Y., MOTOIKE, T., DIXON, S. & SEINFELD, J. E. 2015. Neuromedin s-producing neurons act as essential pacemakers in the suprachiasmatic nucleus to couple clock neurons and dictate circadian rhythms. *Neuron,* 85**,** 1086-1102.

MAYWOOD, E. S., REDDY, A. B., WONG, G. K., O'NEILL, J. S., O'BRIEN, J. A., MCMAHON, D. G., HARMAR, A. J., OKAMURA, H. & HASTINGS, M. H. 2006. Synchronization and maintenance of timekeeping in suprachiasmatic circadian clock cells by neuropeptidergic signaling. *Current biology : CB,* 16**,** 599-605.

ONO, D., HONMA, S. & HONMA, K.-I. 2016. Differential roles of AVP and VIP signaling in the postnatal changes of neural networks for coherent circadian rhythms in the SCN. *Science advances,* 2**,** e1600960.

TAKAHASHI, J. S. 2017. Transcriptional architecture of the mammalian circadian clock. *Nature Reviews Genetics,* 18**,** 164-179.

TAYLOR, S. R., WANG, T. J., GRANADOS-FUENTES, D. & HERZOG, E. D. 2017. Resynchronization Dynamics Reveal that the Ventral Entrains the Dorsal Suprachiasmatic Nucleus. *Journal of Biological Rhythms,* 32**,** 35-47.

WEBB, A. B., ANGELO, N., HUETTNER, J. E. & HERZOG, E. D. 2009. Intrinsic, nondeterministic circadian rhythm generation in identified mammalian neurons. *Proceedings of the National Academy of Sciences,* 106**,** 16493-16498.

YAMAGUCHI, S., ISEJIMA, H., MATSUO, T., OKURA, R., YAGITA, K., KOBAYASHI, M. & OKAMURA, H. 2003. Synchronization of cellular clocks in the suprachiasmatic nucleus. *Science,* 302**,** 1408-12.

YAN, L., KARATSOREOS, I., LESAUTER, J., WELSH, D. K., KAY, S., FOLEY, D. & SILVER, R. Exploring spatiotemporal organization of SCN circuits. Cold Spring Harbor symposia on quantitative biology, 2007. Cold Spring Harbor Laboratory Press, 527-541.

YANG, C. F., CHIANG, M. C., GRAY, D. C., PRABHAKARAN, M., ALVARADO, M., JUNTTI, S. A., UNGER, E. K., WELLS, J. A. & SHAH, N. M. 2013. Sexually

dimorphic neurons in the ventromedial hypothalamus govern mating in both sexes and aggression in males. *Cell,* 153**,** 896-909.

YOO, S. H., YAMAZAKI, S., LOWREY, P. L., SHIMOMURA, K., KO, C. H., BUHR, E. D., SIEPKA, S. M., HONG, H. K., OH, W. J., YOO, O. J., MENAKER, M. & TAKAHASHI, J. S. 2004. PERIOD2::LUCIFERASE real-time reporting of circadian dynamics reveals persistent circadian oscillations in mouse peripheral tissues. *Proc Natl Acad Sci U S A,* 101**,** 5339-46.

Chapter 4.

VIP SCN Neurons contribute to the daily rhythm in glucocorticoids

This chapter includes data for an ongoing project on the role of VIP neurons in glucocorticoid rhythms

Abstract

In mammals, the daily surge in glucocorticoids primes the body for increased arousal. This hormonal rhythm depends on signals from the master circadian pacemaker, the suprachiasmatic nucleus (SCN), through the paraventricular nucleus of the hypothalamus (PVN) to ultimately stimulate production of glucocorticoids in the adrenal glands. However, very little is known about which circuits and cell types drive this daily rhythm. In this study, we sought to understand the role of VIP SCN neurons by i) characterizing which VIP SCN neurons project dorsally to the PVN and ii) testing whether deletion of VIP SCN neurons alters the circadian rhythm in corticosterone. Ultimately, we find that a small bilateral subset of VIP SCN neurons projects to each PVN. Interestingly, we find that deletion of VIP SCN neurons dampens the circadian rhythm in corticosterone suggesting that VIP SCN neurons help stimulate the daily surge in corticosterone.

Introduction

Located in the ventral hypothalamus, the suprachiasmatic nucleus (SCN) is required for circadian timing of behavior, including but not limited to rest/activity cycles, alertness, hunger and thirst (Eastman et al., 1984). Underlying these behaviors are daily rhythms in autonomic and neuroendocrine function. Of particular interest is the pronounced circadian rhythm in glucocorticoids. Daily increases in glucocorticoids including cortisol and corticosterone play a critical role in priming an organism for increased arousal (Kolber et al., 2008) and deficiencies in this rhythm correlate with increased risk of mood disorders (Bao et al., 2007). However, it is unclear how SCN neurons mediate these rhythms.

Neuronal projections from the SCN to the paraventricular nucleus of the hypothalamus (PVN) and adjacent areas are necessary for the daily rhythm in glucocorticoids. Importantly, electrolytic lesions of the SCN result in loss of glucocorticoid rhythms (Buijs et al., 1993). Though rhythms in locomotor behavior can be rescued through fetal SCN transplants, hormonal rhythms cannot suggesting that these rhythms require specific mature SCN circuitry (Meyer-Bernstein et al., 1998). A model for SCN regulation of glucocorticoids suggests that inhibitory and stimulatory signals from the SCN occur at different phases to time the daily peak (Kalsbeek et al., 2008).

Several different classes of SCN neuropeptidergic neurons project dorsally to the PVN including vasoactive intestinal polypeptide (VIP), arginine vasopressin (AVP) and gastrin releasing peptide (GRP) (Abrahamson and Moore, 2001). Researchers have suggested that AVP neurons function as the inhibitory component in the model of circadian glucocorticoid regulation. In mice, AVP microinjections into the PVN acutely decrease corticosterone (Kalsbeek et al., 1992, Kalsbeek et

al., 1996) and deficiencies in AVP expression alter the timing of circadian glucocorticoids (Zelena et al., 2009). Both GRP and VIP signaling have been proposed as stimulatory components (Kalsbeek et al., 2012). In the case of VIP, microinjections into the PVN increase corticosterone (Alexander and Sander, 1994) and *Vip* null mice lose rhythmicity in circadian corticosterone rhythms (Loh et al., 2007). However, these manipulations were not SCN specific and involved mice developing in the absence of neuropeptidergic signaling, limiting the conclusions that can be drawn.

In this study, we address the role of SCN VIP neurons in the daily regulation of circadian glucocorticoids. We approach the question by dissecting the SCN to PVN circuitry specific to VIP neurons in three parts. I) We seek to understand which VIP SCN neurons project to the PVN and the nature of these connections II) We test whether VIP SCN neurons are necessary for the circadian rhythm in glucocorticoids and III) We will ultimately test whether activation of VIP SCN neurons can alter glucocorticoid levels at specific times of day.

Results

A small bilateral subset of VIP SCN neurons project to each PVN

SCN VIP neurons project to the PVN and the surrounding sub-PVN (Abrahamson and Moore, 2001), however little is known about quantity or localization of these neurons within the SCN. To address this question, we injected an eYFP or Alexa-Fluor488 retrograde tracer carrying into one unilateral PVN of transgenic mice expressing tdTOMATO fluorescence in VIP neurons (VIPCre/+; floxed-tdTOM/+). In effect, only VIP SCN neurons that project to the PVN expressed both fluorophores (**Figure 1A**).

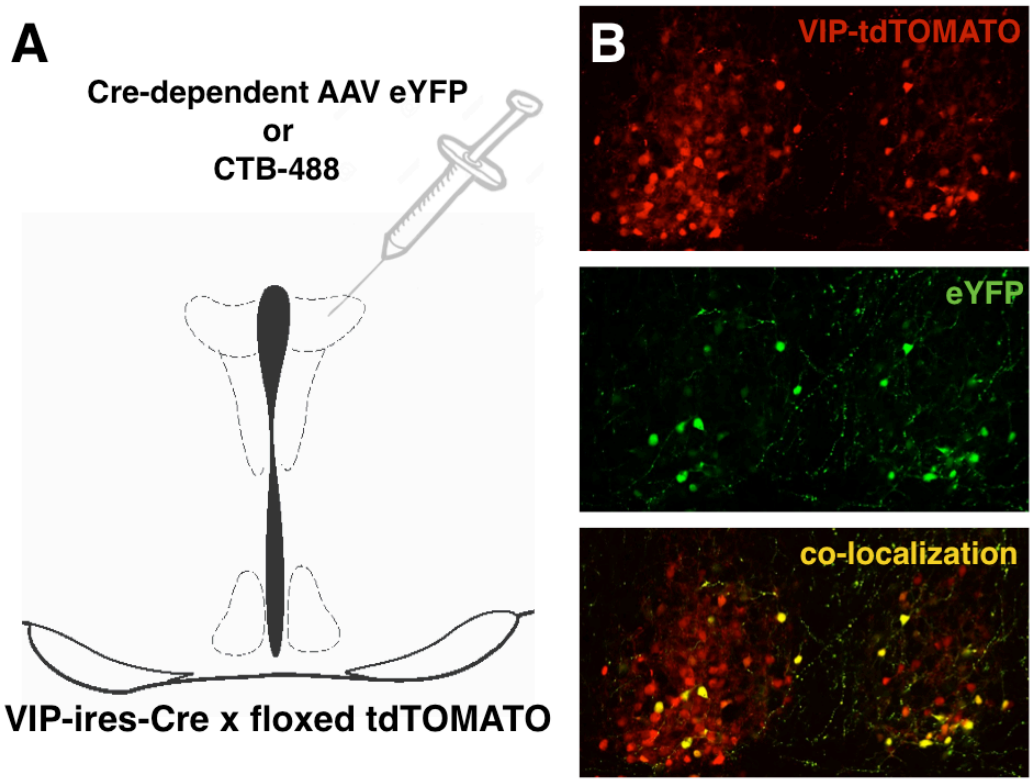
A
Cre-dependent AAV eYFP
or
CTB-488
VIP-ires-Cre x floxed tdTOMATO
B
VIP-tdTOMATO
eYFP
co-localization

Figure 1. A small bilateral subset of VIP neurons projects dorsally to the PVN.

(Preliminary Results)

A) Depiction of the experimental design. A cre-dependent AAV eYFP virus (n=3) or CTB-488 (n=1) retrograde tracer was injected into the PVN of mice that expressed tdTOMATO only in VIP neurons. This resulted in a subset of tdTOMATO-positive VIP neurons expressing eYFP as shown in representative image **B** Preliminary quantification results indicate that on average 5-10% of VIP SCN neurons per side expressed eYFP, indicating that the unilateral PVN receives projections from the bilateral SCN. (20 ± 3 ipsilateral to injection compared to 12 ± 3 contralateral to injection double-labeled VIP neurons)

To test reproducibility, we used two independent tract tracing methods, an AAV cre-dependent eYFP (N=3) and the retrograde tracer cholera-toxin-B 488 (CTB-488, N=1). In all four cases, we visually confirmed that infection was limited to the unilateral PVN.

We observed a small subset of SCN VIP neurons that were double-labeled with tdTOMATO and eYFP/488 (**Figure 1B**). Interestingly, these neurons were present in both the ipsi- and contralateral- SCN relative to the injection site. Preliminary analyses showed roughly 10% of the ipsilateral and 5% of the contralateral SCN neurons project to each PVN (20 ± 3 ipsilateral compared to 12 ± 3 contralateral double-labeled VIP neurons; mean ± SEM, each 40um section of SCN contained roughly 200-250 VIP neurons).

Deletion of SCN VIP neurons drastically dampens the circadian rhythm in corticosterone

To test whether SCN VIP neurons are necessary for the circadian rhythm in corticosterone, we deleted VIP neurons in the adult mouse using Cre-mediated activation of apoptosis. Specifically, mice expressing Cre-recombinase selectively in VIP neurons (heterozygous VIP-ires-Cre) were stereotactically injected with an AAV Cre-dependent Caspase3 construct (Yang et al., 2013). As previously demonstrated (Chapter 3) this resulted in substantial loss of SCN VIP neurons *in vivo*, however more than 80% of VIP-deleted mice retained circadian rhythms in locomotor activity. This experimental system allows us to test the role of VIP neurons in SCN outputs without confounds that result from global loss of circadian rhythmicity seen in *Vip* null mice.

Following locomotor activity recordings, we placed VIP-deleted mice and controls lacking Cre expression in cages custom-built to allow frequent, noninvasive collection of fecal matter (see methods). Under constant darkness, mice were habituated to the cages for 2 days before around-the-clock collection of fecal matter at 4 h intervals. Following steroid hormone extraction, corticosterone levels were measured using a competitive enzyme-linked immunosorbent (ELISA) assay.

VIP-deleted mice had drastically dampened corticosterone levels as compared to controls (**Figure 2**). Specifically, the peak corticosterone was significantly lower indicating a severely blunted corticosterone rhythm. Ultimately, this suggests that activity from VIP SCN neurons functions as a stimulatory element in the daily rhythms of glucocorticoids.

Discussion

This study represents the first direct evidence that SCN VIP neurons play a role in the daily rhythms in glucocorticoids. Prior studies have suggested a role for VIP neurons through PVN-directed microinjections or corticosterone changes in *Vip* and *Vipr2* null mice (Loh et al., 2007, Fahrenkrug et al., 2012). Critically, since VIP signaling is present in the adrenal glands where corticosterone is synthesized and over 60% of mice developing in the absence of VIP signaling lose systemic behavioral circadian rhythms (HÖKfelt et al., 1981, Aton et al., 2005, Harmar et al., 2002, Colwell et al., 2003, Brown et al., 2007); this makes it difficult to conclusively determine the role of VIP SCN neurons in glucocorticoid rhythms. Our study strengthens the existing literature in three ways i) we specifically delete only VIP neurons of the SCN ii) deletion occurs in adult mice avoiding developmental defects and iii) over 80% of our mice have

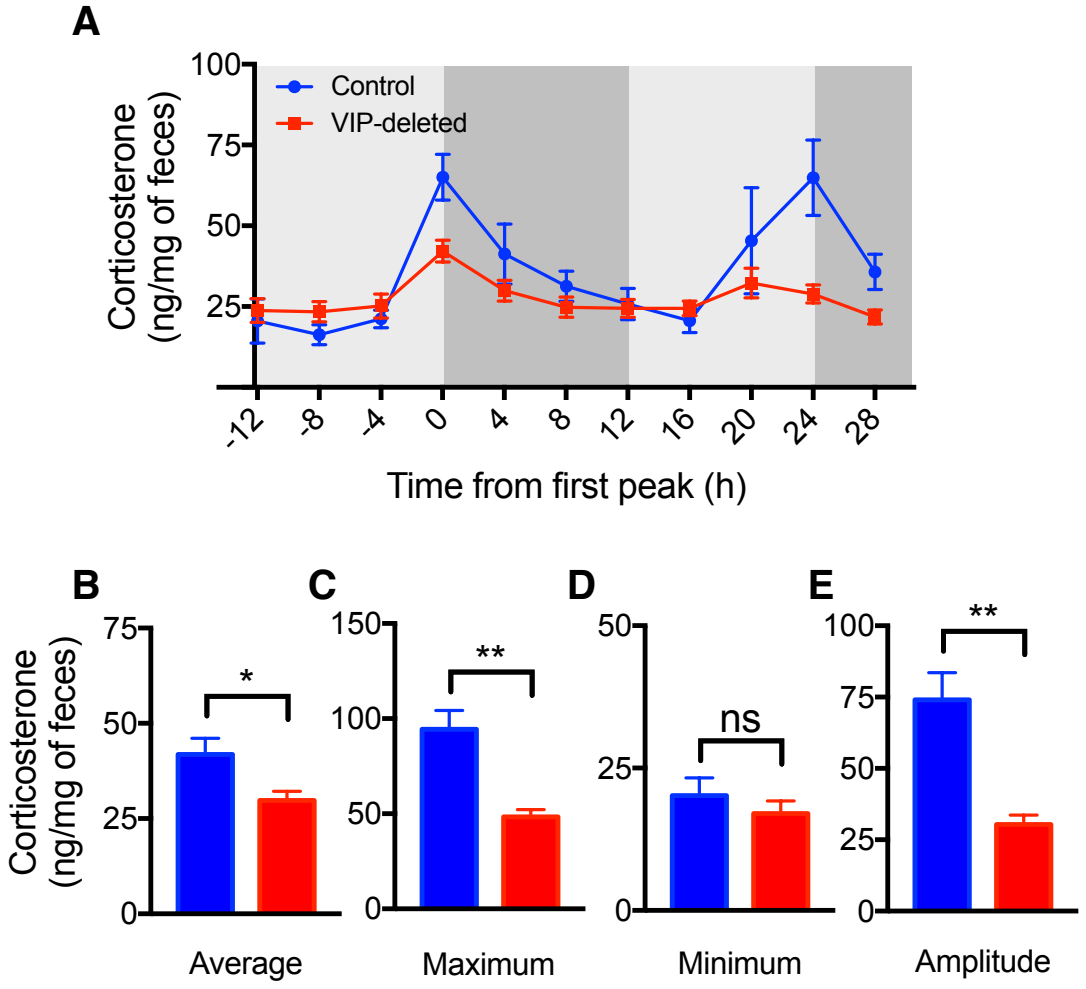
A
Corticosterone (ng/mg of feces)
100
75
50
25
Control
VIP-deleted
-12
-8
-4
0
4
8
12
16
20
24
28
Time from first peak (h)
B
C
D
E
75
50
25
0
*
150
100
50
0
**
50
25
0
ns
100
75
50
25
0
**
Average
Maximum
Minimum
Amplitude

Figure 2. Deletion of VIP SCN neurons dampens corticosterone rhythms. **A** Group data normalized to the first peak of corticosterone (control n=7, VIP-deleted n=11). **B** Average corticosterone was significantly lower in VIP-deleted animals than in controls (*29.8 ± 2.4 VIP-deleted, 41.9 ± 4.2, Control). **C** Lower average values resulted from decreases in peak corticosterone (*48.3 ± 3.8, VIP-deleted; 94.4 ± 9.9, Control) **D** and not from decreases in trough corticosterone (17.04 ± 2.2, VIP-deleted; 20.2 ± 3.1, Control). **E** Overall, corticosterone rhythms were dampened (**peak-to-trough amplitude, 30.4 ± 3.3, VIP-deleted; 74.1 ± 9.5, Control; all units in ng/mg of feces, *$p < 0.05$ unpaired t-test and **$p< 0.01$ unpaired t-test with Welch's correction).

circadian behavioral rhythms suggesting that our phenotype is not driven by single-cell SCN desynchronization.

SCN neuronal projections to nuclei involved in neuroendocrine and autonomic function are well established, however little is known about projections from specific SCN cell types. Our retrograde experiment circumvents many of the prior technical difficulties by using a unique two-fluorophore design. As previously validated (Hermanstyne et al., 2016), tdTOMATO is transgenically expressed solely in VIP SCN neurons through Cre-lox recombination, which bypasses the technical difficulties of staining for VIP neuropeptide. Importantly, we have preliminary but comparable results from two separate retrograde tracers. Interestingly, these results suggest that VIP neurons from the bilateral SCN innervate each PVN. Additionally our preliminary observations suggest that the VIP neurons that project to the PVN are not the same VIP neurons with dense arborizations within the SCN. This supports the idea that there are multiple classes of VIP neurons with separate anatomical and functional roles, specifically those interneurons that densely innervate and synchronize the SCN and the projection neurons that carry signals out of the SCN to regulate SCN output.

Ultimately, our results suggest that VIP SCN neurons stimulate the release of corticosterone in the mouse. Mechanistically we do not yet know what specific circuit mediates the changes in corticosterone. VIP SCN neurons are part of a multi-synaptic autonomic pathway that directly innervates the adrenal glands through the splanchnic nerve (Buijs et al., 1999). Conversely, VIP neurons may directly affect the hypothalamic-pituitary-axis and release of adrenocorticotropnin-

releasing hormone (ACTH). Finally, we cannot discount the possibility that loss of VIP neurons may alter the output activity of other SCN cell types including AVP neurons (Watanabe et al., 2000). Since AVP plays an inhibitory role in circadian glucocorticoid regulation, increased activity of AVP neurons may lower corticosterone levels. However, in our VIP-deleted animals, we detect no significant changes in AVP neuropeptidergic expression within the SCN following VIP-deletion (Chapter3).

Ultimately, these results form a crucial basis for the further investigation of VIP circuitry in regulating daily rhythms in glucocorticoids.

Future Directions

Does activation of VIP neurons increase levels in corticosterone?

Our previous results suggest that VIP neurons play a stimulatory role in corticosterone release. We propose to directly test this by activating VIP neurons using designer receptors exclusively activated by designer drugs (DREADDs) (Urban and Roth, 2015). VIP-ires-Cre mice will be injected with cre-dependent Gq DREADD receptors to allow robust activation of VIP SCN neurons at specific times of day. Control mice receive cre-dependent fluorophores. This technique has previously been utilized in VIP SCN neurons (Brancaccio et al., 2013) and reduces the stimulation variables inherent to optogenetic experiments (duration and frequency of stimulation, light delivery, i.e.).

After recovery, mice will be housed in the fecal matter collection cages in entrained conditions (LD 12:12). Separate experimental runs will test the activation of VIP neurons at the peak of

corticosterone rhythms (CT 12 or lights-off) and the trough of corticosterone rhythms (CT 0 or lights-on) in the same mice. Specifically, we will deliver Clozapine N-Oxide (CNO) through intraperitoneal injections into all animals and collect fecal matter at 3h intervals for 12 h before and after injections. This experiment will then be reproduced under constant conditions (constant darkness DD).

Ultimately, if this experiment provides evidence for mediation of corticosterone rhythms through VIP firing, we can probe this question with more finesse. Experimental possibilities including using optogenetics to understand the role of VIP firing patterns, using microdialysis to measure free-floating corticosterone levels from the interstitial fluid (ISF) with finer temporal precision (30min as opposed to 3-4h) (Qian et al., 2012), and severing the splanchnic nerve to identify whether the effects occur through neuroendocrine (HPA axis) or autonomic circuits.

Methods

Animals Mice were housed in the temperature and humidity controlled Danforth Animal Facility at Washington University in St. Louis with ad lib access to food and water. For the experiments, heterozygote combinations of the following genotypes were used: VIP-ires-Cre knockin ($VIP^{tm1(creZjh}$, Jackson Laboratories), tdTOMATO reporter (B6.Cg-Gt(ROSA)26Sor$^{tm9(CAG-tdTomato)Hze}$/J, Jackson Laboratories) and C57J. All procedures were approved by the Animal Care and Use Committee of Washington University in St. Louis and adhered to National Institutes of Health guidelines

Retrograde Tracing Experiments We injected retrograde tracers into the PVN of VIPCre/+; tdTOM/+ mice during stereotactic surgery. Briefly, mice were kept anesthetized using isofluorane (2%) and placed into a stereotactic device. Either a cre-dependent eYFP virus (AAV9-DIO-eYFP, UPenn viral core) or CTB488 (Cholera Toxin Subunit B – Recombinant, Alexa Fluor 488 Conjugate, ThermoFisher Scientific) was injected into the unilateral PVN at 0.0mm anterior, +/- 0.2 mm lateral and -4.3mm ventral to Bregma. Mice received analgesic treatment during recovery.

After 4-12 weeks, mice were perfused for tissue processing. Briefly, mice were anesthetized with 1.25% Avertin (2,2,2-tribromoethanol and tert-amyl alcohol in 0.9% NaCl; 0.025 ml/g body weight) and transcardially perfused with phosphate-buffered saline (PBS) and 4% paraformaldehyde (PFA). The brain was dissected and transferred to 30% sucrose in PBS the following day. Coronal sections were cut using a Leica Cryostat at 40um thickness in 3 separate wells, washed in PBS, mounted onto glass slides and cover-slipped with DABCO (1,4-Daizobicycol[2,2,2]-octane) mounting medium.

Sections were imaged first on a epifluorescent microscope to verify green spectrum fluorescence in the SCN. Then sections were imaged on a Nikon A1 confocal microscope. The number of tdTOMATO positive cells, and co-localized cells was counted manually. Future quantification and analysis of the images will take place at a later time.

Circadian Corticosterone Analysis Mice were injected with AAV8-DIO-Caspase3-TevP as described in Chapter 3. Following locomotor activity recordings, mice were transferred to

custom-built cages for fecal matter collection. These cages consisted of a wire stage where mice could comfortably sit with easy access to ad lib food and water. The majority of feces and urine would fall through the wire stage onto a piece of filter paper at the bottom of the cage. A slot was cut out of the bottom front of the cage that allowed an investigator to easily collect and replace the filter paper. We estimate 85-100% of feces per time point were collected.

After two days in constant darkness habituating to the cages, investigators collected fecal samples in 3-4h time bins for up to 48h. Samples were immediately transferred to -20 to -80C until processing. For steroid extraction, samples were baked at 50C for 3-4 hours until completely dry before being ground into a powder using a mortar and pestle. Total weight per time point was calculated and steroids were extracted from 25mg of powdered fecal matter using 80% methanol. After agitation, the supernatant was transferred to new tubes and methanol was evaporated off inside a hood. The remaining extracts were suspended in 500 ul of ELISA buffer and diluted to a concentration of 1:2500. Samples were processed for corticosterone concentration using the ELISA kit instructions (Cayman Chemicals, Corticosterone EIA). Comparable results were achieved with 4 separate rounds of collection.

References

ABRAHAMSON, E. E. & MOORE, R. Y. 2001. Suprachiasmatic nucleus in the mouse: retinal innervation, intrinsic organization and efferent projections. *Brain Research,* 916**,** 172-191.

ALEXANDER, L. D. & SANDER, L. D. 1994. Vasoactive intestinal peptide stimulates ACTH and corticosterone release after injection into the PVN. *Regulatory peptides,* 51**,** 221-227.

ATON, S. J., COLWELL, C. S., HARMAR, A. J., WASCHEK, J. & HERZOG, E. D. 2005. Vasoactive intestinal polypeptide mediates circadian rhythmicity and synchrony in mammalian clock neurons. *Nat.Neurosci,* 8**,** 476-483.

BAO, A. M., MEYNEN, G. & SWAAB, D. F. 2007. The stress system in depression and neurodegeneration: Focus on the human hypothalamus. *Brain Res Rev.*

BRANCACCIO, M., MAYWOOD, E. S., CHESHAM, J. E., LOUDON, A. S. I. & HASTINGS, M. H. 2013. A Gq-Ca 2+ axis controls circuit-level encoding of circadian time in the suprachiasmatic nucleus. *Neuron,* 78**,** 714-728.

BROWN, T. M., COLWELL, C. S., WASCHEK, J. A. & PIGGINS, H. D. 2007. Disrupted neuronal activity rhythms in the suprachiasmatic nuclei of vasoactive intestinal polypeptide-deficient mice. *Journal of neurophysiology,* 97**,** 2553-2558.

BUIJS, R. M., KALSBEEK, A., VAN DER WOUDE, T. P., VAN HEERIKHUIZE, J. J. & SHINN, S. 1993. Suprachiasmatic nucleus lesion increases corticosterone secretion. *Am.J.Physiol,* 264**,** R1186-R1192.

BUIJS, R. M., WORTEL, J., VAN HEERIKHUIZE, J. J., FEENSTRA, M. G., TER HORST, G. J., ROMIJN, H. J. & KALSBEEK, A. 1999. Anatomical and functional demonstration of a multisynaptic suprachiasmatic nucleus adrenal (cortex) pathway. *Eur.J.Neurosci.,* 11**,** 1535-1544.

COLWELL, C. S., MICHEL, S., ITRI, J., RODRIGUEZ, W., TAM, J., LELIEVRE, V., HU, Z., LIU, X. & WASCHEK, J. A. 2003. Disrupted circadian rhythms in VIP- and PHI-deficient mice. *American journal of physiology. Regulatory, integrative and comparative physiology,* 285**,** R939-49.

EASTMAN, C. I., MISTLBERGER, R. E. & RECHTSCHAFFEN, A. 1984. Suprachiasmatic nuclei lesions eliminate circadian temperature and sleep rhythms in the rat. *Physiol Behav.,* 32**,** 357-368.

FAHRENKRUG, J., GEORG, B., HANNIBAL, J. & JØRGENSEN, H. L. 2012. Altered rhythm of adrenal clock genes, StAR and serum corticosterone in VIP receptor 2-deficient mice. *Journal of molecular neuroscience : MN,* 48**,** 584-596.

HARMAR, A. J., MARSTON, H. M., SHEN, S., SPRATT, C., WEST, K. M., SHEWARD, W. J., MORRISON, C. F., DORIN, J. R., PIGGINS, H. D., REUBI, J. C., KELLY, J. S., MAYWOOD, E. S. & HASTINGS, M. H. 2002. The VPAC(2) receptor is essential for circadian function in the mouse suprachiasmatic nuclei. *Cell,* 109**,** 497-508.

HERMANSTYNE, T. O., SIMMS, C. L., CARRASQUILLO, Y., HERZOG, E. D. & NERBONNE, J. M. 2016. Distinct Firing Properties of Vasoactive Intestinal Peptide-Expressing Neurons in the Suprachiasmatic Nucleus. *Journal of biological rhythms,* 31**,** 57-67.

HÖKFELT, T., LUNDBERG, J. M., SCHULTZBERG, M. & FAHRENKRUG, J. A. N. 1981. Immunohistochemical evidence for a local VIP-ergic neuron system in the adrenal gland of the rat. *Acta Physiologica,* 113**,** 575-576.

KALSBEEK, A., BUIJS, R. M., VAN HEERIKHUIZE, J. J., ARTS, M. & VAN DER WOUDE, T. P. 1992. Vasopressin-containing neurons of the suprachiasmatic nuclei inhibit corticosterone release. *Brain research,* 580**,** 62-67.

KALSBEEK, A., VAN DER SPEK, R., LEI, J., ENDERT, E., BUIJS, R. M. & FLIERS, E. 2012. Circadian rhythms in the hypothalamo-pituitary-adrenal (HPA) axis. *Molecular and cellular endocrinology,* 349**,** 20-29.

KALSBEEK, A., VAN DER VLIET, J. & BUIJS, R. M. 1996. Decrease of endogenous vasopressin release necessary for expression of the circadian rise in plasma corticosterone: a reverse microdialysis study. *Journal of neuroendocrinology,* 8**,** 299-307.

KALSBEEK, A., VERHAGEN, L. A., SCHALIJ, I., FOPPEN, E., SABOUREAU, M., BOTHOREL, B., BUIJS, R. M. & PÉVET, P. 2008. Opposite actions of hypothalamic vasopressin on circadian corticosterone rhythm in nocturnal versus diurnal species. *The European journal of neuroscience,* 27**,** 818-827.

KOLBER, B. J., WIECZOREK, L. & MUGLIA, L. J. 2008. Hypothalamic-pituitary-adrenal axis dysregulation and behavioral analysis of mouse mutants with altered glucocorticoid or mineralocorticoid receptor function. *Stress (Amsterdam, Netherlands),* 11**,** 321-338.

LOH, D. H., ABAD, C., COLWELL, C. S. & WASCHEK, J. A. 2007. Vasoactive intestinal peptide is critical for circadian regulation of glucocorticoids. *Neuroendocrinology,* 88**,** 246-255.

MEYER-BERNSTEIN, E. L., JETTON, A. E., MATSUMOTO, S. I., MARKUNS, J. F., LEHMAN, M. N. & BITTMAN, E. L. 1998. Effects of suprachiasmatic transplants on circadian rhythms of neuroendocrine function in golden hamsters. *Endocrinology,* 140**,** 207-218.

QIAN, X., DROSTE, S. K., LIGHTMAN, S. L., REUL, J. M. H. M. & LINTHORST, A. C. 2012. Circadian and ultradian rhythms of free glucocorticoid hormone are highly synchronized between the blood, the subcutaneous tissue, and the brain. *Endocrinology,* 153**,** 4346-4353.

URBAN, D. J. & ROTH, B. L. 2015. DREADDs (designer receptors exclusively activated by designer drugs): chemogenetic tools with therapeutic utility. *Annual review of pharmacology and toxicology,* 55**,** 399-417.

WATANABE, K., VANECEK, J. & YAMAOKA, S. 2000. In vitro entrainment of the circadian rhythm of vasopressin-releasing cells in suprachiasmatic nucleus by vasoactive intestinal polypeptide. *Brain research,* 877**,** 361-366.

YANG, C. F., CHIANG, M. C., GRAY, D. C., PRABHAKARAN, M., ALVARADO, M., JUNTTI, S. A., UNGER, E. K., WELLS, J. A. & SHAH, N. M. 2013. Sexually dimorphic neurons in the ventromedial hypothalamus govern mating in both sexes and aggression in males. *Cell,* 153**,** 896-909.

ZELENA, D. R., LANGNAESE, K., DOMOKOS, A. G., PINTÉR, O., LANDGRAF, R., MAKARA, G. B. & ENGELMANN, M. 2009. Vasopressin administration into the paraventricular nucleus normalizes plasma oxytocin and corticosterone levels in Brattleboro rats. *Endocrinology,* 150**,** 2791-2798.